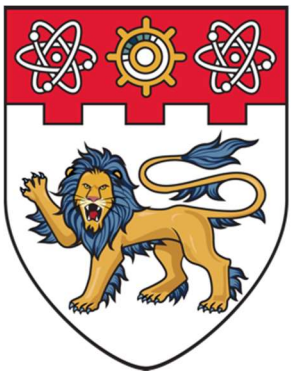

NANYANG TECHNOLOGICAL UNIVERSITY
SINGAPORE

Synthesis of Functional Polymers via Oxyanion and Iodide Catalyzed Living Radical Polymerizations in Emulsion, Solution and Bulk Systems and Their applications

Weijia MAO

SCHOOL OF PHYSICAL AND MATHEMATICAL SCIENCES

2021

Synthesis of Functional Polymers via Oxyanion and Iodide Catalyzed Living Radical Polymerizations in Emulsion, Solution and Bulk Systems and Their applications

Weijia MAO

SCHOOL OF PHYSICAL AND MATHEMATICAL SCIENCES

A thesis submitted to the Nanyang Technological University in partial fulfilment of the requirement for the degree of Doctor of Philosophy

2021

Statement of Originality

I hereby certify that the work embodied in this thesis is the result of original research done by me except where otherwise stated in this thesis. The thesis work has not been submitted for a degree or professional qualification to any other university or institution. I declare that this thesis is written by myself and is free of plagiarism and of sufficient grammatical clarity to be examined. I confirm that the investigations were conducted in accord with the ethics policies and integrity standards of Nanyang Technological University and that the research data are presented honestly and without prejudice.

31 Jul 2021

Date

Weijia MAO

Supervisor Declaration Statement

I have reviewed the content and presentation style of this thesis and declare it of sufficient grammatical clarity to be examined. To the best of my knowledge, the thesis is free of plagiarism and the research and writing are those of the candidate's except as acknowledged in the Author Attribution Statement. I confirm that the investigations were conducted in accord with the ethics policies and integrity standards of Nanyang Technological University and that the research data are presented honestly and without prejudice.

. . . . . .
Date

. . . . . .
Atsushi GOTO

Authorship Attribution Statement

This thesis contains material from [1] paper published in the following peer-reviewed journal(s) where I was the first author.

Chapter 2 is published as W. Mao, C.-G. Wang, Y. Lu, W. Faustinelie, and A. Goto. Carboxylate, nitrate, sulfonate, and phosphate catalysts for living radical polymerization *via* oxygen–iodine halogen bonding catalysis. *Polymer Chemistry.* **11**, 53-60 (2020). DOI: 10.1039/C9PY01533G.

The contributions of the co-authors are as follows:

- I and Dr. C.-G. Wang proposed the initial project.
- I performed the experimental work and analysis (GPC, NMR) except the work of natural carboxylates, which is performed by W. Faustinelie.
- Dr. Y. Lu performed the DFT calculation of catalytic activities.
- Prof. A. Goto and Dr. C.-G. Wang provided guidance in the interpretation of the experimental data.

I and Dr. C.-G. Wang prepared the manuscript drafts. Prof. A. Goto finalized the manuscript.

31 Jul 2021

Date

Weijia MAO

Abstract

Chapter 1 introduced the general concept of living radical polymerization (LRP), three most widely-used LRP methods were introduced, and their advantages and disadvantages were discussed. The mechanism of reversible complexation mediated polymerization (RCMP) was introduced, and its advantages over other LRPs have been discussed. The current catalysts and current limitations of RCMP were also introduced. The motivations and aims for the works in this Thesis were explained.

In Chapter 2, oxyanions (carboxylate, nitrate, phosphate, and sulfonate) were systematically studied as new RCMP catalysts. The oxyanion-catalyzed RCMP yielded polymers with relatively high conversion in short reaction times, maintaining low dispersity. The high chain-end iodide livingness of the obtained polymers also enabled the synthesis of block copolymers. Oxyanion compounds are inexpensive, little toxic, and amenable to broad molecular structures. These features are attractive for RCMP catalysis. The development of oxyanions as RCMP catalysts also contributed to development of air-tolerant RCMP in Chapter 3.

In Chapter 3, air-tolerant RCMP was developed. The air-tolerant RCMP system employed an aldehyde, *N*-hydroxyphthalimide (NHPI), and an amine for both oxygen consumption and catalysis. The aldehyde (RCHO) consumed oxygen and was converted to a carboxylic acid (RCOOH) catalyzed by NHPI. The carboxylic acid was subsequently converted to a carboxylate anion ($RCOO^-$) in the presence of the amine. The generated $RCOO^-$ worked as an RCMP catalyst. This system does not require deoxygenation before polymerization and is amenable to methacrylates and styrene. The development of air-tolerant RCMP enhances the practicality of RCMP.

In Chapter 4, RCMP was explored in the emulsion system. We systematically studied the effect of emulsifiers, catalysts, and alkyl iodide initiating dormant species in emulsion

RCMP for homopolymerization. The kinetic and mechanistic aspects of emulsion RCMP were also elucidated by partitioning tests of the initiating dormant species and particle number analysis in the course of polymerization. Emulsion RCMP can afford stable polymer latex with relatively high solid contents (up to nearly 50%). The emulsion RCMP combines the advantages of emulsion polymerization such as efficient heat transfer, low viscosity, and high polymerization rate with those of RCMP, such as no use of special capping agents or toxic catalysts. The high solid content, high chain-end fidelity, good monomer versatility achievable in the emulsion RCMP would also be attractive for polymer material design and industrial applications.

In Chapter 5, we further explored emulsion RCMP for copolymerization. We carried out block copolymerization exploiting the high iodide chain-end fidelity of poly(methacrylate) −I (PMMA−I) obtained in Chapter 4, successfully yielding block copolymers with high monomer conversions in relatively short reaction times. Random copolymerizations were also carried out in emulsion RCMP, various gradient copolymers were obtained, and monomer sequence can be tuned by the reaction temperature. We also studied using solution RCMP for the synthesis of hydrophilic-amphiphilic block copolymers using monomers with anti-fouling properties and applied the obtained block copolymers for anti-fouling coating on membranes. The accessibility of RCMP in aqueous media to a wide range of monomers was successfully demonstrated.

Acknowledgements

I would like to thank my supervisor, Professor Atsushi Goto, for his guidance and support in the four years. He provided me an opportunity to pursue a Ph.D. degree in my hard time, corrected my mistakes, and provided useful advice during my research. When I faced difficulties in my Ph.D. career, he always helped and encouraged me to overcome and keep moving on. I benefited a lot from Professor Goto for not only my research, but also the integrity and ethics of a researcher, which is valuable for my whole life. I had a wonderful time in his group, and it will be a precious memory.

I also want to thank my thesis advisory committee (TAC) members, Professor Yanli Zhao and Professor Xiao Hu, for their kind suggestions for my research when evaluating my progress report.

I want to thank Nanyang Technological University, SPMS, CBC for providing such a wonderful condition for research and Singapore government for offering the scholarship.

I appreciate all my labmates. Especially, I want to thank Dr. Chen-Gang Wang and Dr. Jit Sarkar for their great help in my research projects. I also want to thank Chen Chen, Xin Yi Oh, Dr. Xu Liu, Dr. Xiaolu Wu, and Dr. Shuaiyuan Han for our friendship and their encouragement when I faced obstacles.

I want to thank Paradox Interactive for its masterpieces, Europa Universalis IV, Crusader Kings III and Hearts of Iron IV, which occupied a large fraction of my holidays and brought so much joy during the spread of COVID-19.

At last, I want to thank my family and friends for their company and support in the 4 years. I have the most incredible family who raised me up and taught me to be a good person and willing to contribute to society. I will do my best in return after my graduation. I would like to thank my best friends, Alice Su, Toransu Chen and Rui Zhang for their unreserved support. I really hope our friendship can be long and prosperous.

Table of Contents

Abstract 1

Acknowledgements 3

Table of Contents 4

Chapter 1 Introduction **7**

1.1 Living Radical Polymerization 7

1.2 Reversible Complexation Mediated Polymerization (RCMP) 10

1.3 Aim in Chapter 2 11

1.4 Air-tolerant LRP Methods 13

1.5 Aim in Chapter 3 13

1.6 Emulsion Polymerization and Emulsion LRP 14

1.7 Anti-fouling in Membrane Technology 17

1.8 Aims in Chapters 4 and 5 18

References 20

Chapter 2 Carboxylate, Nitrate, Sulfonate, and Phosphate Catalysts for Living Radical Polymerization via Oxygen−Iodine Halogen Bonding Catalysis. **23**

2.1 Introduction 24

2.2 Results and Discussion 27

Experimental Proof of the Generation of R• from R–I 27

Polymerizations of MMA with Carboxylate Catalysts 29

Nitrate, Sulfonate and Phosphate Catalysts 32

Increase in Polymerization Rate 35

Naturally Existing Oxyanions as Catalysts 38

Chain-end Fidelity 38

Polymerizations of Functional Methacrylates, Styrene and Acrylonitrile 39

Block Copolymerization 41

2.3 Conclusions 43

2.4 Experimental 44

References 48

Chapter 3 Development of Air-tolerant RCMP system 50

3.1 Introduction 51

3.2 Results and Discussion 55

Oxidation of Aldehydes. 55

Two-step Polymerizations of MMA 57

One-step Polymerizations of MMA 59

Increase in the Polymerization Rate 62

Polymerization of Other Methacrylates and St 64

3.3 Conclusions 65

3.4 Experimental 66

References 68

Chapter 4 Aqueous Emulsion Polymerizations of Methacrylates and Styrene via Reversible Complexation Mediated Polymerization (RCMP) 69

4.1 Introduction 70

4.2 Results and Discussion 74

Polymerizations of MMA 74

Studies on Emulsifiers 74

Studies on Catalysts 76

Studies on Alkyl Iodide Dormant Species 79

Study on Nucleation 84
Chain-end Fidelity 87
Higher Molecular Weights and Higher Solid Contents 89
Functional Methacrylates 89
Styrene 91
4.3 Conclusions 94
4.4 Experimental 95
References 99

Chapter 5 Systematic Studies of Copolymer Synthesis in Aqueous Media via RCMP 101
5.1 Introduction 102
5.2 Results and Discussion 106
Synthesis of Block Copolymers via Emulsion RCMP 106
Synthesis of Gradient Copolymers via Emulsion RCMP 108
Preparation of Macroinitiators via Solution RCMP for the Synthesis of Anti-fouling Block Copolymers 113
Synthesis of Block Copolymers via Solution RCMP 115
Anti-fouling Test 117
5.3 Conclusions 119
5.4 Experimental 120
References 124

Chapter 6 Conclusions 126

Chapter 1. General Introduction.

In synthetic polymer chemistry, radical polymerization is widely used. Radical polymerization contributes to nearly 50% of the commercial polymers produced globally.[1] Compared with other polymerizations such as ionic polymerizations, radical polymerization is advantageous in the good tolerance to impurities and moisture. Radical polymerization is compatible with polar solvents and can be conducted in suspension and emulsion systems.[2-3] However, in conventional radical polymerization, the molecular architecture, molecular weight, molecular weight distribution, and functionality of the obtained polymer cannot be well controlled.

1.1 Living Radical Polymerization.

To synthesize well-defined polymers, living radical polymerization (LRP) was developed.[4] The mechanism of LRP is based on the reversible activation of a dormant species (Polymer–X) to a propagating radical (Polymer•) (active species) by thermal or chemical stimulus, where X is a capping agent (Scheme 1.1).

Scheme 1.1. Reversible activation of LRP (general scheme).

In LRP, Polymer• propagates (reacts with monomers) until it is deactivated (capped with X) back to Polymer–X. There are nearly equal chances for every polymer chain to propagate when the activation-deactivation between dormant species and active species is sufficiently fast in terms of propagation rate, which results in nearly uniform chain length (low dispersity). This mechanism enables the number-average molecular weight (M_n) of the polymer to be controlled by the molar ratio of the monomer and initiator. After the monomer is

consumed completely, the polymer can react with another monomer to produce a block copolymer upon the addition of another monomer. Several LRP methods using different X groups have been developed in the past three decades. Representative LRP methods include nitroxide-mediated radical polymerization (NMP), atom transfer radical polymerization (ATRP), and reversible addition-fragmentation chain transfer (RAFT) polymerization.

NMP utilizes nitroxides as the X. Solomon et al. studied polymerizations of methyl methacrylate (MMA) in the presence of nitroxides and obtained oligomers, which was a pioneering work in developing NMP.[5] In 1993, Georges et al. reported the use of a nitroxide to synthesize polymers (polystyrenes) with narrow molecular weight distribution ($Đ$ (= M_w/M_n) < 1.30, where $Đ$ is the dispersity and M_w is the weight-average molecular weight). This work was the first synthesis of low-dispersity polymers via NMP. The nitroxide was 2,2,6,6-tetramethyl-1-piperidinyloxy (TEMPO). The dormant species (Polymer–TEMPO) reversibly dissociated at a high temperature (125-150 ℃) (Scheme 1.2).[6]

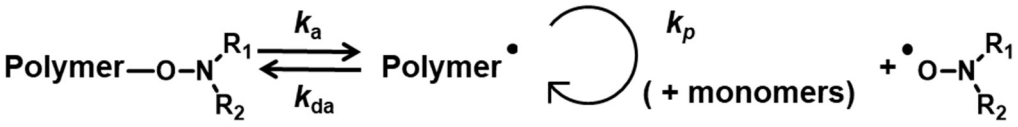

Scheme 1.2. Mechanism of NMP.

Subsequently, other nitroxides were developed for expanding the monomer scope of NMP.[7] NMP is amenable to a range of monomers, including styrene and its derivatives, vinyl pyridines, acrylates, acrylonitrile, acrylic acids, and dienes. NMP also enables the synthesis of architecturally controlled polymers such as star, comb, and hyperbranched polymers. The obtained polymers found applications in microelectronics, nano-porous materials, and additive manufacturing materials.[7] However, NMP has some limitations. The polymerization requires high temperature, and many nitroxide agents are expensive or synthesized.[8]

ATRP was first reported in 1995 independently by two research groups, i.e., Matyjaszewski et al. and Sawamoto et al.[9-10] ATRP utilizes halogen atoms as the X. The ATRP system contains monomer(s), an alkyl halide (R–X, where X = Cl or Br) (initiator), a transition metal halide ($M_t^mX_n$), and a ligand (L) of the metal. The transition metal halide complex ($M_t^mX_n/L_n$) works as the catalyst to reversibly generate Polymer$^\bullet$ from Polymer–X (Scheme 1.3).

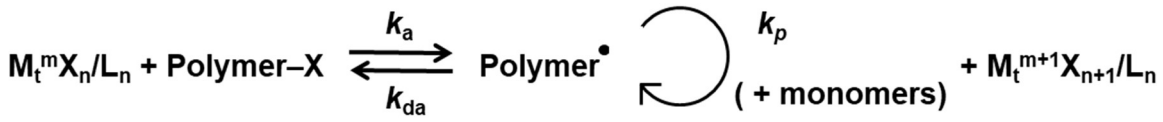

Scheme 1.3. Mechanism of ATRP.

Among the transition metals, Cu is the most widely used. Other utilized metals include Ru, Fe, and Os.[11-12] ATRP is amenable to a wide range of monomers such as styrene, methacrylates, acrylates, and acrylamides. However, relatively large amounts of metals are used in normal ATRP, which can limit the practical use. In recent years, several approaches have been developed to successfully reduce catalyst loading, while maintaining the amenability to a wide range of monomers. These approaches include continuous activator re-generation (ICAR) ATRP,[13] activators regenerated by electron transfer (ARGET) ATRP,[14-16] and electrochemically mediated ATRP (*e*ATRP).[17-18]

RAFT polymerization was first reported by Thang, Rizzardo, and Moad et al. in 1998.[19] RAFT polymerization uses thiocarbonylthio compounds (Z–C(=S)–SR) including dithioesters, xanthates, trithiocarbonates, dithiocarbamates and dithiophosphonates, where R is the leaving alkyl group and Z is the stabilizing group.[20] Mechanistically, Polymer$^\bullet$ ($P_m^\bullet$) undergoes addition to the dormant species (P_n–S–C(=S)–Z), generating an intermediate radical (Scheme 1.4). The fragmentation of ($P_n^\bullet$) from the intermediate completes the RAFT process.

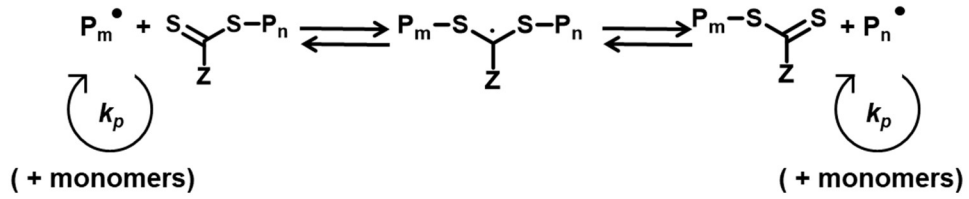

Scheme 1.4. Mechanism of RAFT.

RAFT polymerization can be conducted at a range of temperatures (-15 ℃ to 180 ℃),[21-22] in various solvents,[23-25] and for various monomers such as methacrylates, acrylates, styrenics, acrylamides, vinyl esters, and dienes.[26] RAFT polymerization has been widely used in optoelectronics, therapeutic delivery, and rheology control agents.[27] A possible problem is that the product contains a thiocarbonylthio group at the polymer chain-end, which causes undesirable color and odor. In addition, similar to NMP, many RAFT agents are required to synthesize before polymerization.

1.2 Reversible Complexation Mediated Polymerization (RCMP).

The use of organic (non-metal) catalysts in polymer chemistry has gained increasing interest in recent years for avoiding metal removal, reducing toxicity, and applying to a wider range of use in, e.g., electronic and biological materials.[28] In 2011, our group reported a new type of LRP termed reversible complexation mediated polymerization (RCMP).[29] RCMP contains a monomer, an alkyl iodide (R–I) as an initiating dormant species, and an organic molecule as a catalyst. Mechanistically RCMP catalysis utilizes halogen bonding (XB) in its organocatalysis. XB is a noncovalent bond between an electron halogen (X) (R–I) and an electron donor (B) (catalyst) (Scheme 1.5). Because iodide is the strongest electron acceptor among halides, RCMP uses iodide (R−I) for X. In RCMP, the dormant species (Polymer–I) forms an XB complex with the organic catalyst, and the complex reversibly generates the Polymer•. This reversible complexation mediates the polymerization (Scheme 1.6).[29-31]

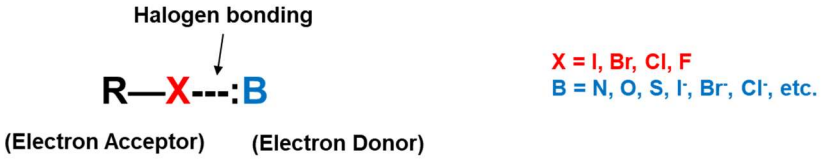

Scheme 1.5. Halogen bonding (XB).

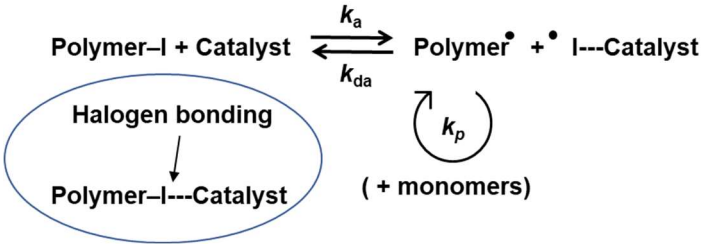

Scheme 1.6. Mechanism of RCMP.

RCMP is an attractive LRP method, as no special capping agents or metals are used. The catalysts employed in RCMP are little toxic, free from odor, and easy to handle (no sensitive to humid and air). RCMP is amenable to a wide range of monomers, including methacrylates, acrylates, styrene, acrylonitrile, and itaconate. Non-cojugated monomer (e.g. vinyl acetate and *N*-vinylpyrrolidone), however, cannot be polymerized trough RCMP in the current studies.[31] In addition, various polymer architectures can be obtained via RCMP, including ABA and CABC block copolymers,[32-34] star copolymers,[35-36] surface-modified polymer brushes,[35,37-39] and chain-end functionalized polymers.[38,40-41]

1.3 Aim in Chapter 2.

Our research group has used tertiary amines,[29-30] iodide anion,[42] pseudohalide anions,[43] and pyridine *N*-oxides,[44] as effective catalysts. Compared with neutral tertiary amines, iodide anion and pseudohalide anions, which are ions, have stronger electron-donating abilities (stronger XB with the dormant species) and showed higher catalytic activities. Compared with iodide anion and pseudohalide anions, pyridine *N*-oxides, which are also ions, were advantageous as by modifying the substituents of pyridine *N*-oxide, the catalytic activity can

be adjusted (Scheme 1.7). Pyridine *N*-oxides form an O···I halogen bonding, which is the first use of an O···I halogen bonding in RCMP catalysis (Scheme 1.7).

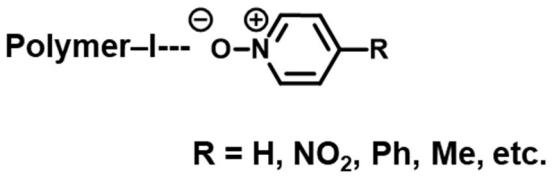

Scheme 1.7. An XB complex generated from pyridine *N*-oxide and Polymer–I.

However, pyridine *N*-oxides require multi-step synthesis and are not well dissolved in hydrophilic solvents, limiting possible applications. Oxyanions such as carboxylates, nitrates, sulfonates, and phosphates are generally less toxic and widespread in nature and synthetic compounds. Hence, we aimed to use oxyanions as alternative RCMP catalysts to pyridine *N*-oxides. Oxyanions are less toxic and also water-soluble, inexpensive, and flexible in structural design. We systematically studied the catalytic abilities of oxyanions in RCMP (Figure 1.1), demonstrating that oxyanions are good catalysts in RCMP. The details will be discussed in Chapter 2 of this thesis.

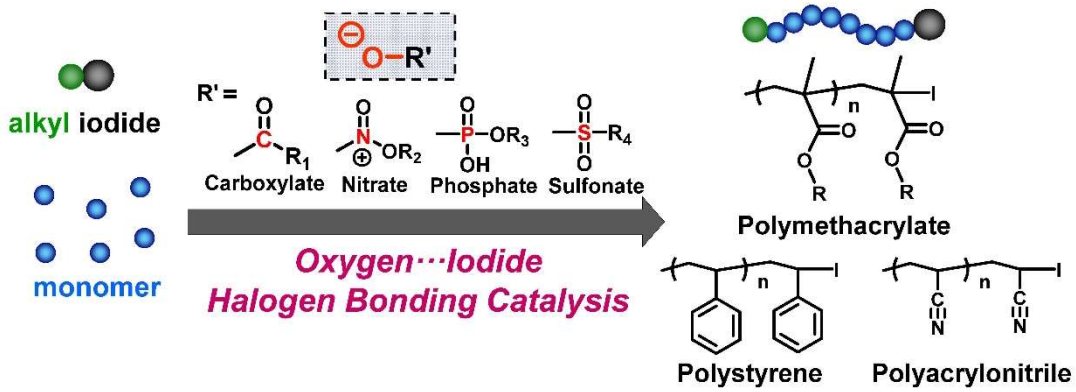

Figure 1.1. Halogen bonding catalysis of RCMP using oxyanions as catalysts.

1.4 Air-tolerant LRP methods.

LRP is a radical polymerization, and hence is sensitive to oxygen (air). Oxygen can trap the propagating radical, therefore inhibits the polymerization.[45] Thus, the reaction mixture needs to be deoxygenated using an inert (nitrogen or argon) gas before the polymerization, which is a possible limitation in industrial applications and low-volume reactions in labs. To overcome this limitation, several methods have been developed for removing oxygen or converting oxygen to inert species. For example, in ATRP, an effective method is ARGET ATRP. ARGET ATRP employs reducing agents. The catalyst (copper (I) species) is oxidized by oxygen to generate copper (II) species. The copper (II) species is subsequently reduced to the copper (I) species in the presence of a reducing agent. The use of an excess amount of the reducing agent can ensure that all oxygen is consumed in the system.[14,46-51] The addition of enzymes such as glucose oxidase (GOx) is a useful approach in RAFT polymerization. GOx consumes oxygen and generates hydrogen peroxide through the oxidation of glucose upon the addition of glucose. The hydrogen peroxide is subsequently reduced to hydroxyl radical in the presence of a reducing agent, and the hydroxyl radical initiates the RAFT polymerization.[52-53] Photoinduced electron transfer RAFT (PET-RAFT) polymerization with air-tolerant properties was also reported. The photoredox catalysts (e.g., zinc tetraphenylporphine (ZnTPP) and *fac*-$[Ir(ppy)_3]$ (ppy = 2-pyridylphenyl)) used in PET-RAFT polymerization are capable of reducing oxygen to inactive hydroxide anion. The electron or energy transfer between the catalyst and the RAFT chain transfer agent mediates the polymerization.[54-55]

1.5 Aim in Chapter 3.

RCMP also requires oxygen removal and has been conducted after argon bubbling. In Chapter 3, we demonstrate air-tolerant RCMP, i.e., oxygen removal in situ in the polymerization. In Chapter 2, oxyanions (carboxylates, nitrates, phosphates, and sulfates) were

successfully employed for RCMP catalysis via oxygen-iodine halogen bonding. Among these oxyanion catalysts, carboxylate anions exhibited the highest catalytic activities, achieving high monomer conversions in short reaction times, maintaining low polydispersity, and accessibility to a wide range of monomers. Carboxylates were proved to be good RCMP catalysts and are abundant in nature or easy to synthesize.

In Chapter 3, we propose air-tolerant RCMP (in situ oxygen removal) utilizing a recently developed aldehyde oxidation method to carboxylic acids and the mentioned use of carboxylate anions as RCMP catalysts. The air-tolerant RCMP utilizes an aldehyde. Oxygen is consumed via the conversion of the aldehyde to a carboxylic acid (Scheme 1.8a). The generated carboxylic acid is further converted to carboxylate anion using a base, and the generated carboxylate anion acts as a catalyst for RCMP (Scheme 1.8b). We studied four different aldehydes for their oxidation in air. Cyclohexanecarboxaldehyde (CHCA) showed the highest oxidation ability, and we used CHCA to demonstrate two-step and one-step air-tolerant RCMPs. The results will be discussed in Chapter 3 of this thesis.

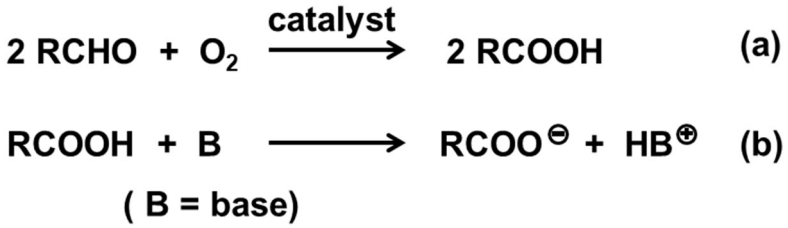

Scheme 1.8. Mechanism of air-tolerant RCMP catalysis: (a) oxidation of aldehyde to carboxylic acid and (b) transformation of carboxylic acid to carboxylate anion.

1.6 Emulsion Polymerization and Emulsion LRP.

Radical polymerization is widely conducted in emulsion systems (heterogeneous systems) as well as in solution and bulk systems (homogeneous systems). In emulsion systems, monomers (typically hydrophobic monomers) are immiscible with the reaction medium

(typically hydrophilic reaction medium such as water), and the reaction occurs in the monomer loci (dispersed phase) dispersed in the reaction medium (continuous phase).[56] A typical oil-in-water emulsion polymerization system contains hydrophobic monomer(s), an initiator, water, and emulsifier (surfactant). Compared with homogenous systems, emulsion radical polymerization has several significant advantages. For example, (i) it enables efficient heat transfer, because the aqueous phase can absorb the heat generated from exothermic polymerization effectively. (ii) It utilizes water as a solvent and a more sustainable manufacturing process. (iii) Compared with bulk and solution polymerization, emulsion polymerization can afford a high polymerization rate because of the segregation effect and compartment effect.[57-59] These features are attractive for large-scale industrial synthesis. Emulsion polymerization is widely used in industry for manufacturing synthetic rubbers, coating materials, adhesive, and so on.[60-67]

Not only conventional radical polymerization but also LRP has extensively been studied in emulsion systems. However, compared with conventional emulsion radical polymerization, there are challenges for conducting emulsion LRP. A challenge is mass transport, i.e., transportation of initiators and catalysts to the polymerization loci through the aqueous phase, leading to broad molecular weight distribution. Secondly, at an early stage of LRP, short oligomer chains are generated. The chain lengths of the oligomers are not long enough to stabilize the particle (polymerization loci). Short oligomers can also exit from the particle (polymerization loci), leading to a reduced polymerization rate.[3]

The first emulsion LRP was conducted in a homopolymerization. In 1997, Klumperman et al. reported the first Emulsion LRP using styrene as a monomer via NMP. The polymerization was conducted at 125 °C at 15 bar.[68] Later on, *N*-(tert-butyl)-*N*'-(1-diethylphosphono-2,2'-dimethylpropyl)nitroxide (SG1) was used, and monomer scope was expanded to methacrylates and acrylates.[69-70] Emulsion NMP was difficult to conduct below

90 ℃. Below 90 ℃, the latex was unstable. Matyjaszewski et al. reported the first emulsion ATRP using *n*-butyl methacrylate as a monomer in 1998, showing living characters, i.e., a linear increase in the molecular weight with the monomer conversion and narrow molecular weight distribution.[71] ATRP uses a copper (I) complex as the catalyst, for example. The transportation of the catalyst was a challenge for controlling the polymerization. The use of ARGET ATRP can significantly reduce the catalyst loading and facilitate the emulsion ATRP.[3,72-73] Emulsion RAFT polymerization was first conducted by Thang, Rizzardo, and Moad et al.[19] Early studies on emulsion RAFT polymerization also faced problems such as poor colloidal stability and inefficient transportation of RAFT agents to the polymerization loci through the continuous phase.[74-76] In order to overcome these problems, miniemulsion or seeded emulsion polymerization, where the monomer-containing micelles (polymerization loci) are pre-created before the polymerization, were employed.[75,77-79]

Copolymerization was also studied in emulsion LRP. Conventional emulsion radical polymerization generally allowed only random copolymerization. In contrast, emulsion LRP allows block copolymerizations as well as random copolymerizations. Interestingly, block copolymerizations via emulsion LRP do not require surfactants. The technique is termed polymerization-induced self-assembly (PISA). In PISA, a hydrophilic monomer A is polymerized first, and then a hydrophobic polymer B is added. The amphiphilic block copolymer can undergo self-assembly to form nano-structures such as spherical micelles, worms, and vesicles.[80] Gilbert et al. first introduced PISA in emulsion RAFT polymerization to synthesize hydrophilic-hydrophobic block copolymers in 2002.[81] Since then, PISA has widely been used to synthesize a series of block copolymers with various morphologies.[82-84] The assembly structures depend on the fractions of the block segments and solid contents. The process is surfactant-free, which reduced the cost and purification step compared with conventional emulsion polymerization. Not only PISA emulsion LRP but also normal

(surfactant-containing) emulsion LRP has been studied to generate block copolymers. The obtained particles (polymerization loci) can take unique morphologies such as core-shell and multi-layered spheres. Triblock copolymers, e.g., "hard-soft-hard" copolymers consisting of polystyrene and poly(*n*-butyl acrylate) segments were also obtained via emulsion RAFT polymerization.[85]

1.7 Anti-fouling in Membrane Technology.

Because of the growing global demand for clean water, the production of clean water has been extensively studied.[86] Clean water is currently produced mainly by desalination.[87] Membranes are widely used for desalination due to the high energy efficiency, low operation cost, and facile operation.[88] Reverse osmosis (RO) system is currently used for 50% of the desalinated water globally.[89-91] In long-term operations, membrane fouling is a common problem for membrane-based desalination. Fouling is caused by the undesirable deposition of colloidal materials, accumulation of organic materials, and microbial growth. Membrane fouling does not only reduce the flux (desalination performance) but also shortens the membrane lifetime, increasing the operation cost.[91-92]

Roughness, hydrophobicity, and charge of the membrane surface are key factors that control fouling. A membrane with a rough, hydrophobic, and positively charged surface exhibits a high adsorption tendency to common hydrophobic foulants such as proteins and bacteria.[92-93] Therefore, various methods have been developed for reducing the fouling by introducing smooth, hydrophilic, and negatively charged surfaces to the membrane. An effective and industrially translational way is to modify the membrane surface with a thin hydrophilic layer. The hydrophilic layer can create a hydration layer (a water layer via hydrogen bonding), which may suppress the deposition of foulants.[94-95] However, the deposited hydrophilic layer may be washed away in a long-term use, and hence the development of new

hydrophilic (polymer) layer with strong anchoring ability and excellent anti-fouling properties is important.

1.8 Aims in Chapters 4 and 5.

We studied RCMP in emulsion systems, which would be useful for large-scale synthesis and industrial applications. Therefore, we systematically studied emulsion RCMP using various emulsifiers, alkyl iodide initiators, and catalysts ~~(Figure 1.2)~~. Figure 1.2 represents one type of emulsion RCMPs, where monomer and initiator are insoluble/slightly soluble in water. Another type of emulsion RCMPs, where monomer and initiator are soluble in aqueous medium to different degrees, was also stuided. The kinetic and mechanistic aspects of the polymerizations were elucidated by the partitioning tests of the species in the aqueous and organic phases and the particle number analysis in the course of the polymerization. We studied the polymerizations of MMA and also functional methacrylates and styrene. The results will be discussed in Chapter 4 of this thesis.

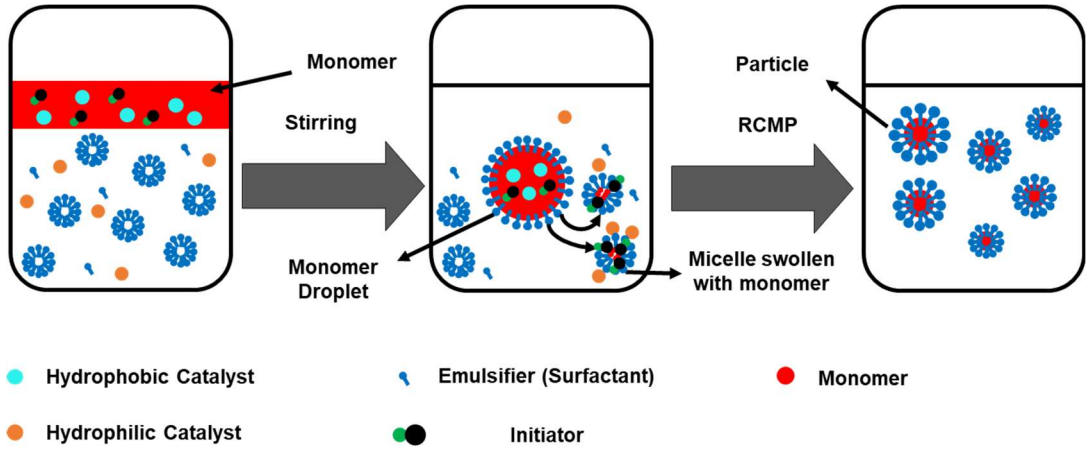

Figure 1.2. Illustration of emulsion RCMP (under condition in which monomer and initiator are insoluble/slightly in water).

In Chapter 5, we aimed to study random and block copolymerizations via emulsion RCMP. Exploiting the high chain-end iodide fidelity of the polymers, we successfully obtained

random, gradient, and block copolymers. Gradient copolymers are copolymers with a gradual change in monomer composition from one species to the other. In Chapter 5, as a separate topic, we also synthesized hydrophilic-amphiphilic block copolymers in solution RCMP for anti-fouling coating on water-purification membranes (Figure 1.3). The obtained block copolymers were tested for anti-fouling coatings, and the results were compared with those of corresponding random copolymers and homopolymers.

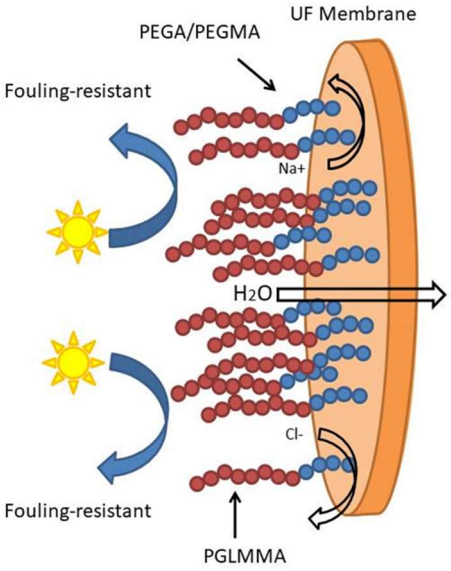

Figure 1.3. An example of membrane modification by block copolymers for anti-fouling coating.

References.

1. Matyjaszewski, K.; Spanswick, J. *Materials Today* **2005,** 8 (3), 26-33.
2. Hong, K.; Zhang, H.; Mays, J. W.; Visser, A. E.; Brazel, C. S.; Holbrey, J. D.; Reichert, W. M.; Rogers, R. D. *Chem. Commun.* **2002**, 13, 1368-1369.
3. Oh, J. K. *J. Polym. Sci. Part A: Polym. Chem.* **2008**, 46, 6983-7001.
4. Braunecker, W. A.; Matyjaszewski, K. *Prog. Polym. Sci.* **2007**, 32, 93-146.
5. Solomon, D. H. *J. Polym. Sci. Part A: Polym. Chem.* **2005**, 43, 5748-5764.
6. Georges, M. K.; Veregin, R. P. N.; Kazmaier, P. M.; Hamer, G. K. *Macromolecules* **1993**, 26, 2987-2988.
7. Likhtenshtein, G. I., Chapter 7 Nitroxide-Mediated Polymerization. In *Nitroxides: Brief History, Fundamentals, and Recent Developments*. Springer Nature: **2020**; pp 161-186.
8. Grubbs. R. B. *Polymer Reviews*, **2011**, 51, 104-137.
9. Wang, J.-S.; Matyjaszewski, K. *J. Am. Chem. Soc*. **1995,** 117, 5614-5615.
10. Kato, M.; Kamigaito, M.; Sawamoto, M.; Higashimura, T. *Macromolecules* **1995,** 28, 1721-1723.
11. di Lena, F.; Matyjaszewski, K. *Prog. Polym. Sci.* **2010**, 35, 959-1021.
12. Matyjaszewski, K. *Macromolecules* **2012,** 45, 4015-4039.
13. Konkolewicz, D.; Magenau, A. J. D.; Averick, S. E.; Simakova, A.; He, H.; Matyjaszewski, K. *Macromolecules* **2012,** 45, 4461-4468.
14. Matyjaszewski, K.; Dong, H.; Jakubowski, W.; Pietrasik, J.; Kusumo, A. *Langmuir* **2007**, 23, 4528-4531.
15. Simakova, A.; Averick, S. E.; Konkolewicz, D.; Matyjaszewski, K. *Macromolecules* **2012,** 45, 6371-6379.
16. Lee, H.-C.; Antonietti, M.; Schmidt, B. V. K. J. *Polym. Chem.* **2016**, 7, 7199-7203.
17. Chmielarz, P.; Fantin, M.; Park, S.; Isse, A. A.; Gennaro, A.; Magenau, A. J. D.; Sobkowiak, A.; Matyjaszewski, K. *Prog. Polym. Sci.* **2017**, 69, 47-78.
18. Liu, Q.; Ma, K.; Wen, D.; Wang, Q.; Sun, H.; Liu, Q.; Kong, J. *Journal of Electroanalytical Chemistry* **2018**, 823, 20-25.
19. Chiefari, J.; Chong, Y. K. B.; Ercole, F.; Krstina, J.; Jeffery, J.; Le, T. P. T.; Mayadunne, R. T. A.; Meijs, G. F.; Moad, C. L.; Moad, G.; Rizzardo, E.; Thang, S. H. *Macromolecules* **1998,** 31, 5559-5562.
20. Keddie, D. J.; Moad, G.; Rizzardo, E.; Thang, S. H. *Macromolecules* **2012**, 45, 5321-5342.
21. Sun, X.-L.; He, W.-D.; Li, L.-Y.; Zhang, B.-Y.; Pan, T.-T. *J. Polym. Sci. Part A: Polym. Chem.* **2009**, 47, 6863-6872.
22. Bekanova, M. Z.; Neumolotov, N. K.; Jablanović, A. D.; Plutalova, A. V.; Chernikova, E. V.; Kudryavtsev, Y. V. *Polymer Degradation and Stability* **2019**, 164, 18-27.
23. Benaglia, M.; Rizzardo, E.; Alberti, A.; Guerra, M. *Macromolecules* **2005**, 38, 3129-3140.
24. Zhang, X.; Rieger, J.; Charleux, B. *Polym. Chem.* **2012**, 3, 1502-1509.
25. Puttick, S.; Davis, A. L.; Butler, K.; Irvine, D. J.; Licence, P.; Thurecht, K. J. *Polym. Chem.* **2013**, 4, 1337-1344.
26. Hill, M. R.; Carmean, R. N.; Sumerlin, B. S. *Macromolecules* **2015**, 48, 5459-5469.
27. Moad, G.; Rizzardo, E.; Thang, S. H. *Chem. Asian J.* **2013**, 8, 1634-1644.
28. Theriot, J. C.; Lim, C.-H.; Yang, H.; Ryan, M. D.; Musgrave. C. B.; Miyake, G. M. *Science* **2016**, 352, 1082-1086.
29. Goto, A.; Suzuki, T.; Ohfuji, H.; Tanishima, M.; Fukuda, T.; Tsujii, Y.; Kaji, H. *Macromolecules* **2011**, 44, 8709-8715.
30. Goto, A.; Ohtsuki, A.; Ohfuji, H.; Tanishima, M.; Kaji, H. *J. Am. Chem. Soc*. **2013**, 135,

11131-11139.
31. Wang, C.-G.; Chong, A. L. C.; Pan, H. M.; Sarkar, J.; Tay, X. T.; Goto, A. *Polym. Chem.* **2020**, 11, 5559-5571.
32. Zheng, J.; Wang, C.-G.; Yamaguchi, Y.; Miyamoto, M.; Goto, A. *Angew. Chem.* **2018**, 130, 1568-1572.
33. Zheng, J.; Chen, C.; Goto, A. *Angew. Chem.* **2020**, 132, 1957-1965.
34. Zheng, J.; Goto, A. *Polym. Chem.* **2021**, 11, 3987-3993.
35. Tanishima, M.; Goto, A.; Lei, L.; Ohtsuki, A.; Kaji, H.; Nomura, A.; Tsujii, Y.; Yamaguchi, Y.; Komatsu, H.; Miyamoto, M. *Polymers* **2014**, 6, 311-326.
36. Zheng, Y.; Sarkar, J.; Niino, H.; Chatani, S.; Hsu, S. Y.; Goto, A. *Polym. Chem.* **2021**.
37. Wang, C.-G.; Yong, H. W.; Goto, A. *ACS Appl. Mater. Interfaces* **2019**, 11, 14478-14484.
38. Chen, C.; Wang, C.-G.; Guan, W.; Goto, A. *Polym. Chem.* **2019**, 10, 5913-5919.
39. Sim, X. M.; Chen, C.; Goto, A. *ACS Appl. Mater. Interfaces* **2021**, 13, 24183-24193.
40. Chen, C.; Xiao, L.; Goto, A. *Macromolecules* **2016**, 49, 9425-9440.
41. Chen, C.; Wang, C.-G.; Xiao, L.; Goto, A. *Chem. Commun.* **2018**, 54, 13738-13741.
42. Sarkar, J.; Xiao, L.; Goto, A. *Macromolecules* **2016**, 49, 5033-5042.
43. Wang, C.-G.; Goto, A. *J. Am. Chem. Soc*. **2017**, 139, 10551-10560.
44. Xu, H.; Wang, C.-G.; Lu, Y.; Goto, A. *Macromolecules* **2019**, 52, 2156-2163.
45. Corrigan, N.; Rosli, D.; Jones, J. W. J.; Xu, J.; Boyer, C. *Macromolecules* **2016**, 49, 6779-6789.
46. Król, P.; Chmielarz, P. *Express Polymer Letters* **2013**, 7 (3), 249-260.
47. Zhang, L.; Cheng, Z.; Shi, S.; Li, Q.; Zhu, X. *Polymer* **2008**, 49, 3054-3059.
48. Dong, H.; Matyjaszewski, K. *Macromolecules* **2008**, 41, 6868-6870.
49. Kwak, Y.; Matyjaszewski, K. *Polym Int* **2009**, 58, 242-247.
50. Quirós-Montes, L.; Carriedo, G. A.; García-Álvarez, J.; Soto, A. P. *Green Chem.* **2019**, 21, 5865-5875.
51. Zhou, Y.; Wang, K.; Hu, D. *Scientific Reports* **2019**, 9, 9789.
52. Chapman, R.; Gormley, A. J.; Herpoldt, K.-L.; Stevens, M. M. *Macromolecules* **2014**, 47, 8541-8547.
53. Wang, M.; Zhang, J.; Guerrero-Sanchez, C.; Schubert, U. S.; Feng, A.; Thang, S. H. *ACS Comb. Sci.* **2019**, 21, 643-649.
54. Xu, J.; Jung, K.; Atme, A.; Shanmugam, S.; Boyer, C. *J. Am. Chem. Soc.* **2014**, 136, 5508-5519.
55. Shanmugam, S.; Xu, J.; Boyer, C. *J. Am. Chem. Soc.* **2015**, 137, 9174-9185.
56. Wang, Q.; Fu, S.; Yu, T. *Prog. Polym. Sci.* **1994**, 19,703-753.
57. Kemmere, M. F.; Meuldijk, J.; Drinkenburg, A. A. H.; German, A. L. *Polymer Reaction Engineering* **2000**, 8 (3), 271-297.
58. Zhang, Y.; Dubé, M. A., Chapter 3 Green Emulsion Polymerization Technology. In *Polymer Reaction Engineering of Dispersed Systems Springer*, Springer, Cham: **2017**; pp 65-100.
59. Zetterlund, P. B.; Kagawa, Y.; Okubo, M. *Chem. Rev.* **2008**, 108, 3747-3794.
60. Morton, M. *Journal of Macromolecular Science-Chemistry* **1981**, 15 (7), 1289-1302.
61. Eknoian, M. W.; Worley, S. D.; Bickert, J.; Williams, J. F. *Polymer* **1999**, 40, 1367-1371.
62. Huynh, V. T.; Nguyen, D.; Such, C. H.; Hawkett, B. S. *J. Polym. Sci. Part A: Polym. Chem.* **2015**, 53, 1413-1421.
63. Jovanović, R.; Dubé, M. A. *Journal of Macromolecular Science, Part C: Polymer Reviews* **2004**, 44 (1), 1-51.
64. Mabrouk, A. B.; Dufresne, A.; Boufi, S. *Carbohydrate Polymers* **2020**, 229, 115504.
65. Sanyal, S.; Huang, H.-C.; Rege, K.; Dai, L. L. *Journal of Nanomedicine and Nanotechnology* **2011**, 2 (7).

66. Yadav, H. K. S.; AI Halabi, N. A.; Alsalloum, G. A. *J. Pharm. Pharm. Res* **2017**, 1 (5).
67. Martín-Fabiani, K.; de la Haye, J. L.; Schulz, M.; Liu, Y.; Lee, M.; Duffy, B.; D'Agosto, F.; Lansalot, M.; Keddie, J. L. *ACS Appl. Mater. Interfaces* **2018**, 10, 11221-11232.
68. Bon, S. A. F.; Bosveld, M.; Klumperman, B.; German, A. L. *Macromolecules* **1997**, 30, 324-326.
69. Nicolas, J.; Charleux, B.; Guerret, O.; Magnet, S. *Angew. Chem. Int. Ed.* **2004**, 43, 6186-6189.
70. Nicolas, J.; Charleux, B.; Guerret, O.; Magnet, S. *Macromolecules* **2005**, 38, 9963-9973.
71. Qiu, J.; Gaynor, S. G.; Matyjaszewski, K. *Macromolecules* **1999**, 32, 2872-2875.
72. Cheng, C.; Shu, J.; Gong, S.; Shen, L.; Qiao, Y.; Fu, C. *New J. Chem.* **2010**, 34, 163-170.
73. Surmacz, K.; Chmielarz, P. *Materials* **2020**, 13, 1717.
74. Ferguson, C. J.; Hughes, R. J.; Nguyen, D.; Pham, B. T. T.; Gilbert, R. G.; Serelis, A. K.; Such, C. H.; Hawkett, B. S. *Macromolecules* **2005**, 38, 2191-2204.
75. Monteiro, M. J.; Hodgson, M.; Brouwer, H. D. *J. Polym. Sci. Part A: Polym. Chem.* **2000**, 38, 3864-3874.
76. Zhou, J.; Yao, H.; Ma, J. *Polym. Chem.* **2018**, 9, 2532-2561.
77. Lansalot, M.; Davis, T. P.; Heuts, J. P. A. *Macromolecules* **2002**, 35, 7582-7591.
78. Butté, A.; Storti, G.; Morbidelli, M. *Macromolecules* **2000**, 33, 3485-3487.
79. Prescott, S. W.; Ballard, M. J.; Rizzardo, E.; Gilbert, R. G. *Macromolecules* **2002**, 35, 5417-5425.
80. Liu, C.; Hong, C.-Y.; Pan, C.-Y. *Polym. Chem.* **2020**, 11, 3673-3689.
81. Ferguson, C. J.; Hughes, R. J.; Pham, B. T. T.; Hawkett, B. S.; Gilbert, R. G.; Serelis, A. K.; Such, C. H. *Macromolecules* **2002**, 35, 9243-9245.
82. Khor, S. Y.; Truong, N. P.; Quinn, J. F.; Whittaker, M. R.; Davis, T. P.; *ACS Macro Lett.* **2017**, 6, 1013-1019.
83. Guimarães, T. R.; Bong, Y. L.; Thompson, S. W.; Moad, G.; Perrier, S.; Zetterlund, P. B. *Polym. Chem.* **2021**, 12, 122-133.
84. Qiao, X. G.; Lambert, O.; Taveau, J.-C.; Dugas, P.-Y.; Charleux, B.; Lansalot, M.; Bourgeat-Lami, E. *Macromolecules* **2017**, 50, 3796-3806.
85. Fang, J.; Gao, X.; Luo, Y. *Polymer* **2020**, 201, 122602.
86. Subramaniam, M., Chapter 1 Introduction: Water Crisis. In *Contesting Water Rights*, Palgrave Macmillan, Cham: **2018**; pp 1-23.
87. Prihasto, N.; Liu, Q.-F.; Kim, S.-H. *Desalination* **2009**, 249, 308-316.
88. Qasim, M.; Badrelzaman, M.; Darwish, N. N.; Darwish, N. A.; Hilal, N. *Desalination* **2019**, 459, 59-104.
89. Anis, S. F.; Hashaikeh, R.; Hilal, N. *Desalination* **2019**, 452, 159-195.
90. Goh, P. S.; Lau, W. J.; Othman, M. H. D.; Ismail, A. F. *Desalination* **2018**, 425, 130-155.
91. Sim, L. N.; Chong, T. H.; Taheri, A. H.; Sim, S. T. V.; Lai, L.; Krantz, W. B.; Fane, A. G. *Desalination* **2018**, 434, 169-188.
92. Shahkaramipour, N.; Tran, T. N.; Ramanan, S.; Lin, H. *Membranes* **2017**, 7 (1), 13.
93. Rana, D.; Matsuura, T. *Chem. Rev.* **2010,** 110, 2448-2471.
94. Choudhury, R. R.; Gohil, J. M.; Mohanty, S.; Nayak, S. K. *J. Mater. Chem. A* **2018**, 6, 313-333.
95. Sun, W.; Liu, J.; Chu, H.; Dong, B. *Membranes* **2013**, 3, 226-241.

Chapter 2. Carboxylate, Nitrate, Sulfonate, and Phosphate Catalysts for Living Radical Polymerization via Oxygen−Iodine Halogen Bonding Catalysis

Abstract.

Four families of oxyanions, i.e., carboxylate, nitrate, phosphate, and sulfonate, were studied as novel catalysts in living (or reversible deactivation) racial polymerization via oxygen-iodine halogen bonding catalysis. Oxyanions with sodium and tetraalkylammonium counter-cations exhibited good catalytic activities as well as high solubilities in hydrophilic and hydrophobic monomers. These oxyanion catalysts were amenable to methyl methacrylate, functional methacrylates, styrene, and acrylonitrile, and also afforded block copolymers with low dispersities. The catalytic activities of the oxyanions were also theoretically studied using density functional theory (DFT) calculation. The studied four families of oxyanions are abundant in natural and synthetic compounds. Non-toxic natural carboxylates were successfully used to synthesize well-defined biocompatible polymers. The low cost, low toxicity, and accessibility to a range of polymer designs are attractive features for practical use.

2.1. Introduction.

Halogen bonding is a noncovalent attractive interaction between an electron-accepting halogen (X) and an electron-donating group (B). Halogen bonding generates a directional 180° interaction (R–X···B), and the strength of halogen bonding increases for heavier halogens, i.e., R–I > R–Br > R–Cl >> R–F. The B group can be anions and electro-donating neutral species such as halide anions and oxygen- and nitrogen-containing species.[1,2] A variety of halogen bonding donor-acceptor pairs have been found and applied in crystal engineering[3–5] and molecular recognition.[6–8] Recently, solution-phase halogen-bonding-promoted organocatalysis has attracted emerging attention in organic synthesis and supramolecular chemistry.[9–11]

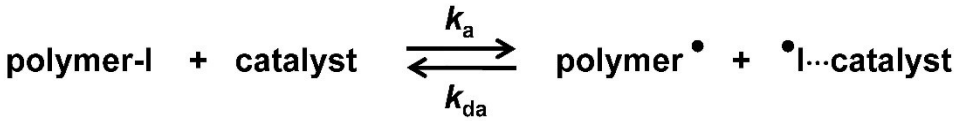

Scheme 2.1. Reversible activation in RCMP.

Living radical polymerization, also termed reversible-deactivation radical polymerization, is an effective method to synthesize well-defined polymers with predictable molecular weights and narrow molecular weight distributions.[12–17] Our research group developed an organocatalyzed living radical polymerization using an alkyl iodide (R–I) as an initiator and an organic molecule as a catalyst.[18–26] Mechanistically, the dormant polymer–iodide (polymer–I) and the catalyst are supposed to form a halogen-bonding complex (polymer–I···catalyst). The complex subsequently reversibly generates the propagating radical (polymer•) (Scheme 2.1). We term this polymerization reversible complexation mediated polymerization (RCMP). RCMP is attractive because no special capping agents or metals are required while it is amenable to a wide range of monomers and polymer structures. Several effective catalysts such as iodide (I^-) and pseudo-halide anions have been utilized in RCMP.[19,21] Recently, we reported that pyridine *N*-oxide ($C_5H_5N^+–O^-$) derivatives worked as

efficient catalysts.[27] The use of oxygen-centered anions (O^{-}) opened a new avenue in the catalyst development in RCMP. However, the rigid aromatic structure and multi-step synthesis of pyridine *N*-oxide derivatives limited practical applications.

An oxyanion is generally described as a polyatomic anion with the chemical formula $[E_xO_y]^{z-}$, where E is an element and O is oxygen. E can be various elements and bonds to one or more oxygen atoms to form functional oxyanions such as carboxylate (E = C, x = 1, y = 2, and z = 1), nitrate (E = N, x = 1, y = 3, and z = 1), sulfonate (E = S, x = 1, y = 3, and z = 1 or 2) and phosphate (E = P, x = 1, y = 4, and z = 1, 2 or 3). Oxyanions are widely witnessed in natural and synthetic compounds such as enzymes, lipids, drugs, and surfactants for biomedical and industrial applications.[28–30] While the halogen bonding of oxyanions such as carboxylates and sulfates has been used in crystal engineering, little attention has been paid to their use in halogen bonding catalysis (catalytic reactions). Poli et al. recently reported the use of several oxyanions (or oxygen-centered anions) including carbonates, bicarbonates, sulphates, bisulphates, and nitrates as catalysts in atom transfer radical polymerization with ethyl α-bromophenylacetate as an initiator. While a comprehensive and elegant study was performed, the weak halogen bonding interaction between the alkyl bromide and oxyanions led to relatively low monomer conversions (up to 37.5% conversion) and relatively large polydispersity indexes ($Đ \geq 1.34$), where $Đ$ is M_w/M_n, and M_n and M_w are the number-average and weight-average molecular weights, respectively.[31]

Herein, we report the use of carboxylates, nitrates, sulfonates, and a phosphate as RCMP oxyanion catalysts combined with an alkyl iodide initiator (not an alkyl bromide initiator). Unlike pyridine *N*-oxide derivatives, these oxyanion families enable a diverse molecular design because of their simple structures and abundance in natural, biological, and synthetic chemistries. These oxyanion catalysts were amenable to a broad range of monomers including methyl methacrylate, functional methacrylates, styrene, and acrylonitrile, which is

advantageous over the previous pyridine *N*-oxide catalysts. Such wide scopes in catalyst structures and amenable monomers are attractive features. The catalytic activities of the oxyanion catalysts were also theoretically studied via density functional theory (DFT) calculation. Figure 2.1 shows the studied alkyl iodide initiator, oxyanion catalysts, and ethers to dissolve the catalysts. Block copolymers with hydrophobic and hydrophilic segments were also successfully synthesized using the oxyanion catalysts.

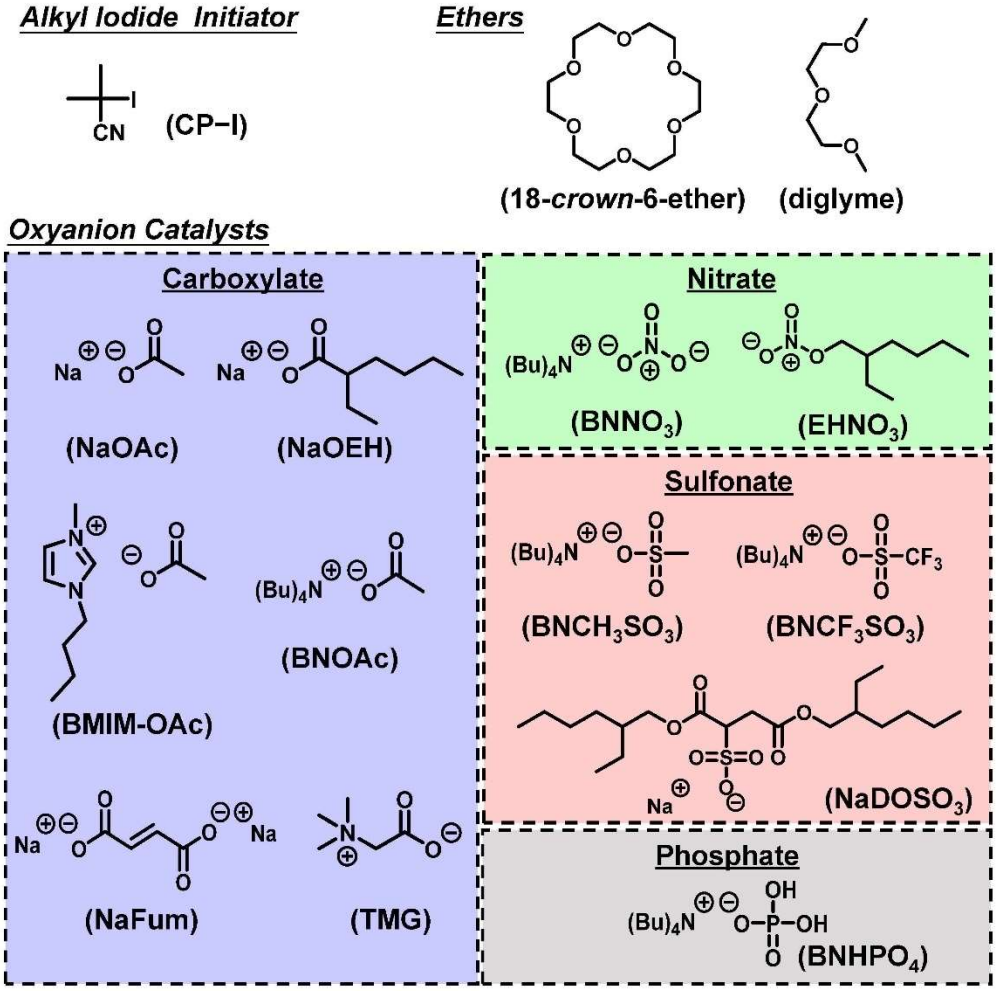

Figure 2.1. Structures of the alkyl iodide, ethers, and oxyanion catalysts used in this work.

2.2. Results and Discussion.

Experimental proof of the generation of R• from R–I.

A radical trap experiment[19,32] was carried out to prove the generation of an alkyl radical (R•) from an alkyl iodide using oxyanions. We heated 2-iodo-2-methylpropionitrile (CP–I (Figure 2.1), 40 mM) (alkyl iodide), sodium acetate (NaOAc, 80 mM) or tetrabutylammonium acetate (BNOAc, 40 mM) (catalyst), and 2,2,6,6-tetramethylpiperidinyl-1-oxy (TEMPO) (80 mM) (radical trap) in a mixture of toluene-d_8 (90%) and acetonitrile-d_3 (10%) at 70 °C for 8 h. We used 18-*crown*-6-ether (80 mM) to dissolve NaOAc. BNOAc is a metal-free organic acetate and was highly soluble in the studied solvent without the crown ether. The mixture of toluene-d_8 (dielectric constant ε = 2.4) and acetonitrile-d_3 (ε = 37.5) is a model of methyl methacrylate (MMA) medium (ε = 7.9). If CP–I generates CP radical (CP•) in the presence of the acetates, CP• is trapped by TEMPO to form CP–TEMPO. Figure 2.2 shows the ^{1}H NMR spectra of pure CP–I and the reaction mixtures after 8 h. The signals (peaks *a'*, *b'* and *c'*) of CP–TEMPO was observed after the 8 h reaction (Figure 2.2b and 2.2c), proving the radical generation from CP–I via the catalytic work of the acetates. The conversion of CP–I to CP–TEMPO was 92% and 49% with NaOAc and BNOAc, respectively. The acetate anions are weak bases, and the basicity can bring about the elimination of HI from CP–I as a side reaction. In the case of NaOAc, only 3% of the elimination product (methacrylonitrile) was generated for 8 h. On the other hand, BNOAc promoted the elimination and gave methacrylonitrile in 51% for 8 h. The results clearly demonstrate the generation of R• from R–I with both acetate catalysts and also the occurrence of a rather significant side reaction (elimination) in the case of BNOAc, suggesting the importance of the choice of the counter cations. NaOAc efficiently catalyzed the radical generation with negligible elimination and should be more suitable to the polymerization catalyst. The elimination product (methacryonitrile), if any generated, may work as a co-monomer in the polymerization. However, the amount of the methactylonitrile

generated during the polymerization would be very small, and the incorporation of methacryronitrile in the obtained polymers may be negligible.

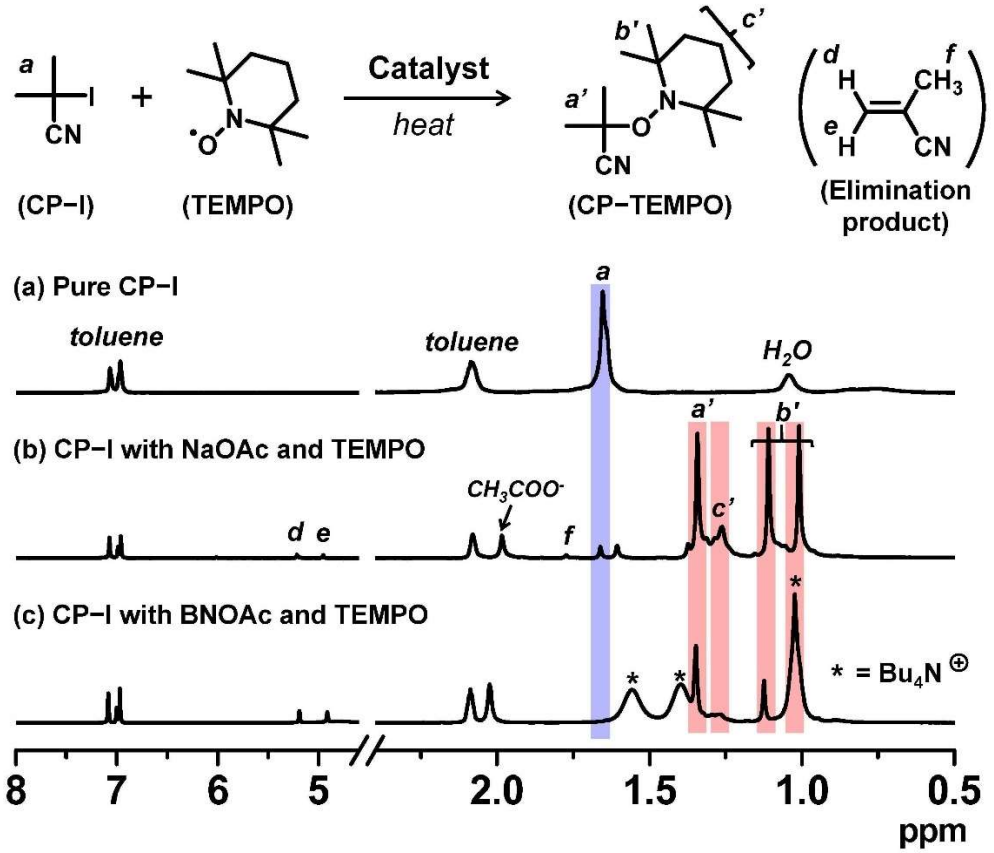

Figure 2.2. ^{1}H NMR spectra (in the range of 0.5–8.0 ppm) of (a) pure CP–I, (b) the solution of CP–I (40 mM), NaOAc (80 mM), 18-*crown*-6-ether (80 mM), and TEMPO (80 mM) heated at 70 °C for 8 h, and (c) the solution of CP–I (40 mM), BNOAc (40 mM), and TEMPO (80 mM) heated at 70 °C for 8 h. The solvent was a mixture of toluene-d_8 and acetonitrile-d_3 (v/v = 9/1).

Table 2.1. Polymerizations of MMA with Oxyanion Catalysts.

entry	Target DP[a]	catalyst	$[MMA]_0/[CP–I]_0/[catalyst]_0/[18\text{-}crown\text{-}6\text{-}ether]_0/[I_2]_0$ (mM)	T (°C)	t (h)	conv (%)	M_n ($M_{n,theo}$[b])	$Đ$
1	100	NaOAc	8000/80/80/80/0	70	10	80	7500 (8000)	1.14
2	100	None	8000/80/0/80/0	70	10	No polymerization		
3	100	NaOAc	8000/80/80/0/0	70	10	No polymerization		
4	100	NaOEH	8000/80/80/80/0	70	3	75	10000 (7500)	1.21
5	100	NaOEH	8000/80/80/80/5	70	8	80	8800 (8000)	1.19
6	200	NaOEH	8000/40/40/40/5	70	8	80	21000 (16000)	1.15
7	400	NaOEH	8000/20/20/20/5	70	24	81	30000 (32000)	1.38
8	100	BMIM-OAc	8000/80/80/0/0[c]	70	8	78	8600 (7800)	1.30
9	100	BNOAc	8000/80/80/0/5	70	6	72	14300 (7200)	1.24
10	100	$BNNO_3$	8000/80/80/0/5	70	8	79	8400 (7900)	1.22
11	100	$EHNO_3$	8000/80/80/0/0	70	24	No polymerization		
12	100	$BNCH_3SO_3$	8000/80/80/0/5	70	24	75	7800 (7500)	1.28
13	100	$BNCF_3SO_3$	8000/80/80/0/5	70	24	No polymerization		
14	100	$BNHPO_4$	8000/80/80/0/5	70	6	82	10500 (8200)	1.20
15	100	NaFum	8000/80/40/80/4	70	24	67	7400 (6700)	1.37

[a]Target degree of polymerization at 100% monomer conversion (calculated by $[MMA]_0/[CP–I]_0$). [b]Theoretical M_n calculated with $[MMA]_0$, $[CP–I]_0$, and monomer conversion. [c]The addition of 10wt% 1-butanol (MMA/1-butanol = 9/1 (w/w).

Polymerizations of MMA with Carboxylate Catalysts.

We studied the bulk polymerizations of MMA using an R–I initiator and oxyanion catalysts, i.e., carboxylates, nitrates, sulfonates, and a phosphate with a wide range of different molecular structures (Figure 2.1). Figure 2.3, Figure 2.4 (circle), and Table 2.1 (entries 1, 3-9,

and 15) show the polymerization results using carboxylate catalysts. We heated a mixture of MMA (8 M), CP–I (80 mM) as an alkyl iodide initiator, NaOAc (80 mM) as a catalyst, and 18-*crown*-6-ether (80 mM) to dissolve the catalyst at 70 °C (Figure 2.3 (circle) and Table 2.1 (entry 1)). An induction period (Figure 2.3a (circle)) was observed in the first 4 h due to a slow dissolution of NaOAc in MMA. (NaOAc was similarly or slightly better dissolved in a toluene-d_8/acetonitrile-d_3 (v/v = 9/1) mixture in the radical trap experiment mentioned above.) Not only the initiation (from the initiating alkyl iodide dormant species) but also the propagation (monomer consumption) was slow. Therefore, chain growth in the induction period would be negligible. This would be the reason why low-dispersity polymers were obtained even at relatively low monomer conversions. Subsequently, the polymerization proceeded up to an 80% monomer conversion in 10 h. The M_n value agreed with the theoretical value ($M_{n,theo}$), and the $Đ$ value was below 1.2 from an early stage of polymerization. No polymerization occurred without the addition of NaOAc or 18-*crown*-6-ether (Table 2.1 (entries 2 and 3)), meaning that the NaOAc dissolved by the crown ether worked as a catalyst.

For a better solubility of the catalyst, we used sodium 2-ethylhexanoate (NaOEH) bearing a 2-ethylhexyl group together with 18-*crown*-6-ether (Figure 2.3 (filled square) and Table 2.1 (entry 4). NaOEH brought no induction period because of the good solubility and hence led to a faster polymerization, reaching a 75% monomer conversion in 3 h. The M_n linearly increased with the monomer conversion but deviated from the $M_{n,theo}$, probably because NaOEH is a highly active catalyst to rapidly generate a large amount of alkyl radicals from alkyl iodides, where the termination among short oligomer radicals significantly took place at an early stage of polymerization (until a sufficient amount of deactivator is accumulated). The generated low-molar-mass terminated species were not counted as polymers in the GPC analysis. In order to suppress the termination, we added a small amount of deactivator, i.e., molecular iodine (I_2) so that the generated alkyl radical can smoothly be capped with iodide to

generate the dormant species. With the addition of I_2 (5 mM), the M_n agreed with the $M_{n,theo}$ and the $Đ$ value was below 1.2 from an early stage of polymerization (Figure 2.3 (open square) and Table 2.1 (entry 5)). The high catalytic activity of NaOEH also allowed the synthesis of higher molecular weight polymers with M_n = 21000–30000 and $Đ$ = 1.15–1.38 (Table 2.1 (entries 6 and 7)). These results demonstrate the effectiveness of the NaOEH catalyst.

As completely metal-free (sodium-free) catalysts, we also used 1-butyl-3-methylimidazolium acetate (BMIM-OAc) (Figure 2.3 (triangle) and Table 2.1 (entry 8)) and BNOAc (Figure 2.4 (circle) and Table 2.1 (entry 9)) and obtained polymers with $Đ$ = 1.24–1.30. 1-Butanol (10wt%) was added to dissolve BMIM-OAc in MMA. Both catalysts are sodium-free and did not require the crown ether for the dissolution. However, the M_n deviated from the $M_{n,theo}$. Unlike NaOEH, the deviation was observed even in the presence of I_2 (deactivator) for both catalysts, probably because the deviation is attributed to the HI elimination (side reaction) from CP–I (and short polymer–I), as was observed in the radical trapping experiment in the case of BNOAc (Figure 2.2c). In general, a higher basicity (a higher nucleophilicity) leads to a stronger halogen bonding and is beneficial to promote the halogen bonding catalysis. However, too high basicity leads to significant elimination as a competitive side reaction. While the ion pair (carboxylate anion and counter cation) is fully dissociated in aqueous solutions, it tends to associate in organic solutions. In the MMA medium, because of this association, the basicity may differ for Na and organic carboxylates. A possible reason why the elimination was insignificant and significant for Na and organic carboxylates, respectively, would be their different basicity in MMA, although the exact mechanism is unclear at the moment.

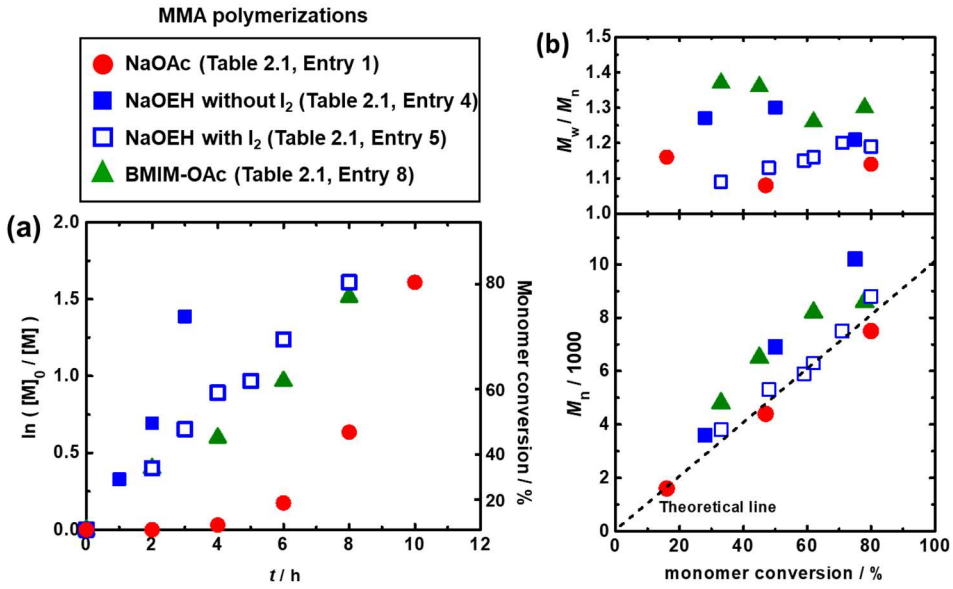

Figure 2.3. Plots of (a) ln([M]$_0$/[M]) vs t and (b) M_n and M_w/M_n vs conversion for the MMA/CP–I/catalyst/I_2 systems (70 °C): [MMA]$_0$ = 8 M; [CP–I]$_0$ = 80 mM; [Catalyst]$_0$ = 80 mM; [I_2]$_0$ = 0 or 5 mM. 18-*crown*-6-ether (80 mM) was added to NaOAc and NaOEH systems. The symbols are indicated in the figure.

Nitrate, Sulfonate and Phosphate Catalysts.

A nitrate has a similarity to a carboxylate in the isoelectronic structures of $O{=}N^{+}{-}O^{-}$ and $O{=}C{-}O^{-}$. However, a nitrate (NO_3^-) is more conjugated than a carboxylate (CO_2^-) (Figure 2.1). Because of the delocalization of the electron, a nitrate is less basic and may suppress the elimination. Figure 2.4 (square) and Table 2.1 (entry 10) show the result using tetrabutylammonium nitrate ($BNNO_3$) as a catalyst. $BNNO_3$ is organic and is also highly soluble in MMA. Unlike BNOAc (carboxylate), $BNNO_3$ (nitrate) led to a good agreement of M_n with $M_{n,theo}$, suggesting the suppression of the elimination. $BNNO_3$ is a bimolecular pair of the cationic BN^+ and anionic NO_3^- ions. An electrically neutral single molecular nitrate ester, i.e., 2-ethylhexyl nitrate ($EHNO_3$), showed a weak catalytic ability and resulted in no polymerization after 24 h (Table 2.1 (entry 11)).

A sulfonate (RSO_3^-) anion is another EO_3^- type anion structurally similar to NO_3^-. Similar to $BNNO_3$, tetrabutylammonium methanesulfonate ($BNCH_3SO_3$) worked as an efficient catalyst and afforded a good agreement of M_n with $M_{n,theo}$ and low $Đ$ values ($\leq$ 1.28)

(Figure 2.4 (triangle) and Table 2.1 (entry 12)), suggesting a minor occurrence of the elimination. In contrast to the successful polymerization with the methyl sulfonate ($BNCH_3SO_3$), no polymerization took place with a trifluoromethanesulfonate (tetrabutylammonium trifluoromethanesulfonate ($BNCF_3SO_3$)) (Table 2.1 (entry 13)). The electron-withdrawing trifluoromethyl group decreases the basicity (nucleophilicity) of SO_3^- and hence suppresses the halogen bonding catalysis, giving no polymerization.

A phosphate (PO_4^-) anion forms a $(RO)_2PO_2^-$ structure. The resonance of PO_2^- is similar to that of a carboxylate (CO_2^-) and hence the basicity PO_4^- is relatively high. Therefore, the polymerization with tetrabutylammonium phosphate monobasic ($BNHPO_4$) led to a marked deviation of M_n from $M_{n,theo}$ due to the elimination (Figure 2.4 (hexagon) and Table 2.1 (entry 14)).

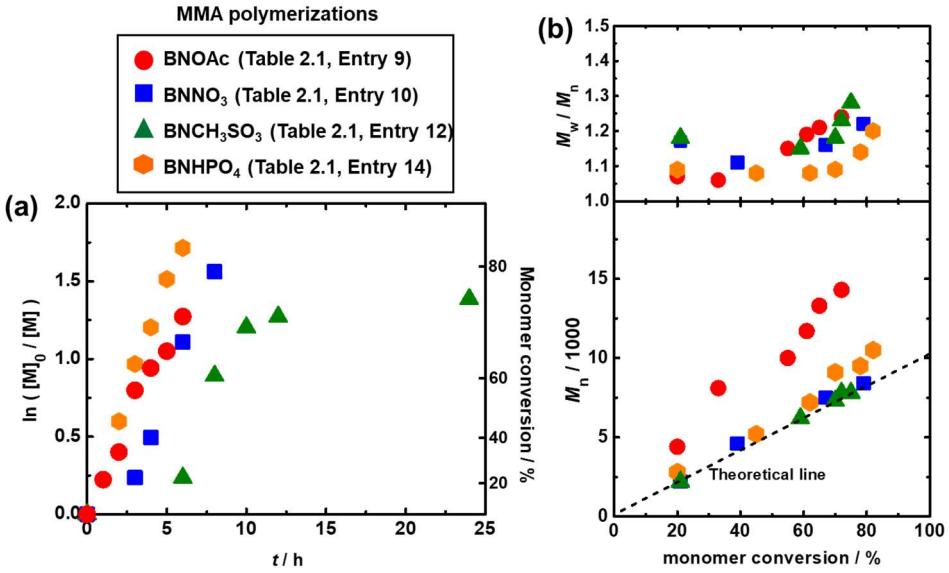

Figure 2.4. Plots of (a) $\ln([M]_0/[M])$ vs t and (b) M_n and M_w/M_n vs conversion for the MMA/CP−I/catalyst/I_2 systems (70 °C): $[MMA]_0 = 8$ M; $[CP-I]_0 = 80$ mM; $[Catalyst]_0 = 80$ mM; $[I_2]_0 = 5$ mM. The symbols are indicated in the figure.

As a whole, all the four families of oxyanions (carboxylate, nitrate, sulfonate, and phosphate) were effective for the halogen bonding catalysis and induced the polymerization.

The four families of oxyanions are abundant in natural and synthetic compounds with biological, enzymatic, and amphipathic functions. The low cost, low toxicity, and accessibility to broad molecular structures are attractive in practical use and future catalyst development. The basicity increases in the order of a sulfonate $CH_3SO_3^-$ (pK_b = 15.92) < a nitrate NO_3^- (15.30) < a phosphate PO_4^- (11.88) < a carboxylate AcO^- (9.24), where the pK_b values are those in aqueous solutions and can be viewed for qualitative comparison in the organic MMA medium. As mentioned, higher basicity (higher nucleophilicity) promotes the halogen bonding catalysis. However, the carboxylate and phosphate are too basic and brought about the elimination, losing the livingness in the polymerization, in the case of the organic (BN) counter cation. Importantly, the carboxylate with the Na counter cation (NaOEH) significantly suppressed the elimination (as observed in the radical trap experiment and will be demonstrated in the chain-end analysis shown below), leading to a good control of polymerization. In summary, among the studied oxyanions, sodium carboxylate (NaOEH) and BN nitrate ($BNNO_3$) are particularly useful catalysts with respect to their high polymerization rate and good livingness (regarding M_n and $Đ$ values).

Density functional theory (DFT) calculation was performed by Dr. Y. Lu to support the experimental results. Methyl 2-iodo-2-methylpropionate (MMA–I (Scheme 2.2)) was studied as a unimer model of poly(methyl methacrylate)-iodide (PMMA–I). We calculated the Gibbs free energy change (ΔG) from MMA–I and oxyanion (reactants) to the corresponding radicals (products) (Scheme 2.2). The ΔG value increased in the order of acetate (69.8 kJ/mol) < nitrate (96.1 kJ/mol) < dihydrogen phosphate (101.1 kJ/mol) < methanesulfonate (102.9 kJ/mol) in the bifurcated asymmetric form (Q form). These ΔG values are smaller than that for the most effective pyridine oxide catalyst (116.1 kJ/mol) previously reported,[27] suggesting the higher catalytic abilities of the studied oxyanions. Acetate has the lowest ΔG value (hence the highest catalytic activity), which is consistent with the strongest basicity among the four types of

oxyanions. The ΔG value was relatively small for nitrate. These results support the experimentally observed effectiveness of Na carboxylate (NaOEH) and BN nitrate ($BNNO_3$) as catalysts. Phosphate has a strong basicity (the second strongest basicity among the four oxyanions) but showed the second-largest ΔG value, probably because the basicity is not always proportional to the nucleophilicity that actually influences the halogen-bonding catalysis. The use of methanesulfonate ($BNCH_3SO_3$) exhibited a relative slow polymerization than the other three catalysts (Figure 2.4), which is consistent with the calculation result showing the largest ΔG value. Not only the bifurcated asymmetric form (Q form) but also the symmetric form (P form) was observed for acetate (ΔG = 81.9 kJ/mol) and nitrate (ΔG = 102.9 kJ/mol). However, the Q form gave smaller ΔG values than the P form, and hence the Q form process is more favourable. The P form was not found for dihydrogen phosphate and methanesulfonate. The mono-coordinate halogen-bonding (R form) of R–O$^{-}\cdots$I$^{\bullet}$ was not found in the DFT calculation, as also reported in the literature.[33,34]

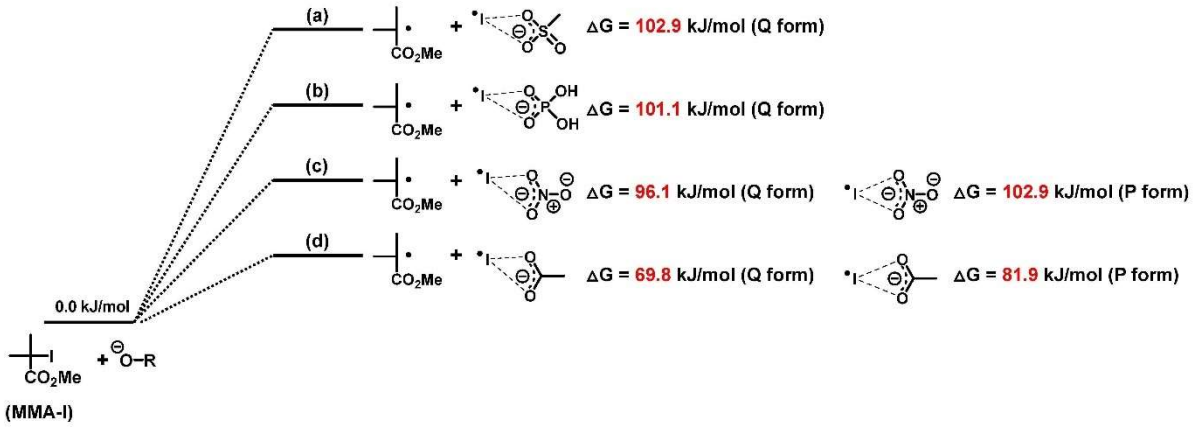

Scheme 2.2. Gibbs free energy change in reaction of MMA–I with (a) methanesulfonate, (b) dihydrogen Phosphate, (c) nitrate, and (d) acetate.

Increase in Polymerization Rate.

In order to suppress the elimination (side reaction), we decreased the polymerization temperature from 70 °C to 60 °C. The slowed polymerization caused by a decreased

temperature was overcome by the addition of a small amount of an azo initiator, i.e., 2,2'-azobis(2,4-dimethylvaleronitrile) (V65). Azo initiators are often used to decrease the deactivator concentration and hence effectively increase the polymerization rate in other living radical polymerizations.[35,36] As Figure 2.5 and Table 2.2 (entries 1-4) show, the addition of V65 (10 mM) maintained the high polymerization rate or even increased the polymerization rate at a lower temperature of 60 °C, reaching 80−90 % monomer conversions in 3−6 h, for the studied four families of oxyanions (NaOEH, $BNNO_3$, $BNCH_3SO_3$, and $BNHPO_4$). Importantly, $BNHPO_4$ afforded a good agreement of M_n with $M_{n,theo}$ at 60 °C (Figure 2.5 (hexagon)), successfully suppressing the elimination that was significant at the higher temperature of 70 °C (Figure 2.4 (hexagon)). It would be possible to reach 100% monomer conversion if the reaction is prolonged. However, the prolonged reaction was avoided in these particular studies (Table 2.2). This is because, in bulk polymerizations, the reaction mixtures will be solidified upon a full monomer conversion, which will cause difficulties in taking polymers from reactors (flasks) for characterizing the polymers.

Table 2.2. Polymerizations of MMA with V65.

entry	Target DP[a]	catalyst	$[MMA]_0/[CP-I]_0/[catalyst]_0/[V65]_0/[I_2]_0$ (mM)	T (°C)	t (h)	conv (%)	M_n ($M_{n,theo}$[b])	$Đ$
1	100	NaOEH	8000/80/80/10/5[c]	60	5	90	9300 (9000)	1.14
2	100	$BNNO_3$	8000/80/80/10/5	60	6	88	8800 (8800)	1.20
3	100	BNCH3SO3	8000/80/80/10/5	60	4	80	7600 (8000)	1.09
4	100	$BNHPO_4$	8000/80/80/10/5	60	3	88	11300 (8800)	1.20
5	100	NaFum	8000/80/40/10/2[c]	60	4	89	8400 (8900)	1.19
6	100	TMG	8000/80/80/10/2	60	6	90	9100 (9000)	1.24
7	100	$NaDOSO_3$	8000/80/80/10/0[c]	60	16	78	8400 (7800)	1.28

[a]Target degree of polymerization at 100% monomer conversion (calculated by $[MMA]_0/[CP-I]_0$). [b]Theoretical M_n calculated with $[MMA]_0$, $[CP-I]_0$, and monomer conversion. [c]The addition of 18-*crown*-6-ether (80 mM).

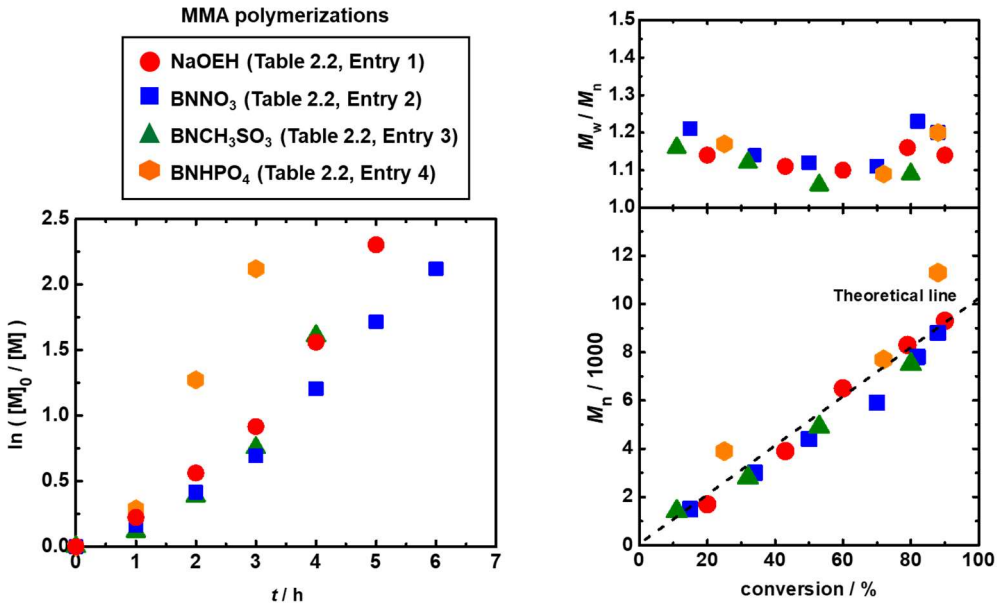

Figure 2.5. Plots of (a) ln([M]$_0$/[M]) vs t and (b) M_n and M_w/M_n vs conversion for the MMA/CP–I/catalyst/V65/I_2 systems (60 °C): [MMA]$_0$ = 8 M; [CP–I]$_0$ = 80 mM; [Catalyst]$_0$ = 80 mM; [V65]$_0$ = 10 mM; [I_2]$_0$ = 5 mM. The symbols are indicated in the figure.

Naturally Existing Oxyanions as Catalysts.

Naturally existing oxyanions were also used as the catalysts for the polymerization of MMA. Sodium fumarate (NaFum) and trimethylglycine (TMG, also known as glycine betaine) are naturally existing and non-toxic carboxylates that used as food additives.[37,38] NaFum showed a relatively slow polymerization rate in the absence of V65 (Table 2.1 (entry 15)). With a small amount of V65 (10 mM), NaFum and TMG yielded polymers at high monomer conversions (≥ 89%) and low $Đ$ values (≤ 1.24) in 6 h (Table 2.2 (entries 5 and 6)). Sodium dioctyl sulfosuccinate ($NaDOSO_3$) is a commercial laxative.[39] This alkyl sulfonate drug also worked as an efficient catalyst (Table 2.2 (entry 7)). (This part of the work is done by W. Faustinelie.)

Chain-end Fidelity.

We studied the iodide chain-end fidelity (livingness) of a PMMA synthesized with the NaOEH catalyst. The PMMA obtained after 2 h (monomer conversion = 33%) in Figure 2.3 (open square) was purified through the reprecipitation from hexane (non-solvent) and subsequently with preparative GPC (M_n = 4000 and $Đ$ = 1.14 after purification) and analyzed with a high-resolution ^{1}H NMR (500 MHz) (Figure 2.6). The signals of the methoxyl protons (*a*, *a'*, and *a''*) at the side chain appeared at 3.58–3.67 ppm. The main peak at 3.58–3.62 ppm was assigned to the repeating MMA units (*a*) in the middle of the chain. The downfield-shifted peak at 3.65–3.67 ppm was assigned to the ω-terminal chain-end unit (*a'*) adjacent to the chain-end iodide. The peak at 3.62–3.65 ppm was assigned to the α-terminal chain-end unit (*a''* adjacent to the initiating 2-methylpropionitrile (CP) group.) From the ^{1}H NMR peak area and the M_n (= 4000) determined by GPC, the fraction of the iodine chain end was calculated to be 94%, meaning a high iodide-chain-end fidelity. A small amount of dead polymers should be generated via radical-radical termination, because this polymerization is a radical polymerization. A minor elimination may also occur, as observed in the radical trap experiment

(3% elimination product at 70 °C for 8 h). This result clearly shows the good livingness (high iodide-chain-end fidelity) with the NaOEH catalyst. The obtained (purified) PMMA was used as a macroinitiator in the block copolymerizations shown below.

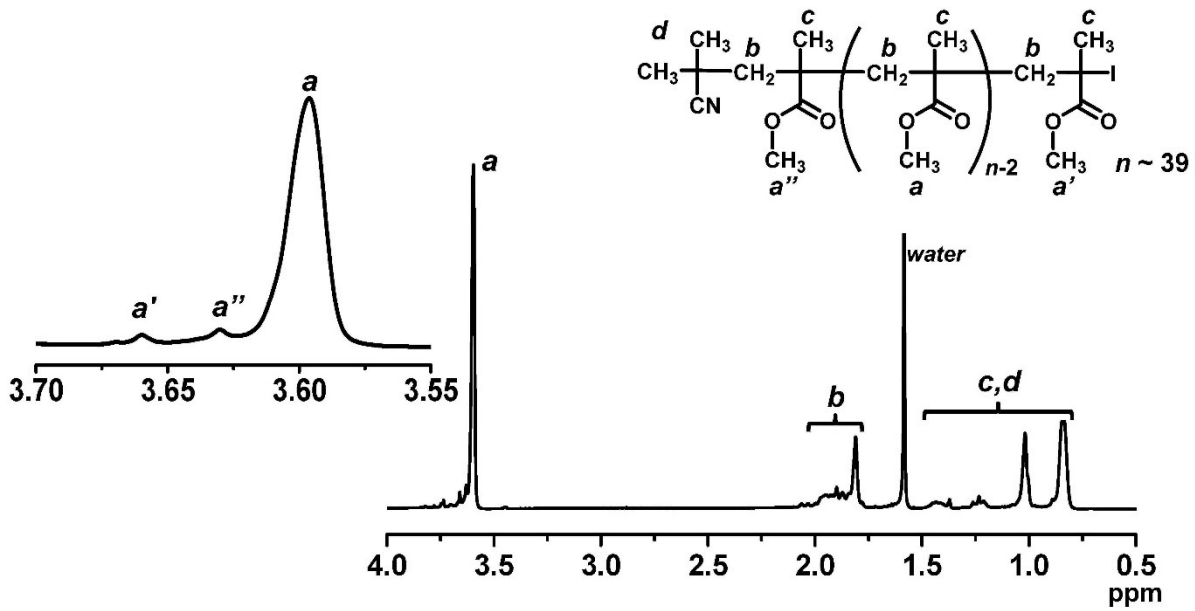

Figure 2.6. ^{1}H NMR spectrum ($CDCl_3$) of PMMA–I obtained with NaOEH (Figure 2.3 (open square) for 2 h) (M_n = 4000 and $Đ$ = 1.14 after purification).

Polymerizations of functional methacrylates, styrene and acrylonitrile.

The monomer scope encompassed functional methacrylates, styrene, and acrylonitrile. Table 2.3 (entries 1-8) summarizes the polymerizations of butyl methacrylate (BMA), benzyl methacrylate (BzMA), 2-methoxyethyl methacrylate (MEMA), 2-(dimethylamino)ethyl methacrylate (DMAEMA), di(ethylene glycol) methyl ether methacrylate (DEGMA), and poly(ethylene glycol)methyl ether methacrylate (PEGMA) using the NaOEH, NaFum and TMG carboxylate catalysts. Low-dispersity ($Đ$ = 1.14–1.24) polymers were obtained for the hydrophobic BMA, BzMA, and MEMA monomers with 70−80% monomer conversions at 70 °C for 4–12 h. A lower polymerization temperature (50 °C) was used for the hydrophilic DMAEMA, DEGMA, and PEGMA monomers in order to suppress the HI elimination from the polymer chain end. The HI elimination is promoted in polar conditions. For DMAEMA, DEGMA, and PEGMA, V65 was added to increase the polymerization rate at the lower

temperature (50 °C), yielding low-dispersity ($Đ$ = 1.28–1.40) polymers. Poly(di(ethylene glycol) methyl ether methacrylate) and poly(poly(ethylene glycol)methyl ether methacrylate) are biocompatible and may be used in biomedical materials.[40] The use of naturally existing non-toxic NaFum and TMG as polymerization catalysts offers an attractive route to synthesize well-defined biomedically useful polymers without the remaining toxic catalyst residues. Besides methacrylates, styrene and acrylonitrile were also successfully used. Table 2.3 (entries 9-14) shows the polymerizations of styrene and acrylonitrile using NaOEH (carboxylate), $BNNO_3$ (nitrate), and $BNCH_3SO_3$ (sulfonate) as catalysts, yielding low-dispersity ($Đ$ = 1.31–1.41) polymers. These results demonstrate the oxyanion catalysts are amenable to various monomer families and functional monomers. Oxyanion catalysts are amenable to styrene and acrylonitrile, which is another advantage compared to pyridine *N*-oxide catalysts, as pyridine *N*-oxide catalysts are not amenable to styrene and acrylonitrile.[27]

Table 2.3. Polymerizations of Methacrylates, Styrene, and Acrylonitrile with Oxyanion Catalysts.

entry	Monomer	Catalyst	Azo initiator	$[Monomer]_0/[CP–I]_0/[Catalyst]_0/[Azo\ initiator]_0$ (mM)	T (°C)	t (h)	Conv (%)	M_n[a] ($M_{n,theo}$[b])	$Đ$[a]
1	BMA	NaOEH	None	8000/80/80/0[e,f]	70	12	80	15000 (14000)	1.14
2	BzMA	NaOEH	None	8000/80/80/0[e]	70	8	70	14000 (12000)	1.24
3	MEMA	NaOEH	None	8000/80/80/0[e]	70	4	75	15000 (12000)	1.24
4	DMAEMA	NaOEH	V65	8000/80/80/20[e]	50	5	55	8100 (8600)	1.34
5	DEGMA	NaFum	V65	8000/80/40/40[e,f]	50	4	97	17000 (18000)	1.39
6	DEGMA	TMG	V65	8000/80/40/40[f]	50	4	81	15000 (15000)	1.34
7	PEGMA	NaOEH	V65	8000/80/80/10[e]	50	8	60	24000 (18000)	1.40
8	PEGMA	NaFum	V65	8000/80/40/40[e,f]	50	4	67	17000 (20000)	1.28
9	Styrene	NaOEH	AIBN	8000/80/80/30[c]	80	7	70	7000 (7300)	1.41
10	Styrene	$BNNO_3$	AIBN	8000/80/80/30	80	4	80	8400 (8300)	1.37
11	Styrene	$BNCH_3SO_3$	AIBN	8000/80/80/40	80	5	89	8700 (9200)	1.31
12	Acrylonitrile	NaOEH	AIBN	8000/80/160/10[d]	75	4	54	5000 (3000)	1.40
13	Acrylonitrile	$BNNO_3$	AIBN	8000/80/160/10[d]	75	2	57	8000 (3500)	1.34
14	Acrylonitrile	$BNCH_3SO_3$	AIBN	8000/80/160/10[d]	75	3	90	12000 (4800)	1.39

[a]PMMA-calibrated THF-GPC values for entries 1-3. Polystyrene-calibrated THF-GPC values for entries 9-11. PMMA-calibrated DMF-GPC values for entries 4-8 and 12-14. [b]Theoretical M_n calculated with $[Monomer]_0$, $[CP–I]_0$, and monomer conversion. [c]The addition of diglyme (25wt%). NaOEH was dissolved in this solution polymerization. [d]The addition of ethylene carbonate (EC) (50wt%). NaOEH was dissolved in this solution polymerization (entry 12). [e]The addition of 18-*crown*-6-ether (80 mM). [f]The addition of I_2 (2 mM).

Block Copolymerization.

Exploiting the living character, block polymerizations were performed using the NaOEH catalyst. We used the purified PMMA-iodide (PMMA–I) (M_n = 4000 and $Đ$ = 1.14) presented in Figure 2.6 as a macroinitiator. Diglyme was used as the solvent to dissolve NaOEH. The block polymerizations with BzMA, MEMA, and DMAEMA gave well-defined hydrophobic-hydrophobic and hydrophobic-hydrophilic block copolymers with low polydispersity (M_n = 11000–19000 and $Đ$ = 1.37–1.42) (Table 2.4). Figure 2.7 shows the GPC chromatograms before and after the block polymerization. In all cases, a large fraction of the

macroinitiator extended to the block copolymers, demonstrating the high block efficiency. The results show the accessibility to various block copolymers.

Table 2.4. Block Polymerizations from PMMA–I macroinitiator (M_n = 4000 and $Đ$ = 1.14).

Entry	Monomer	Target DP	$[Monomer]_0/[PMMA{-}I]_0/[NaOEH]_0/[V65]_0$ (mM)[a]	T (°C)	t (h)	Conv (%)[b]	M_n[c] ($M_{n,theo}$)[d]	$Đ$[c]
1	BzMA	100	8000/80/80/0	70	5	80	19000 (18000)	1.37
2	MEMA	100	8000/80/80/0	70	5	60	13000 (13000)	1.40
3	DMAEMA	100	8000/80/80/20	50	6	50	11000 (12000)	1.42

[a]The addition of diglyme (25wt% of diglyme and totally 75% of monomer and PMMA−I). [b]Calculated with ^{1}H NMR. [c]PMMA-calibrated THF-GPC values for entries 1 and 2. PMMA-calibrated DMF-GPC values for entry 3. [d]Theoretical M_n calculated with $[Monomer]_0$, $[PMMA{-}I]_0$, and monomer conversion.

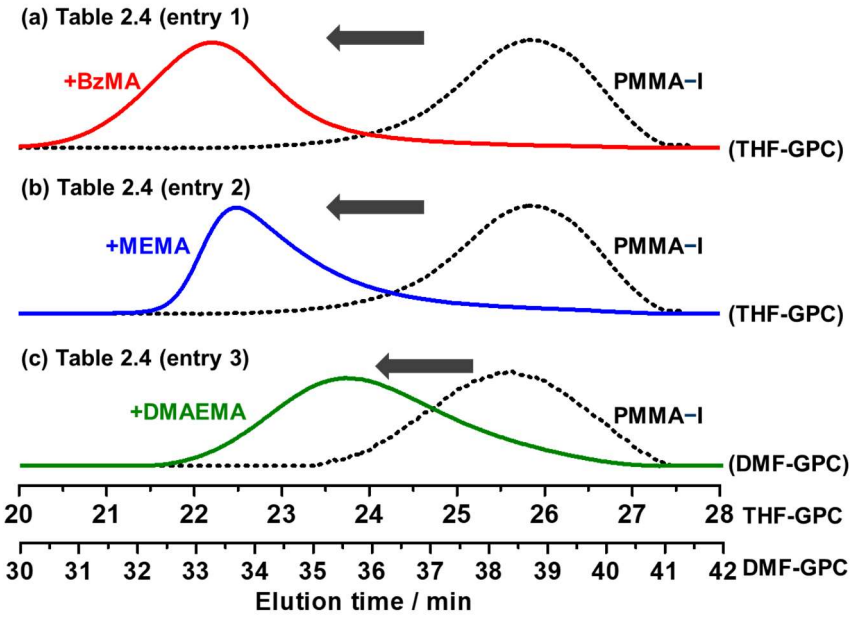

Figure 2.7. GPC chromatograms before (dashed lines) and after (solid lines) the block polymerizations in Table 2.4.

2.3. Conclusions.

The four families of oxyanions (carboxylate, nitrate, sulfonate, and phosphate) were effective for the halogen bonding catalysis and induced the polymerization. Among the studied catalysts, sodium carboxylate (NaOEH) and BN nitrate ($BNNO_3$) are particularly effective with negligible side reaction (elimination), keeping good livingness. Naturally existing non-toxic sodium fumarate (NaFum) and trimethylglycine (TMG) also successfully worked as catalysts. These catalysts were amenable to MMA, functional methacrylates, styrene, and acrylonitrile and also successfully yielded block copolymers. The four families of oxyanions are abundant in natural and synthetic compounds. The low cost, low toxicity, and accessibility to broad molecular structures are attractive features in practical use and future catalyst development. In addition, upon possible conversion of the carboxylic acids to the carboxylate anions in basic conditions, carboxylic acid-containing monomers may work as monomers and catalysts simultaneously and may lead self-catalyzed polymerizations. This is a fascinating perspective and will be studied in the future.

2.4. Experimental.

Materials.

Methyl methacrylate (MMA) (>99.8%, Tokyo Chemical Industry (TCI), Japan), butyl methacrylate (BMA) (>99.0%, TCI), benzyl methacrylate (BzMA) (>98.0%, TCI), 2-methoxyethyl methacrylate (MEMA) (>98.0%, TCI), poly(ethylene glycol) methyl ether methacrylate (PEGMA) (average molecular weight = 300) (98.0%, Sigma-Aldrich, USA), 2-(dimethylamino)ethyl methacrylate (DMAEMA) (>98.5%, TCI), di(ethylene glycol) methyl ether methacrylate (DEGMA) (95.0%. Sigma-Aldrich), styrene (>99.0%, TCI), acrylonitrile (>99%, Kanto Chemical, Japan), sodium acetate (NaOAc) (>98.5%, TCI), sodium 2-ethylhexanote (NaOEH) (>98.0%, TCI), 1-butyl-3-methylimidazolium acetate (BMIM-OAc) (>95.0%, Sigma-Aldrich), tetrabutylammonium acetate (BNOAc) (>90.0%, TCI), sodium fumarate (NaFum) (>99.0%, Sigma-Aldrich), trimethylglycine (TMG) (>97.0%, TCI), tetrabutylammonium methanesulfonate ($BNCH_3SO_3$) (≥97.0%, Sigma-Aldrich), tetrabutylammonium trifluoromethanesulfonate ($BNCF_3SO_3$) (>98.0%, TCI), dioctyl sulfosuccinate sodium salt ($NaDOSO_3$) (≥97%, Sigma-Aldrich), 2-ethylhexyl nitrate ($EHNO_3$) (97%, Sigma-Aldrich), tetrabutylammonium nitrate ($BNNO_3$) (97%, Sigma-Aldrich), tetrabutylammonium phosphate monobasic ($BNHPO_4$) (≥99.0%, Sigma-Aldrich), 2-iodo-2-methylpropionitrile (CP–I) (>96.0%, TCI), iodine (I_2) (>98.0%, TCI), diethylene glycol dimethyl ether (diglyme) (>99.0%, TCI), 18-*crown*-6-ether (>98.0%, TCI), 2,2′-azobis(2,4-dimethylvaleronitrile) (V65) (95%, Wako Pure Chemical, Japan), 2,2'-azobis(isobutyronitrile) (AIBN) (95%, Wako), 2,2,6,6-tetramethylpiperidine-1-oxyl (TEMPO) (≥98.0%, Sigma-Aldrich), 1-butanol (>99.0%, TCI), *N*,*N*-dimethylformamide (DMF) (>99.5%, Kanto Chemical), tetrahydrofuran (THF) (>99.5%, Kanto Chemical), and hexane (>99%, International Scientific, Singapore) were used as received.

Measurements.

The GPC analysis using THF as the eluent was performed on a Shimadzu LC-2030C Plus liquid chromatograph (Kyoto, Japan) equipped with both a Shodex KF-804L mixed gel column (300 × 8.0 mm; bead size = 7 μm; pore size = 1500 Å) and a Shodex LF-804 mixed gel column (300 × 8.0 mm; bead size = 6 μm; pore size = 3000 Å). The eluent was THF at a flow rate of 0.7 mL/min. Sample detection and quantification were conducted using a Shimadzu differential refractometer RID-20A. The column system was calibrated with standard poly(methyl methacrylate)s (PMMAs) and polystyrenes (PSts). The monomer conversion was determined from the GPC peak area for the polymerizations of MMA.

The GPC analysis using DMF as the eluent was performed on a Shimadzu LC-2030C Plus liquid chromatograph equipped with two Shodex LF-804 mixed gel columns. The eluent was DMF (containing LiBr (10 mM)) at a flow rate of 0.5 mL/min (40 °C). Sample detection was conducted using a Shimadzu differential refractometer RID-20A. The column system was calibrated with standard PMMAs.

The NMR spectra were recorded on Bruker (Germany) AV500 spectrometer (500 MHz) or AV 300 (300 MHz) at ambient temperature. $CDCl_3$, toluene-d_8, acetone-d_6, and acetonitrile-d_3 (Cambridge Isotope Laboratories, USA) were used as the solvents for the NMR analysis, and the chemical shift was calibrated using residual undeuterated solvents or tetramethylsilane (TMS) as the internal standard. The monomer conversion (except for the polymerization of MMA) and the monomer composition in the obtained copolymers were determined with ^{1}H NMR.

Polymers were purified with a preparative GPC (LC-9204, Japan Analytical Industry, Tokyo) equipped with JAIGEL 1H and 2H polystyrene gel columns (600×40 mm; bead size = 16 μm; pore size = 20-30 (1H) and 40-50 (2H) Å). Chloroform was used as the eluent at a flow rate of 14 mL/min (room temperature).

Radical trapping experiment.

A mixture of toluene-d_8 (0.9 mL), acetonitrile-d_3 (0.1 mL), CP–I (40 mM), sodium acetate or NaOAc (80 mM), 18-*crown*-6-ether (80 mM), and TEMPO (80 mM) was heated in a Schlenk flask at 70 °C for 8 h under argon atmosphere with magnetic stirring and subsequently cooled to room temperature. The mixtures before and after the heat treatment were analyzed by ^{1}H NMR. No 18-*crown*-6-ether was used in the cases of tetrabutylammonium salts (40 mM).

General procedure for polymerization.

In a typical run, a mixture of a monomer (1.5 g), an alkyl iodide initiator, and a catalyst was heated in a Schlenk flask at 50–80 °C under argon atmosphere with magnetic stirring. After a prescribed time *t*, an aliquot (0.1 mL) of the solution was taken out by a syringe, cooled to room temperature, and analyzed with GPC and ^{1}H NMR.

Synthesis of PMMA–I macroinitiator.

A mixture of MMA (3.0 g, 30 mmol), CP–I (58.4 mg, 0.3 mmol), NaOEH (49.8 mg, 0.3 mmol), and 18-*crown*-6-ether (79.2 mg, 0.3 mmol) was heated in a Schlenk flask at 70 °C for 2 h under an argon atmosphere with magnetic stirring. The mixture was cooled to room temperature and diluted with THF (10 mL). The polymer was purified by reprecipitation from hexane (200 mL) (non-solvent) and subsequently with preparative GPC. The polymer solution was evaporated and dried in vacuo to give PMMA–I (M_n = 4000 and $Đ$ = 1.14, monomer conversion = 33%) as a yellow solid. The PMMA–I was used as a macroinitiator for the block copolymerizations.

Block polymerizations.

In a typical run, a mixture of monomer (1.0 g), the PMMA–I macroinitiator, NaOEH (catalyst), V65 (azo initiator), and diglyme (solvent) was heated in a Schlenk flask at 70 °C

under argon atmosphere with magnetic stirring. After cooling to room temperature, the solution was analyzed with GPC and ^{1}H NMR.

Density Functional Theory (DFT) Calculation.

All calculations were performed by Dr. Y. Lu with Gaussian 09 (Rev. E.01) programs. Geometry optimization was conducted by M062X functional.[2] The Def2-TZVPP set was employed for all atoms and pseudo potential was used for iodine atom.[3] Vibrational frequency calculations were performed on all the optimized geometry both to validate they are the stable geometry and to calculate zero-point energy (ZPE) values.

References.

1. Politzer, P.; Lane, P.; Concha, M. C.; Ma, Y.; Murray, J. S. *J. Mol. Model.* **2007**, 13, 305-311.
2. Cavallo, G.; Metrangolo, P.; Milani, R.; Pilati, T.; Priimagi, A.; Resnati, G.; Terraneo, G. *Chem. Rev.* **2016**, 116, 2478-2601.
3. Mukherjee, A.; Tothadi, S.; Desiraju, G. R. *Acc. Chem. Res.* **2014**, 47, 2514-2524.
4. Christopherson, J.-C.; Topić, F.; Barrett, C. J.; Friščić, T. *Cryst. Growth Des.* **2018**, 18, 1245-1259.
5. Corpinot, M. K.; Bučar, D.-K. *Cryst. Growth Des.* **2019**, 19, 1426-1453.
6. Metrangolo, P.; Meyer, F.; Pilati, T.; Resnati, G.; Terraneo, G. *Angew. Chem. Int. Ed.* **2008**, 47, 6114-6127.
7. Gilday, L. C.; Robinson, S. W.; Barendt, T. A.; Langton, M. J.; Mullaney B. R.; Beer, P. D. *Chem. Rev.* **2015**, 115, 7118-7195.
8. Brown, A.; Beer, P. D. *Chem. Commun.* **2016**, 52, 8645-8658.
9. Beale, T. M.; Chudzinski, M. G.; Sarwar, M. G. Taylor, M. S. *Chem. Soc. Rev.* **2013**, 42, 1667-1680.
10. Bulfield, D.; Huber, S. M. *Chem. Eur. J.* **2016**, 22, 14434-14450.
11. Tepper, R.; Schubert, U. S. *Angew. Chem. Int. Ed.* **2018**, 57, 6004-6016.
12. Matyjaszewski, K. *Adv. Mater.* **2018**, 30, 1706441.
13. Nicolas, J.; Guillaneuf, Y.; Lefay, C.; Bertin, D.; Gigmes, D. Charleux, B. *Prog. Polym. Sci.* **2013**, 38, 63-235.
14. Keddie, D. J.; Moad, G.; Rizzardo, E.; Thang, S. H. *Macromolecules* **2012**, 45, 5321-5342.
15. Matyjaszewski, K.; Tsarevsky, N. V. *J. Am. Chem. Soc.* **2014**, 136, 6513-6533.
16. Discekici, E. H.; Anastasaki, A.; de Alaniz, J. R. Hawker, C. J. *Macromolecules* **2018**, 51, 7421-7434.
17. Ni, Y.; Zhang, L.; Cheng, Z.; Zhu, X. *Polym. Chem.* **2019**, 10, 2504-2515.
18. Goto, A.; Suzuki, T.; Ohfuji, H.; Tanishima, M.; Fukuda, T.; Tsujii, Y.; Kaji, H. *Macromolecules* **2011**, 44, 8709-8715.
19. Goto, A.; Ohtsuki, A.; Ohfuji, H.; Tanishima, M.; Kaji, H. *J. Am. Chem. Soc*. **2013**, 135, 11131-11139.
20. Ohtsuki, A.; Lei, L.; Tanishima, M.; Goto, A.; Kaji, H. *J. Am. Chem. Soc.* **2015**, 137, 5610-5617.
21. Wang, C.-G.; Goto, A. *J. Am. Chem. Soc*. **2017**, 139, 10551-10560.
22. Wang, C.-G.; Hanindita, F.; Goto, A. *ACS Macro Lett.* **2018**, 7, 263-268.
23. Zheng, J.; Wang, C.-G.; Yamaguchi, Y.; Miyamoto, M.; Goto, A. *Angew. Chem.* **2018**, 130, 1568-1572.
24. Wang, C.-G.; Chen, C.; Sakakibara, K.; Tsujii, Y.; Goto, A. *Angew. Chem. Int. Ed.* **2018**, 57, 13504-13508.
25. Liu, X.; Wang, C.-G.; Goto, A. *Angew. Chem. Int. Ed.* **2019**, 58, 5598-5603.
26. Wang, C.-G.; Oh, X. Y.; Liu, X.; Goto, A. *Macromolecules* **2019**, 52, 2712-2718.
27. Xu, H.; Wang, C.-G.; Lu, Y.; Goto, A. *Macromolecules* **2019**, 52, 2156-2163.
28. Gangolli, S. D.; van den Brandt, P. A.; Feron, V. J.; Janzowsky, C.; Koeman, J. H.; Speijers, G. J. A.; Spiegelhalder, B.; Walker, R.; Wishnok, J. S. *Eur. J. Pharmacol. Environ. Toxicol. Pharmacol. Sect.* **1994**, 292, 1-38.
29. Raghothama, K. G. *Annu. Rev. Plant Physiol. Plant Mol. Biol.* **1999**, 50, 665-693.
30. Czajka, A.; Hazell, G.; Eastoe, J. *Langmuir* **2015**, 31, 8205-8217.
31. Wang, J.; Han, J.; Peng, H.; Tang, X.; Zhu, J.; Liao, R.-Z.; Xie, X.; Xue, Z.; Fliedel, C.; Poli, R. *Polym. Chem.* **2019**, 10, 2376-2386. The data in Table 1 (entries 20-34) in this reference are related to oxyanion (oxygen-centered anion) catalysts.

32. Moad, G. Rizzardo, E. *Macromolecules* **1995**, 28, 8722-8728.
33. Saha, S.; Ganguly, S.; Desiraju, G. R. *Aust. J. Chem.* **2014**, 67, 1840-1848.
34. Tothadi, S.; Sanphui, P.; Desiraju, G. R. *Cryst. Growth Des.* **2014**, 14, 5293-5302.
35. Goto, A.; Fukuda, T. *Prog. Polym. Sci.* **2004**, 29, 329-385.
36. Fischer, H. *Chem. Rev.* **2001**, 101, 3581-3610.
37. Das, R. K.; Brar, S. K.; Verma, M. *Pharmacol. Rep.* **2016**, 68, 404-414.
38. de Zwart, F. J.; Slow, S.; Payne, R. J.; Lever, M.; George, P. M.; Gerrard, J. A.; Chambers, S. T. *Food Chemistry* **2003**, 83, 197-204.
39. Donowitz, M.; Binder, H. J. *Gastroenterology* **1975**, 69, 941-950.
40. Lutz, F. *J. Polym. Sci. Pol. Chem.* **2008**, 46, 3459-3470.

Chapter 3. Development of Air-tolerant RCMP System.

Abstract.

Air-tolerant reversible complexation mediated polymerization (RCMP) was explored. The system contained a monomer, an alkyl iodide initiating dormant species, air (oxygen), an aldehyde, *N*-hydroxyphthalimide (NHPI), and an amine. The aldehyde (RCHO) was converted to a carboxylate anion ($RCOO^-$) in the presence of the amine. $RCOO^-$ worked as an RCMP catalyst. As a result, the system does not require deoxygenation before the polymerization; namely, oxygen was in situ consumed in the mentioned sequence of reactions, and after the consumption of oxygen, the polymerization started with monomer, an alkyl iodide dormant species, and an $RCOO^-$ catalyst. The proof of concept and an attempt to speed up the polymerization with the addition of an azo compound are described in this chapter. This air-tolerant RCMP method is also amenable to several methacrylates and styrene.

3.1 Introduction.

Living radical polymerization (LRP) can generate polymers with narrow molecular weight distributions, controlled architectures, and chain-end functionalities. Examples of LRP systems are atom transfer radical polymerization (ATRP), reversible addition-fragmentation chain transfer (RAFT) polymerization, and nitroxide-mediated radical polymerization (NMP).[1-3] Our research group developed an organocatalyzed living radical polymerization, which is termed as reversible complexation mediated polymerization (RCMP), using an alkyl iodide (R−I) as an initiator and an organic compound as a catalyst (Scheme 3.1). Mechanistically, the dormant species (Polymer–I) and the catalyst are supposed to form a halogen bonding complex (Polymer–I···catalyst), which subsequently reversibly generates the propagating radical (Polymer•) and the •I···catalyst complex.[4-5]

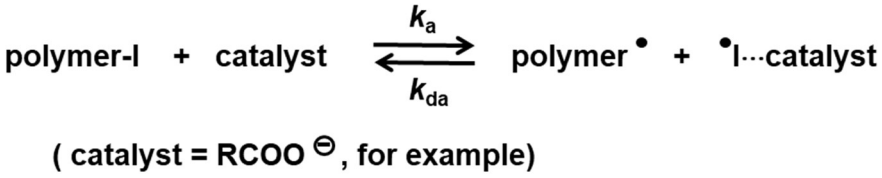

Scheme 3.1. Reversible Activation of RCMP.

A common concern in LRP is the adverse effect of air (oxygen). LRP is a radical polymerization, and oxygen works as an inhibitor of the polymerization. In ATRP, the transition metal catalysts are sensitive to oxygen. The activator catalysts (such as copper (I) complexes) are oxidized to the deactivator catalysts (such as copper (II) complexes), thereby slowing down the polymerization in the presence of air.[6] Therefore, the reaction mixture must be rigorously deoxygenated before polymerization proceeds, which limits applications in industry and low-volume reactions in labs. To overcome this limitation, several methods to remove oxygen or to convert oxygen to inert species in situ in the polymerization were developed. In ATRP, activators regenerated by electron transfer (ARGET) was developed, in

which reducing agents such as copper (0), tin (II) 2-ethylhexanoate, triethylamine, and vitamin C, were added to reduce the oxidized copper (II) to regenerate the copper (I) in situ in the polymerization.[7-12] Other effective air-tolerant methods for ATRP include the use of photoredox catalysts[6] and electrochemical ATRP (*e*ATRP).[13] In the RAFT polymerization, enzymes such as glucose oxidase (GOx) were added to convert oxygen to inert (non-radical quenching) species.[14-15] Photocatalyzed RAFT polymerizations with air-tolerant properties were also reported; namely, visible-light-induced activation of photoredox catalysts enabled electron or energy transfer from the catalysts to the dormant species to mediate polymerization.[16-17]

For RCMP, our research group developed a series of effective catalysts, including tertiary amine, iodide anion, pseudo-halide anions, and pyridine *N*-oxides.[4,18-21] In Chapter 2, oxyanion catalysts (carboxylates, nitrates, phosphates, and sulphates) were systematically studied. Among these oxyanion catalysts, carboxylate anions exhibited the best catalytic performance and were amenable to a range of monomers including methacrylates, styrene, and acrylonitrile.[22]

Carboxylic acids are abundant in nature and also easy to synthesize. Hence, carboxylic acids are widely used in the medicinal, food, and agriculture industries.[23] Improvement in catalytic processes from aldehydes to carboxylic acids has actively been studied in recent years, because traditional methods use expensive or toxic oxidants such as $KMnO_4$ and CrO_3, and more environmentally benign catalytic process has been desired. Molecular oxygen is a clean and sustainable oxidant. In 2016, Ma et al. reported the use of a catalytic amount of $Fe(NO_3)_3$/TEMPO/MCl (M = Na or K) to convert a wide range of aldehydes and alcohols to carboxylic acids with high conversions (> 90%) under O_2 or air.[24] Later on, Kang et al. reported the first metal-free catalytic system for the oxidation of aldehydes to carboxylic acids under O_2 using an organic catalyst, i.e., *N*-hydroxyphthalimide (NHPI). However, they studied the

oxidation under 1 atm O_2 and did not mention the oxidation under the air (oxygen content of 20%).[25]

In RCMP, our research group has performed the polymerizations after the bubbling of the reaction mixtures with argon in order to remove oxygen. Based on the recent development in the oxidation method of aldehydes to carboxylic acids using oxygen and NHPI and our findings of the catalytic activities of carboxylate anions as RCMP catalysts, we are inspired to develop air-tolerant RCMP. Namely, we consume oxygen via the conversion of an aldehyde (RCHO) to a carboxylic acid (RCOOH) using NHPI (Scheme 3.2a). The generated carboxylic acid is subsequently converted to a carboxylate anion ($RCOO^-$) by the addition of a base in the system (Scheme 3.2b). The generated $RCOO^-$ is further used as RCMP catalyst (Scheme 3.1). The air-tolerant nature can be useful for large scale synthesis and also increase the accessibility of RCMP to non-experts in labs. A further marked aspect is that the aldehyde serves as not only an O_2 remover but also a precursor of catalyst. The $RCOO^-$ generated from the aldehyde serves as an RCMP catalyst, and hence no additional catalyst is required in this system. Thus, this system is not only air-tolerant but also an extra catalyst-free system, which would be a further attractive feature. In the present work, we first studied several aldehydes (Figure 3.1) to check their reactivities in the NHPI-catalyzed oxidation in the air. We found that cyclohexanecarboxaldehyde (CHCA) showed the highest conversion to the carboxylic acid. Hence, we further used CHCA to develop air-tolerant RCMP. Namely, we carried out RCMP using a monomer, an alkyl iodide dormant species, CHCA, NHPI, and an amine without deoxygenation (containing oxygen) before the polymerization. Upon heating, oxygen was consumed in the mentioned sequence of reactions (Scheme 3.2) to generate the carboxylate anion from CHCA. After the consumption of oxygen, the polymerization started with monomer, an alkyl iodide dormant species, and the generated carboxylate anion RCMP catalyst. In this

chapter, we describe the proof of principle of the air-tolerant RCMP and the studies of methyl methacrylate (MMA), other methacrylates, and styrene (St).

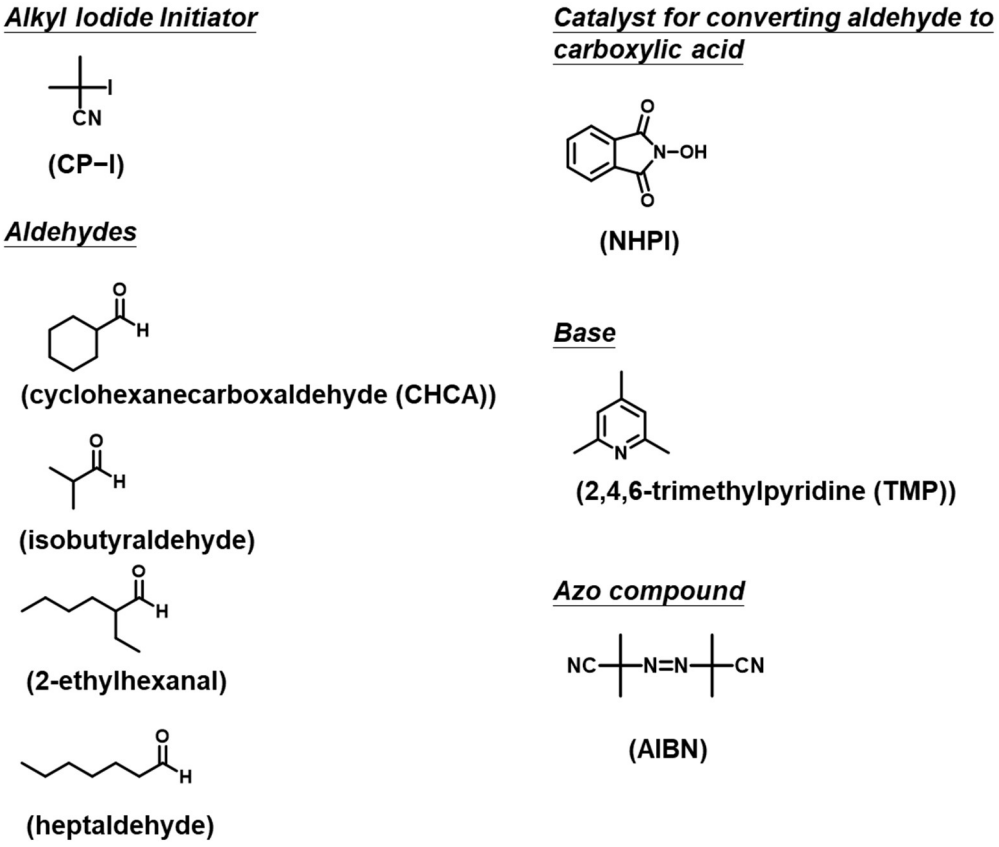

Figure 3.1. Structures of alkyl iodide, aldehydes, and catalyst for converting aldehyde to carboxylic acid, base, and azo compound used in this work.

$$2\ RCHO + O_2 \xrightarrow{NHPI} 2\ RCOOH \qquad (a)$$

$$RCOOH + B \longrightarrow RCOO^{\ominus} + HB^{\oplus} \qquad (b)$$

(B = base (TMP))

Scheme 3.2. (a) Oxidation of aldehyde to carboxylic acid and (b) transformation of carboxylic acid to carboxylate anion.

3.2 Results and discussion.

Oxidation of Aldehydes.

We studied four different aldehydes (Figure 3.1) of their NHPI-catalyzed oxidation in the air. We heated a mixture of an aldehyde (1 mmol), NHPI (0.05 mmol), and a solvent (0.5–1.0 g) in the air at 70 °C for 3 h in a 25 mL Schlenk flask capped with stopper. The 25 mL Schlenk flask contains 5.25 mL O_2 (21% of the air), which is approximately 0.22 mmol at room temperature and 1 atm (ideal gas law). This amount is nearly half of the stoichiometric amount to the aldehyde (1 mmol) and can ensure the complete consumption of O_2.

Table 3.1 (entries 1-4) shows the results of the oxidation of the four aldehydes in acetonitrile-d_3 (CD_3CN) (1.0 g). We used acetonitrile according to the reaction procedure of Kang et al., who used acetonitrile or water as a solvent.[25] Kang et al. used 1 atm O_2 and we used the air (the O_2 content of 20%). Figure 3.2 shows the ^{1}H NMR spectra of the reaction mixtures before (0 h) and after the reaction (3 h) for CHCA. The proton in the aldehyde (*a*) of CHCA appeared at 9.55 ppm. The alpha (C*H*) proton next to the aldehyde (*b*) of CHCA and that next to the carboxylic acid of the converted cyclohexanecarboxylic acid (*b'*) appeared at 2.20–2.31 ppm. From the peak ratio of *a* and *b* before the reaction (Figure 3.2a) and that of *a* and (*b* + *b'*) after the reaction (Figure 3.2b), the conversion of CHCA was determined to be 59% after the 3 h reaction. The conversions of isobutyraldehyde and 2-ethylhexanal were 56% and 10%, respectively. Heptaldehyde, which is a primary alkyl aldehyde, was not converted to carboxylic acid. According to the mechanism hypothesized by Kang et al., an acyl radical is generated as an intermediate in the reaction.[25] The acyl radical can be generated more favorably from secondary alkyl aldehydes than primary alkyl aldehydes, because secondary alkyl groups can better stabilize the acyl radical electronically. No conversion of heptaldehyde would be explained by the unfavorable formation of the acyl radical from the primary alkyl aldehyde. Because CHCA showed the highest conversion, we further studied the oxidation of CHCA in

two other solvents (0.5 g), i.e., dimethyl sulfoxide (DMSO) and diglyme (Table 3.1 (entries 5 and 6)), giving 25% and 66% conversion, respectively. Diglyme did not only give a slightly higher conversion than acetonitrile but is also a less toxic solvent that can be used in RCMP. Therefore, we utilized diglyme for the following RCMP (polymerization) studies.

Table 3.1. Oxidation Results of Aldehydes with NHPI.

Entry	Aldehyde	Solvent[a]	[Aldehyde]$_0$/ [NHPI]$_0$ (mmol)[b]	T (°C)	t (h)	conv (%)
1	CHCA	CD_3CN	1/0.05	70	3	59
2	isobutyraldehyde	CD_3CN	1/0.05	70	3	56
3	2-ethylhexanal	CD_3CN	1/0.05	70	3	10
4	heptaldehyde	CD_3CN	1/0.05	70	3	0
5	cyclohexanecarboxaldehyde	DMSO	1/0.05	70	3	25
6	cyclohexanecarboxaldehyde	Diglyme	1/0.05	70	3	66

[a]The amount of solvent was 1 g for CD_3CN and 0.5 g for DMSO and diglyme. [b]0.22 mmol of O_2.

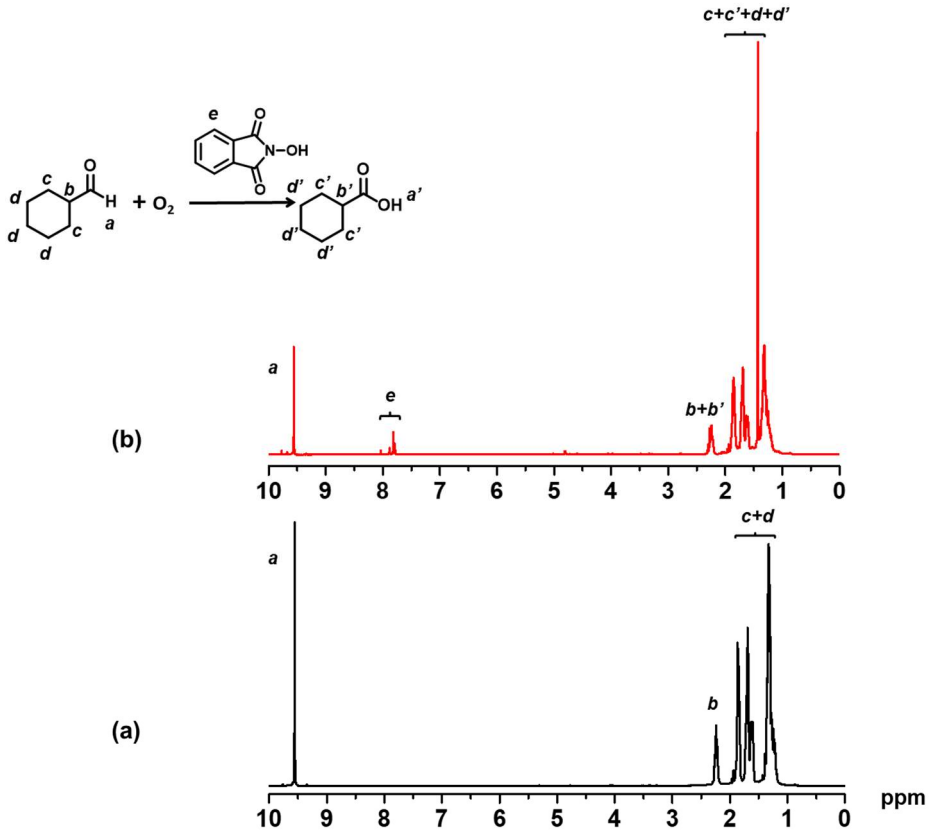

Figure 3.2. ^{1}H NMR spectrum (CD_3CN) for the NHPI-catalyzed oxidation of CHCA (a) before and (b) after the reaction (Table 3.1 (entry 1)).

Two-step Polymerizations of MMA.

Exploiting the successful conversion of CHCA to carboxylic acid, we studied two-step polymerizations (RCMPs) of MMA. In the first step, we carried out the same experiment (Table 3.1 (entry 6)) for the oxidation of CHCA (1 mmol, 2 equiv) with NHPI (0.05 mmol, 0.1 equiv) in diglyme (0.5 g) in the air at 70 °C for 3 h. In the second step, to this reaction mixture, we added a deoxygenated mixture of MMA (20 mmol, 40 equiv, 2.0 g), 2-iodo-2-methylpropionitrile (CP–I (Figure 3.1)) (0.5 mmol, 1 equiv) as an alkyl iodide initiating dormant species, and 2,4,6-trimethylpyridine (TMP (Figure 3.1)) (2 mmol, 4 equiv) as a base using a deoxygenated syringe. The carboxylic acid generated in the first step was converted to the carboxylate anion in the presence of the TMP base, and the resultant carboxylate anion worked as the RCMP catalyst. MMA (monomer), CP–I (initiator), and the carboxylate anion (catalyst) induced and controlled the polymerization. Table 3.2 (entry 1) and Figure 3.3 (circles) show the result. The conversion of MMA reached a relatively high value of 84% in 20 h, at which the number-average molecular weight (M_n) was 5100 and the dispersity ($Đ = M_w/M_n$) was 1.45, where M_w is the weight-average molecular weight. The addition of a small amount of I_2 (0.0125 equiv to CP–I) afforded an even smaller value of 1.26 with keeping a relatively high monomer conversion (86%) in 20 h (Table 3.2 (entry 2) and Figure 3.3 (squares)). I_2 worked as a deactivator of the propagating radical and prevented the addition of many monomers to the propagating radical in an activation-deactivation cycle, resulting in more uniform growth of polymer (narrow molecular weight distribution). Thus, the carboxylate anion generated via the NHPI-catalyzed oxidation of CHCA in the air and the subsequent TMP treatment successfully worked as a catalyst of RCMP.

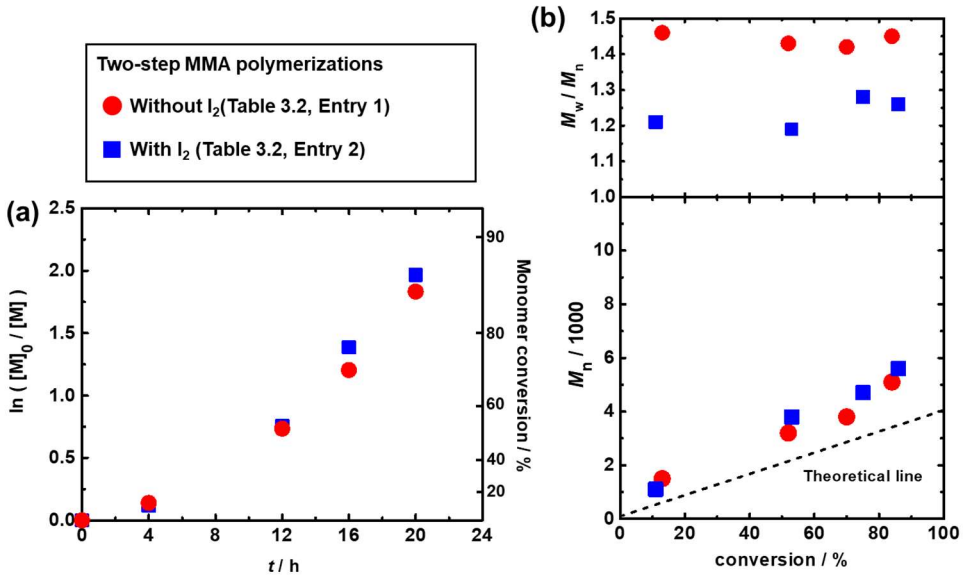

Figure 3.3. Plots of (a) ln([M]$_0$/[M]) vs t and (b) M_n and M_w/M_n vs conversion for the MMA/CP–I/TMP/I$_2$ systems (70 °C). The experimental conditions are indicated in Table 3.2 (entries 1 and 2). The symbols are indicated in the figure.

Table 3.2. Two Step Polymerizations of MMA.

Entry	DP[a]	[MMA]$_0$/[CP–I]$_0$/[TMP]$_0$/[I$_2$]$_0$ (mmol)[b]	T (°C)	t (h)	conv (%)	M_n ($M_{n,theo}$[c])	$Đ$
1	40	20/0.5/2/0	70	4	13	1500 (500)	1.46
				12	52	3200 (2100)	1.43
				16	70	3800 (2800)	1.42
				20	84	5100 (3400)	1.45
2	40	20/0.5/2/0.0125	70	4	11	1100 (500)	1.21
				12	53	3800 (2200)	1.19
				16	75	4700 (3000)	1.28
				20	86	5600 (3600)	1.26

[a]Target degree of polymerization at 100% monomer conversion (calculated by [MMA]$_0$/[CP–I]$_0$). [b]This mixture was added into the reaction mixture of CHCA (1 mmol), NHPI (0.05 mmol), and diglyme (0.5 g) in the air (0.22 mmol of O$_2$) at 70 °C for 3 h in 25 mL flask (Table 3.1 (entry 6)). [c]Theoretical M_n calculated with [MMA]$_0$, [CP–I]$_0$, and monomer conversion.

One-step Polymerizations of MMA.

Instead of the two-step polymerization described above, we studied the one-step polymerization for more practicality of this method. We used the same amounts of CHCA (1 mmol, 2 equiv), NHPI (0.05 mmol, 0.1 equiv), diglyme (0.5 g), MMA (20 mmol, 40 equiv, 2.0 g), CP−I (0.5 mmol, 1 equiv), and TMP (2 mmol, 4 equiv) as in the two-step polymerization

(Table 3.2 (entry 1)) but mixed all of them together in the air in a 25 mL flask with a stopper and heated at 70 °C (Table 3.3 (entry 1) and Figure 3.4 (circles)). There was an induction period (no polymerization took place) for 12 h, during which oxygen was consumed, and CHCA was converted to the RCMP catalyst. The polymerization proceeded relatively slowly after the induction period, reaching a 67% monomer conversion for 48 h. The M_n value nearly twice deviated from the theoretical value, suggesting that, during the long induction period, nearly half of CP–I (initiator) degraded via possible side reactions. The $Đ$ value was 1.16−1.17 until 20 h (36% monomer conversion) and became higher than 1.50 after 20 h, indicating that the prolonged polymerization time also caused less control in the polymerization. Nevertheless, the polymerization proceeded, and low-dispersity polymers were obtained until 20 h, clearly showing that oxygen was consumed in situ in the polymerization and that the carboxylate anion generated from CHCA worked as the RCMP catalysts to generate well-defined polymers in one step. The result proved the proposed principle of the air-tolerant RCMP.

To confirm that the combination of CHCA, NHPI, and TMP generated the RCMP catalyst, we carried out reference experiments (Table 3.3 (entries C1-C5)). Single use of CHCA, TMP, or NHPI resulted in no polymerization (Table 3.3 (entries C1-C3)). TMP and NHPI contain a nitrogen atom, which may coordinate the iodide of polymer–I to generates Polymer$^{\bullet}$ and catalyze RCMP. However the coordination is weak, and hence the single use of TMP or NHPI led to a nearly zero monomer conversion. (Table 3.3 (entry C3)). The combined use of CHCA and NHPI also led to no polymerization, indicating the generated carboxylic acid does not work as a catalyst but must be converted to the carboxylate anion using TMP (Table 3.3 (entry C4)). Furthermore, we removed oxygen via argon bubbling in the combined use of CHCA, NHPI, and TMP. No polymerization took place (Table 3.3 (entry C5)), because the oxidation of aldehyde cannot proceed without oxygen. The results confirmed that the

combination of CHCA, NHPI, and TMP in the presence of oxygen generated the RCMP catalyst.

Table 3.3. One-step Polymerizations of MMA with Target DP of 40.

Entry	Target DP[a]	$[MMA]_0/[CP–I]_0/[CHCA]_0/[NHPI]_0/[TMP]_0$ (mmol)[b]	T (°C)	t (h)	conv (%)	M_n ($M_{n,theo}$)[c]	$Đ$
1	40	20/0.5/2/0.05/4	70	12	0	NA	NA
				16	26	5100 (1000)	1.16
				20	36	5800 (1400)	1.17
				24	42	6800 (1700)	1.55
				32	61	6800 (2400)	1.70
				48	67	8100 (2800)	2.04
C1	40	20/0.5/2/0/0	70	16	16	NA	NA
C2	40	20/0.5/0/0/4	70	16	16	NA	NA
C3	40	20/0.5/0/0.05/0	70	16	16	NA	NA
C4	40	20/0.5/2/0.05/0	70	16	16	NA	NA
C5	40	20/0.5/2/0.05/4 (no air)[d]	70	16	16	NA	NA

[a]Target degree of polymerization at 100% monomer conversion (calculated by $[MMA]_0/[CP–I]_0$). [b]Diglyme (20% wt) as solvent and 0.22 mmol of O_2. [c]Theoretical M_n calculated with $[MMA]_0$, $[CP–I]_0$, and monomer conversion. [d]Argon bubbling was carried out to remove oxygen.

Table 3.4. One-step Polymerizations of MMA with and without AIBN.

Entry	Target DP[a]	$[MMA]_0/[CP–I]_0/[CHCA]_0/[NHPI]_0/[TMP]_0/[AIBN]_0$ (mmol)[b]	T (°C)	t (h)	conv (%)	M_n ($M_{n,theo}$)[c]	$Đ$
1	100	25/0.25/2/0.05/4/0	70	6	0	NA	NA
				12	12	6200 (1200)	1.35
				18	18	7200 (1800)	1.54
				24	33	11400 (3300)	1.97
2	100	25/0.25/2/0.05/4/0	80	4	0	NA	NA
				8	6	4400 (600)	1.24
				12	31	7700 (3100)	1.66
				16	35	9000 (3500)	1.81
3	100	25/0.25/2/0.05/4/0 (with I_2)[d]	70	24	24	12000 (2400)	1.84
4	40	20/0.5/2/0.05/4/0.125	70	4	21	1200 (800)	1.24
				8	34	2100 (1300)	1.27
				12	53	2900 (2100)	1.35
				16	86	4100 (3400)	1.32
5	100	25/0.25/2/0.05/4/0.125	70	2	31	3500 (3100)	1.25
				4	55	6100 (5500)	1.23
				6	87	9000 (8700)	1.38
6	200	25/0.125/2/0.05/4/0.125	70	8	86	19000 (17000)	1.29
7	400	25/0.0625/2/0.05/4/0.125	70	4	74	27000 (27000)	1.34
C1	40	20/0.5/0/0/0/0.125	70	8	0	NA	NA
C2	100	25/0.25/0/0/0/0.125	70	8	6	700 (600)	1.70

[a]Target degree of polymerization at 100% monomer conversion (calculated by $[MMA]_0/[CP–I]_0$). [b]Diglyme (20% wt) as solvent and 0.22 mmol of O_2. [c]Theoretical M_n calculated with $[MMA]_0$, $[CP–I]_0$, and monomer conversion. [d]The addition of I_2 (0.0125 mmol).

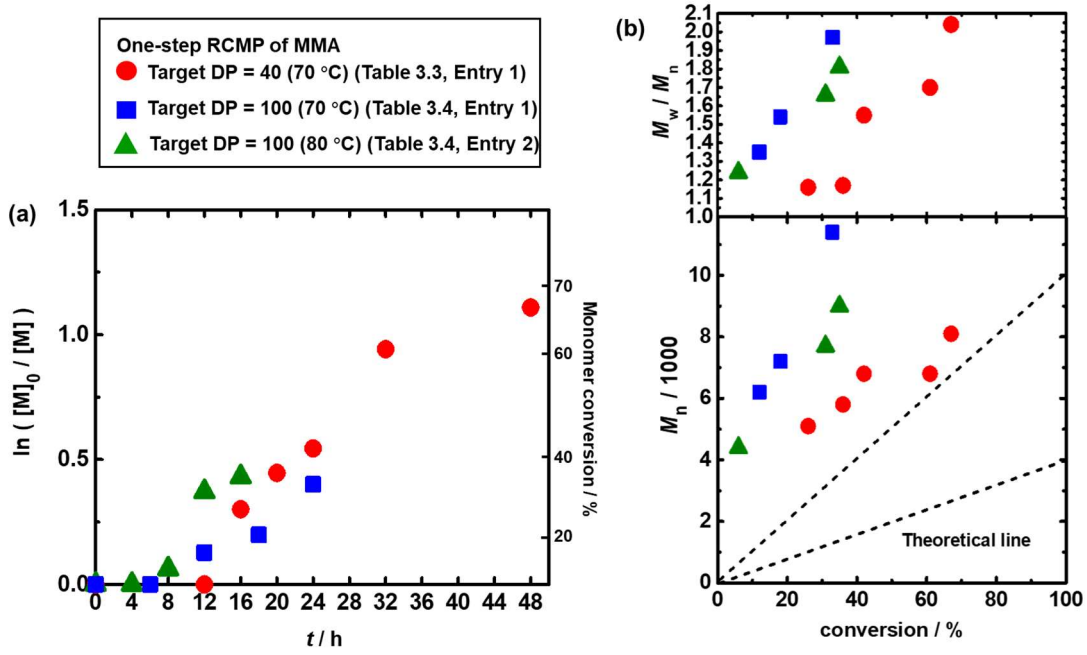

Figure 3.4. Plots of (a) $\ln([M]_0/[M])$ vs t and (b) M_n and M_w/M_n vs conversion for the MMA/CP–I/CHCA/NHPI/TMP systems. The experimental conditions are indicated in Table 3.3 (entry 1) and Table 3.4 (entries 1-2). The symbols are indicated in the figure.

We increased the target DP at a full (100%) monomer conversion from 40 (Table 3.3 (entry 1)) to 100 (Table 3.4 (entry 1)) by changing the $[MMA]_0/[CP–I]_0$ ratio from 40 to 100. The induction period was shortened from 12 h (target DP = 40) to 6 h (target DP = 100). However, the M_n still largely deviated from the theoretical value (Figure 3.4 (squares)). The $Đ$ value was 1.35 for 12 h (12% monomer conversion) and became higher than 1.50 after 18 h. In order to improve the control in the M_n and $Đ$ values, we attempted two approaches. One approach was to increase the reaction temperature from 70 °C (Table 3.4 (entry 1)) to 80 °C (Table 3.4 (entry 2) and Figure 3.4 (triangles)) to reduce the polymerization time and hence reduce side reactions. The induction period was shortened to 4 h, but the $Đ$ value was still relatively large (= 1.66) for 12 h (31% monomer conversion). Side reactions seemed still significant. The other method was to add I_2 (0.05 equiv to CP–I) at 70 °C as in the two-step system (Table 3.2 (entry 2)). However, the polymerization slowed down and the $Đ$ value was 1.84 for 24 h (24% monomer conversion) (Table 3.4 (entry 3)). The two approaches were not effective.

Increase in the Polymerization Rate.

As another approach, we attempted to shorten the polymerization time and hence by adding a small amount of azo compound, i.e., 2,2'-azobis(isobutyronitrile) (AIBN) (0.125 mmol, 0.25 or 0.5 equiv to CP–I) (Table 3.4 (entries 4-5)). In our previously studied RCMP systems, the addition of azo compound effectively decreased the deactivator concentration and therefore increased the polymerization rate.[18-19,22] For the target DP of 40, the induction period was shortened from 12 h (Table 3.3 (entry 1) and Figure 3.4 (circles)) to approximately 0.5 h (Table 3.4 (entry 4) and Figure 3.5 (circles)) with the addition of AIBN. The monomer conversion also increased from 26% (Table 3.3 (entry 1)) to 86% (Table 3.4 (entry 4)) for 16 h. The M_n value well matched the theoretical value, and the $Đ$ value was 1.2–1.4 throughout

the polymerization (Figure 3.5 (circles)). After 16 h, we successfully obtained a polymer with M_n = 4100, $Đ$ = 1.32 (Table 3.4 (entry 4)). Similarly, for the target DP of 100, the polymerization became faster with the addition of AIBN (Table 3.4 (entry 5) and Figure 3.5 (squares)) compared with the system without AIBN (Table 3.4 (entry 1) and Figure 3.4 (squares)). The M_n values matched the theoretical values, yielding a polymer with M_n = 9000 and $Đ$ = 1.38 for 6 h (87% conversion) (Table 3.4 (entry 5) and Figure 3.5 (squares)).

As the controlled experiments, we carried out polymerizations using only MMA, CP–I, and AIBN in the air but without CHCA, NHPI, and TMP, leading to no polymerization or very slow polymerization (Table 3.4 (entries C1 and C2)). The results suggest that the generation of the RCMP catalyst from CHCA, NHPI, and TMP is necessary for the polymerization to proceed. With the addition of AIBN (Table 3.4 (entries 4-5) and Figure 3.5), the induction period was shortened but was still long enough to generate the RCMP catalyst from CHCA, NHPI, and TMP. Thus, the combination of AIBN with CHCA, NHPI, and TMP successfully afforded the fast polymerization and good control in the M_n and $Đ$ values.

We further targeted higher DPs of 200 and 400. We obtained low-dispersity polymers with M_n = 19000–27000 and $Đ$ =1.29–1.34 at high monomer conversions (74%–86%) in relatively short reaction time (4–8 h) (Table 3.4 (entries 6 and 7)).

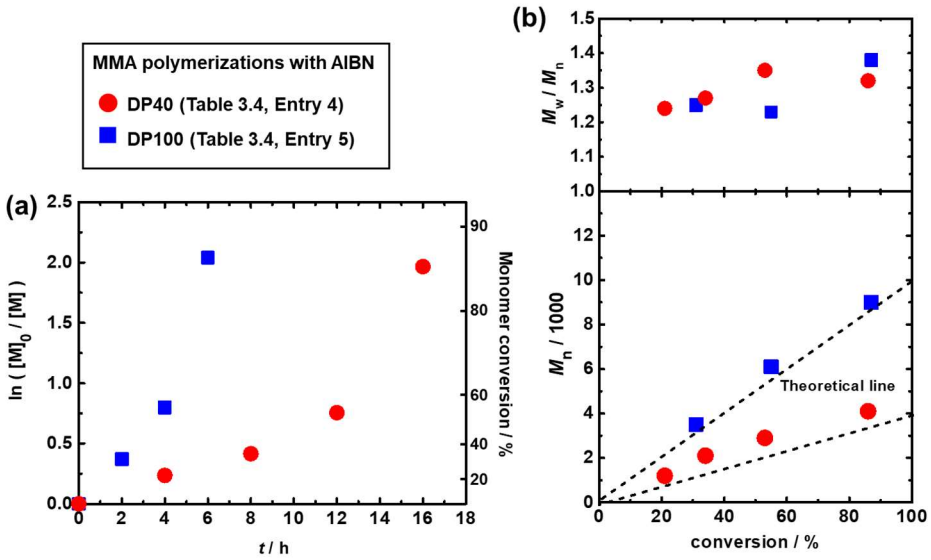

Figure 3.5. Plots of (a) ln([M]$_0$/[M]) vs t and (b) M_n and M_w/M_n vs conversion for the MMA/CP−I/CHCA/NHPI/TMP/AIBN systems (70 °C): The experimental conditions are indicated in Table 3.4 (entries 4-5). The symbols are indicated in the figure.

Table 3.5. Polymerizations of functional methacrylates and styrene.

Entry	Monomer	[M]$_0$/[CP–I]$_0$/[CHCA]$_0$/[NHPI]$_0$ /[TMP]$_0$/[AIBN]$_0$ (mmol)[b]	T (°C)	t (h)	conv (%)	M_n ($M_{n,theo}$)[c]	$Đ$
1	BMA	25/0.25/2/0.05/4/0.125	70	8	46	5700 (6500)	1.40
2	BzMA	25/0.25/2/0.05/4/0.125	70	8	100	13000 (13000)	1.33
3	HEMA	25/0.25/2/0.05/4/0.125	50	24	68	6100 (8000)	1.29
4	St	25/0.25/2/0.05/4/0.125	80	8	87	6500 (9000)	1.49

[a]Target degree of polymerization at 100% monomer conversion (calculated by [MMA]$_0$/[CP–I]$_0$). [b]Diglyme (20% wt) as solvent and 0.22 mmol of O_2. [c]Theoretical M_n calculated with [M]$_0$, [CP–I]$_0$, and monomer conversion.

Polymerization of Other Methacrylates and St.

We studied other methacrylates and St to expand the monomer scope. Table 3.5 shows the polymerizations of hydrophobic methacrylates, i.e., butyl methacrylate (BMA) (entry 1) and benzyl methacrylate (BzMA) (entry 2), and a hydrophilic methacrylate, i.e., 2-hydroxylethyl methacrylate (HEMA) (entry 3). Low-dispersity polymers with M_n = 5700−13000 and $Đ$ = 1.29−1.40 were obtained with 46%−100% monomer conversions. The polymerization of St (entry 4), which is another family of monomer, also yielded a relatively low-dispersity polystyrene with M_n = 6500 and $Đ$ = 1.49 with an 87% monomer conversion. Thus, the air-tolerant RCMP was amenable to several methacrylates and St.

3.3 Conclusion.

Air-tolerant RCMP using CHCA (aldehyde), NHPI, and TMP (amine) was developed. Oxygen was consumed via NHPI-catalyzed oxidation of CHCA to the carboxylic acid. The carboxylic acid was further converted to the carboxylate anion in the presence of TMP (amine), and the carboxylate anion worked as an efficient catalyst of RCMP. Low-dispersity polymers ($Đ$ = 1.2−1.4) were obtained up to M_n = 27000 and up to high monomer conversions (approximately 85%). The monomer scope encompassed MMA, functional methacrylates, and St. No requirement of deoxygenation facilitates the operation of RCMP, enhancing the usefulness of RCMP.

3.4 Experimental.

Materials.

Methyl methacrylate (MMA) (>99.8%, Tokyo Chemical Industry (TCI), Japan), butyl methacrylate (BMA) (>99.0%, TCI), benzyl methacrylate (BzMA) (>98.0%, TCI), 2-hydroxyethyl methacrylate (HEMA) (>95.0%, TCI), styrene (St) (>99.0%, TCI), 2-iodo-2-methylpropionitrile (CP−I) (>96.0%, TCI), iodine (I_2) (>98.0%, TCI), 2,2'-azobis(isobutyronitrile) (AIBN) (95%, Wako Pure Chemical, Japan), cyclohexanecarboxaldehyde (CHCA) (97%, Sigma-Aldrich, USA), isobutyraldehyde (>99.0%, Sigma-Aldrich), 2-ethylhexanal (96%, Sigma-Aldrich), heptaldehyde (95%, Sigma-Aldrich), *N*-hydroxyphthalimide (NHPI) (97%, Sigma-Aldrich), 2,4,6-trimethylpyridine (TMP) (99%, Sigma-Aldrich), and diethylene glycol dimethyl ether (diglyme) (>99.0%, TCI) were used as received.

Measurements.

The GPC measurement using THF as the eluent was performed using the same instrument and procedure as mentioned in Chapter 2 (Section 2.4). The monomer conversion was determined from the peak area.

The ^{1}H NMR spectra were recorded on Bruker (Germany) AV500 spectrometer (500 MHz) or AV 300 (300 MHz) at ambient temperature. Acetonitrile-d_3 and DMSO-d_6 (Cambridge Isotope Laboratories, USA) were used as the solvents for the NMR analysis, and the chemical shift was calibrated using residual undeuterated solvents or tetramethylsilane (TMS) as the internal standard.

Oxidation of Aldehyde.

A mixture of CHCA (0.112 g, 1 mmol), NHPI (0.0082 g, 0.05 mmol) and a solvent (acetonitrile-d_3 (1.0 g) or DMSO-d_6 or diglyme (0.5 g)) was heated in a Schlenk flask at 70 °C

for 3 h with magnetic stirring and subsequently quenched to room temperature. The mixtures before and after the heat treatment were analyzed by ^{1}H NMR.

Two-step Polymerization.

In a typical run, a deoxygenated mixture of MMA (2.0 g), CP−I, and TMP was added into the reaction mixture of aldehyde oxidation (CHCA, NHPI and diglyme) after 3 h (shown above) via a deoxygenated syringe, and heated in a Schlenk flask at 70 °C with magnetic stirring. After a prescribed time *t*, the mixture was quenched to room temperature, an aliquot (0.1 mL) of the solution was taken out by a syringe, diluted by THF to a known concentration, and analyzed by GPC.

One-step Polymerization.

In a typical run, a mixture of monomer (2.0 g), CP−I, CHCA, NHPI, TMP, AIBN, and diglyme (20% wt of the total mixture) was heated in a Schlenk flask at 50–80 °C with magnetic stirring. After a prescribed time *t*, the mixture was quenched to room temperature, an aliquot (0.1 mL) of the solution was taken out by a syringe, diluted by THF to a known concentration, and analyzed by GPC.

References.

1. Matyjaszewski, K. *Macromolecules* **2012**, 45, 4015-4039.
2. Moad, G.; Rizzardo, E.; Thang, S. H. *Chem. Asian J.* **2013**, 8, 1634-1644.
3. Nicolas, J.; Guillaneuf, Y.; Lefay, C.; Bertin, D.; Gigmes, D. Charleux, B. *Prog. Polym. Sci.* **2013**, 38, 63-235.
4. Goto, A.; Suzuki, T.; Ohfuji, H.; Tanishima, M.; Fukuda, T.; Tsujii, Y.; Kaji, H. *Macromolecules* **2011**, 44, 8709-8715.
5. Wang, C.-G.; Chong, A. L. C.; Pan, H. M.; Sarkar, J.; Tay, X. T.; Goto, A. *Polym. Chem.* **2020**, 11, 5559-5571.
6. McCarthy, B.; Miyake, G. M. *ACS Macro Lett.* **2018**, 7, 1016-1021.
7. Matyjaszewski, K.; Dong, H.; Jakubowski, W.; Pietrasik, J.; Kusumo, A. *Langmuir* **2007**, 23, 4528-4531.
8. Zhang, L.; Cheng, Z.; Shi, S.; Li, Q.; Zhu, X. *Polymer* **2008**, 49, 3054-3059.
9. Dong, H.; Matyjaszewski, K. *Macromolecules* **2008**, 41, 6868-6870.
10. Kwak, Y.; Matyjaszewski, K. *Polym Int* **2009**, 58, 242-247.
11. Quirós-Montes, L.; Carriedo, G. A.; García-Álvarez, J.; Soto, A. P. *Green Chem.* **2019**, 21, 5865-5875.
12. Kang, H.; Jeong, W.; Hong, D. *Langmuir* **2019**, 35, 7744-7750.
13. Sun, Y.; Lathwal, S.; Wang, Y.; Fu, L.; Olszewski, M.; Fantin, M.; Enciso, A. E.; Szczpaniak, G.; Das, S. Matyjaszewski, K. *ACS Macro Lett.* **2019**, 8, 603-609.
14. Lv, Y.; Liu, Z.; Zhu, A.; An, Z. *J. Polym. Sci. Part A: Polym. Chem.* **2017**, 55, 164-174.
15. Schneiderman, D. K.; Ting, J. M.; Purchel, A. A.; Miranda Jr, R.; Tirrell, M. V.; Reineke, T. M.; Rowan, S. J. *ACS Macro Lett.* **2018**, 7, 406-411.
16. Wang, J.; Rivero, M.; Bonilla, A. M.; Sanchez-Marcos, J.; Xue, W.; Chen, G.; Zhang, W.; Zhu, X. *ACS Macro Lett.* **2016**, 5, 1278-1282.
17. Li, M.; Fromel, M.; Ranaweera, D.; Rocha, S.; Boyer, C.; Pester, C. W. *ACS Macro Lett.* **2019**, 8, 374-380.
18. Goto, A.; Ohtsuki, A.; Ohfuji, H.; Tanishima, M.; Kaji, H. *J. Am. Chem. Soc*. **2013**, 135, 11131-11139.
19. Sarkar, J.; Xiao, L.; Goto, A. *Macromolecules* **2016**, 49, 5033-5042.
20. Wang, C.-G.; Goto, A. *J. Am. Chem. Soc*. **2017**, 139, 10551-10560.
21. Xu, H.; Wang, C.-G.; Lu, Y.; Goto, A. *Macromolecules* **2019**, 52, 2156-2163.
22. Mao, W.; Wang, C.-G.; Lu, Y. Faustinelie, W.; Goto, A. *Polym. Chem.* **2020**, 11, 53-60.
23. Badea, G. I.; Radu, G. L., Chapter 1: Carboxylic Acids-Key Role in Life Sciences. In *Carboxylic Acid - Key Role in Life Sciences*. BOD: **2018**; pp 1-5.
24. Jiang, X.; Zhang, J.; Ma, S. *J. Am. Chem. Soc.* **2016**, 138, 8344-8347.
25. Dai, P.-F.; Qu, J.-P.; Kang, Y.-B. *Org. Lett.* **2019**, 21, 1393-1396.

Chapter 4. Aqueous Emulsion Polymerizations of Methacrylates and Styrene via Reversible Complexation Mediated Polymerization (RCMP)

Abstract.

Reversible complexation mediated polymerization (RCMP) was successfully exploited in aqueous emulsion polymerization of methyl methacrylate (MMA). The polymerization behavior was comprehensively studied using a series of emulsifiers, alkyl iodide initiating dormant species, and catalysts. The optimized combination of these species generated stable polymer particles up to relatively high solid contents (up to nearly 50%) and achieved nearly quantitative initiation efficiency and low dispersity ($Đ$ = 1.1–1.3). The kinetic and mechanistic aspects of the polymerization were elucidated by the partitioning tests of the species in the aqueous and organic phases and the particle number analysis in the course of polymerization. The emulsion RCMP was amenable to not only MMA but also functional methacrylates and styrene. No use of metal or sulfur compounds, relatively high solid contents, good monomer versatility, and high chain-end fidelity achievable in the emulsion RCMP are attractive features for polymer material applications and industrial applications.

4.1. Introduction.

Emulsion polymerization is an industrially important process owing to the efficient heat transfer, low viscosity, and high polymerization rate.[1] Radical polymerization, which contributes to approximately 50% of the commercial polymers, has been widely conducted in emulsion system. However, similar to homogenous radical polymerizations which were discussed in the previous chapters, conventional free-radical emulsion polymerization cannot control the molecular weight and molecular weight distribution due to the high reactivity of the propagating radicals and their propensity to undergo bimolecular termination, transfer, and other side reactions. Therefore, emulsion polymerization has extensively been studied in living radical polymerization (LRP) (also termed reversible deactivation radical polymerization), which is based on the reversible activation of a dormant species (Polymer–X) to a propagating radical (Polymer$^{\bullet}$) (active species) by thermal or chemical stimulus (introduced in Chapter 1), yielding polymers with predictable molecular weights and narrow molecular weight distributions.[2-3] There are some challenges in using LRP in emulsion polymerization compared with conventional radical polymerization. The transportation and partitioning of the initiating dormant species and catalysts in the dispersed and continuous phases are to be carefully considered to control the polymerization. Also importantly, oligomers are generated at an early stage of polymerization in LRP, making the dispersed phase (particles) hard to stabilize and often causing coagulation of the particles. This is completely different from conventional radical polymerization, where high molecular-weight polymers are generated throughout the polymerization and stabilize the particles even at an early stage of polymerization. Therefore, important issues in emulsion LRP are the choice of appropriate initiating dormant species and catalysts and the stabilization of the particles under optimized reaction conditions using proper emulsifiers (surfactants).

Since the pioneering work of the emulsion polymerization of *n*-butyl methacrylate,[4] atom transfer radical polymerization (ATRP) has been successfully used in emulsion[5-8], mini-emulsion[9-10], and micro-emulsion[11-12] polymerizations for various monomers. Emulsion ATRP has also been controlled by external stimuli such as photo irradiation[13-14] and electrical current.[15-16]

Reversible addition−fragmentation chain-transfer (RAFT) polymerization has most widely been studied in water-borne system. To overcome the initial instability of the particles, macroRAFT agents have been used as emulsifiers. Amphiphilic block copolymers generated from the macroinitiators efficiently stabilized the particles.[17-18] The obtained particles are often well-defined self-assemblies such as micelles, worms, and vesicles. This elegant process is termed polymerization-induced self-assembly (PISA).[19-20] The obtained self-assemblies have been used as drug carriers and imaging particles for biomedical applications and as fillers for rheological improvement of resins, for instance.[21-24]

Nitroxide-mediated radical polymerization (NMP) was the first LRP that was applied in emulsion polymerization. Since then, emulsion NMP has extensively been explored.[25-28] Other LPR systems such as organotellurium mediated radical polymerization (TERP),[29-30] iodine transfer polymerization (ITP),[31-32] and reverse iodine transfer polymerization (RITP)[33-34] have also been successfully utilized in emulsion and mini-emulsion polymerizations. While these emulsion LRP systems are successful and useful, possible limitations are the use of transition metals as catalysts for ATRP, the odor of sulfur compounds used in RAFT, and the high temperature required in NMP.

Our research group has developed reversible complexation mediated polymerization (RCMP), which is an LRP using halogen bonding for catalysis. In RCMP, a polymer-iodide (polymer–I) (dormant species) and a catalyst form a halogen bonding and generate a propagating radical Polymer$^{\bullet}$ (active species).[35-37] For example, Polymer–I coordinates I^{-}

(catalyst) to form a halogen-bonding complex (Polymer–I···I^-). The complex subsequently generates Polymer$^\bullet$ and a deactivator ($I_2^{\bullet-}$) (Scheme 4.1a). Because $I_2^{\bullet-}$ is not a stable radical, two $I_2^{\bullet-}$ species would react (disproportionate) to generate I^- and I_3^- (Scheme 4.1b). I_3^- works as a deactivator (Scheme 4.1c). The regenerated I^- works as an activator (Scheme 4.1a). I^- is used in the form of salts such as tetrabutylammonium iodide ($Bu_4N^+I^-$) (BNI) and alkali iodide (NaI and KI). Advantages of RCMP include no use of heavy metals, sulfur compounds, or special capping agents, no requirement of high temperatures, and robust operation (no oxidation of catalysts in the air in the preparation of the polymerization mixture). RCMP is amenable to a wide range of hydrophobic and hydrophilic monomers in bulk and in solutions using organic solvents and water.[38-40] RCMP has also been combined with PISA (dispersion PISA system) to generate block copolymer self-assemblies.[41-42] However, RCMP has not been used in emulsion polymerization, which is important for industrial applications.

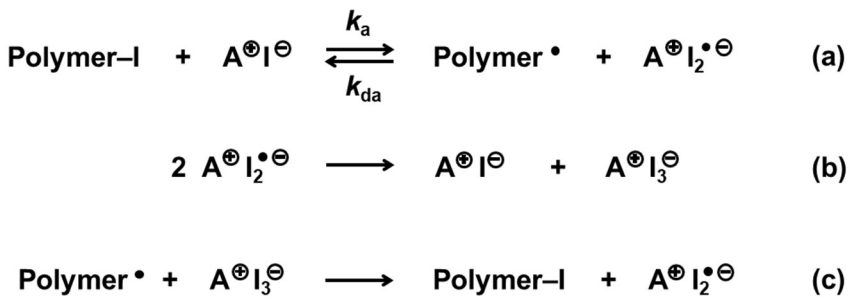

Scheme 4.1. Reversible activation of RCMP.

Herein, we report the first emulsion RCMP. We studied the homopolymerizations of hydrophobic monomers in a water continuous phase. We achieved good stability of the particles using mixed (ionic and neutral) emulsifiers and good control in the polymerization. The studied monomers encompassed methyl methacrylate (MMA), styrene (St), and functional methacrylate monomers. We systematically studied the effects of the initiating dormant species and catalysts with different hydrophobicity in the polymerizations of MMA. The partitioning

of the initiating dormant species in the continuous and dispersed phases and the change in the particle number were also studied for probing the mechanisms of the polymerization. Figure 4.1 shows the studied alkyl iodide initiating dormant species, catalysts, and emulsifiers (surfactants) in this work.

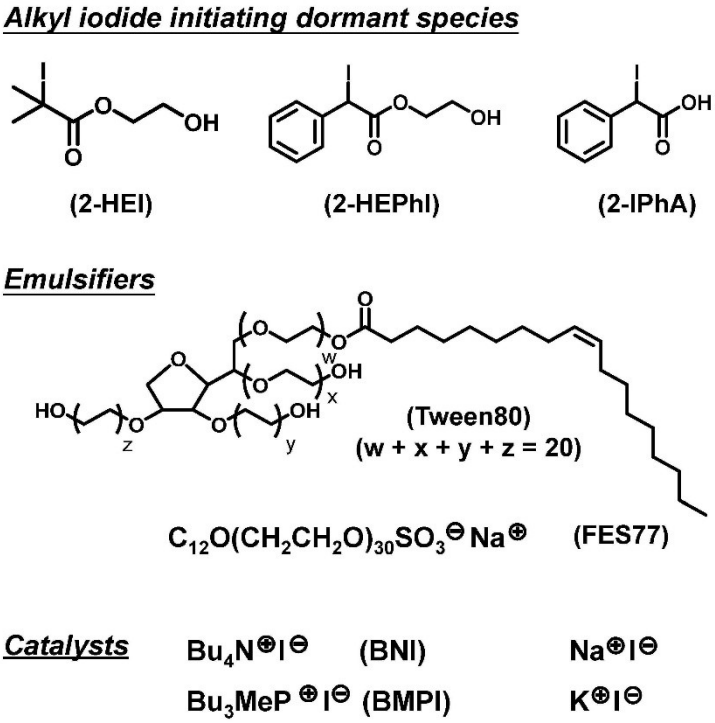

Figure 4.1. Structures of alkyl iodides, emulsifiers, and catalysts used in this work.

4.2. Results and Discussion.

Polymerizations of MMA.

Studies on Emulsifiers.

As mentioned above, the stability of the particles is an important issue in emulsion LRP. We first studied emulsifiers in the polymerizations of MMA. We used a non-ionic emulsifier Tween80 (Figure 4.1), which is non-toxic and biodegradable. We heated a mixture of MMA (monomer, 100 equiv, 30.0 wt%), 2-hydroxyethyl 2-iodoisobutyrate (2-HEI (Figure 4.1), an alkyl iodide initiating dormant species, 1 equiv), NaI (catalyst, 1 equiv), BNI (catalyst, 1 equiv), 2,2'-azobis(2-methylpropionamidine) dihydrochloride (V50) (water-soluble azo initiator, 0.5 equiv), Tween80 (emulsifier, 5.0 wt%), and water (reaction medium, 65.0 wt%) in a reaction vessel under a continuous argon flow using mechanical stirring at 60 °C. A small amount of V50 was added to increase the polymerization rate. In our previously studied RCMP in bulk and solution systems, the polymerization was accelerated by the addition of azo initiators due to the capability of decreasing the deactivator concentration. The monomer conversion reached 52% for 1.5 h, and the number-average molecular weight (M_n) and dispersity $Đ$ (= M_w/M_n) values were 8100 and 1.21, respectively, where M_w is the weight-average molecular weight (Table 4.1 (entry 1) and Figure 4.2 (squares)). However, the particles coagulated and precipitated during the polymerization. Thus, we studied an ionic emulsifier FES77 (1.7 wt%) (Figure 4.1). Stable particles were generated because of the electrostatic repulsion originated from FES77 that covered the particle surfaces. However, the $Đ$ value was relatively large (>1.50) (Table 4.1 (entry 2) and Figure 4.2 (triangles)). Thus, we tried to combine Tween80 and FES77 (3/1 (w/w)) to seek both low dispersity and particle stability. Stable particles were generated and the $Đ$ value became relatively small (1.18–1.33). The monomer conversion reached to ~100% for 100 min, giving a poly(methyl methacrylate) (PMMA) with M_n = 17000 and $Đ$ = 1.33 (Table 4.1 (entry 3) and Figure 4.2 (circles)). We reduced the amount of the

emulsifier (Tween80/FES77 (3/1 (w/w))) from 3.3 wt% (Table 4.1 (entry 3)) to 0.7 wt% (Table 4.1 (entry 4)), resulting in a coagulation of particles and a large *Đ* value (= 2.25). Hence, we utilized the mixture (3.3 wt%) of Tween80 and FES77 (3/1 (w/w)) in the following MMA polymerizations. V50 is a cationic azo initiator, which may associate with the anionic FES77 emulsifier. However, the optimized conditions involved the use of the neutral emulsifier (Tween80) and the anionic emulsifier (FES77) in a mixed manner (3/1 (w/w)). Because of the relatively small fraction of the anionic FES77 emulsifier and the relatively small amount of V50, we observed no coagulation even using the cationic V50 azo initiator.

Table 4.1. Emulsion Polymerizations of MMA using Different Emulsifiers and Catalysts.

Entry	Target DP[a]	Emulsifier	Catalysts A / B	$[MMA]_0/[2HEI]_0/[A]_0/[B]_0/[V50]_0$ (mM)	*T* (°C)	*t* (min)	conv (%)	M_n ($M_{n,theo}$[b])	*Đ*
1	100	Tween80[c]	NaI / BNI	8000/80/80/80/40	60	90	52	8100 (5200)	1.21
2	100	FES 77[d]	NaI / BNI	8000/80/80/80/40	60	90	93	17000 (9300)	1.70
3	100	Tween80 / FES77[e,f]	NaI / BNI	8000/80/80/80/40	60	100	100	17000 (10000)	1.33
4	100	Tween80 / FES77[e,g]	NaI / BNI	8000/80/80/80/40	60	100	77	11000 (7700)	2.25
5	100	Tween80 / FES77[e,f]	none	8000/80/0/0/40	60	20	100	53000 (10000)	2.39
6	100	Tween80 / FES77[e,f]	NaI / none	8000/80/160/0/40	60	60	100	25000 (10000)	1.54
7	100	Tween80 / FES77[e,f]	none / BNI	8000/80/0/160/40	60	120	59	26000 (5900)	1.30
8	100	Tween80 / FES77[e,f]	KI / BNI	8000/80/80/80/40	60	100	100	16000 (10000)	1.38
9	100	Tween80 / FES77[e,f]	NaI / BMPI	8000/80/80/80/40	60	100	100	19000 (10000)	1.49

[a]Target degree of polymerization (DP) at 100% monomer conversion as calculated according to $[MMA]_0/[2\text{-}HEI]_0$. [b]Theoretical M_n value calculated according to ($[MMA]_0/[2\text{-}HEI]_0$) × (monomer conversion) × (molecular weight of MMA). [c]$[MMA]_0/[Tween80]_0/[water]_0$ = 30.0/5.0/65.0 (w/w/w). [d]$[MMA]_0/[FES77]_0/[water]_0$ = 30.0/1.7/68.3 (w/w/w). [e]Tween80/FES77 = 3/1 (w/w). [f]$[MMA]_0/[emulsifier]_0/[water]_0$ = 30.0/3.3/66.7 (w/w/w). [g]$[MMA]_0/[emulsifier]_0/[water]_0$ = 30.0/0.7/69.3 (w/w/w).

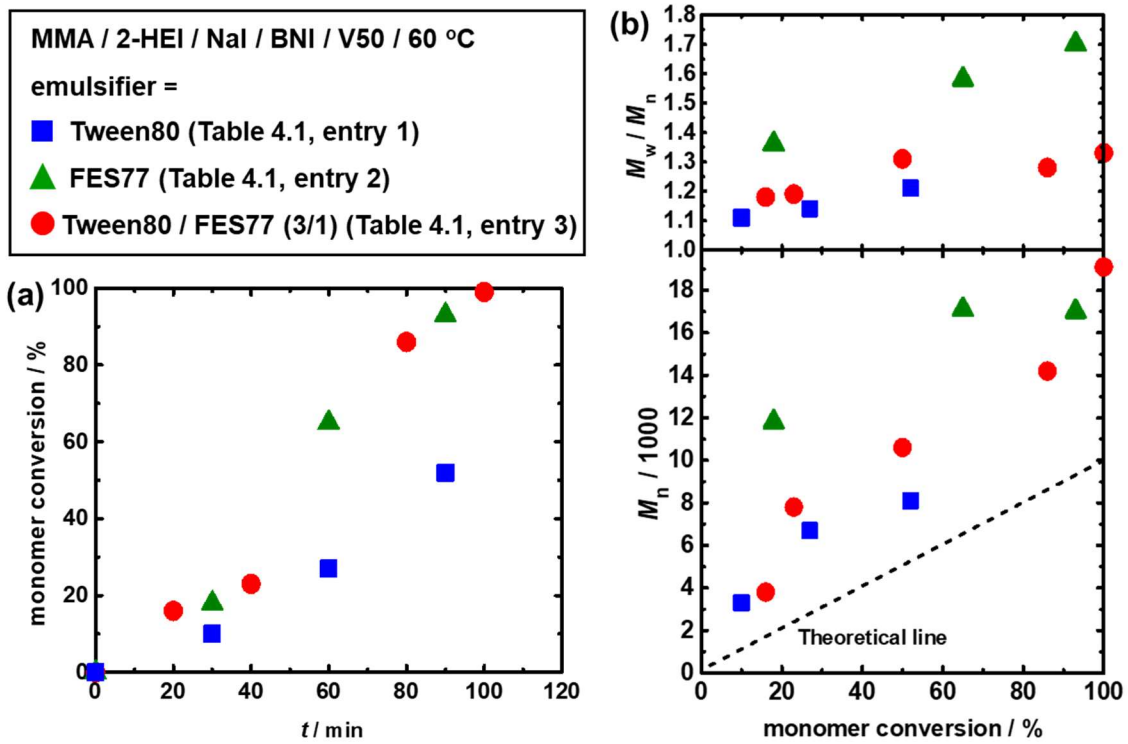

Figure 4.2. Plots of (a) monomer conversion vs t and (b) M_n and M_w/M_n vs conversion for the MMA/2-HEI/NaI/BNI/V50 systems using different emulsifiers (60 °C): $[MMA]_0$ = 8 M; $[2\text{-HEI}]_0$ = 80 mM; $[NaI]_0$ = 80 mM; [BNI] = 80 mM; $[V50]_0$ = 40 mM (Table 4.1, entries 1-3). The symbols are indicated in the figure.

Studies on Catalysts.

In the mentioned Tween80/FES77 combined system (Table 4.1 (entry 3), we co-used NaI and BNI. NaI is soluble in water and is expected to catalyze the polymerization in the water phase. BNI has four hydrophobic butyl groups and is more soluble in the organic phase and therefore is expected to catalyze the polymerization in the organic phase. BNI is also amphiphilic. BNI is slightly soluble in water and may also play some role in catalyzing the polymerization in the water phase.

Mechanistically, in the beginning of polymerization, the hydrophobic MMA monomer would form droplets, which are dispersed in water, and emulsifiers would form micelles in water. At an early stage of polymerization, MMA molecules would diffuse from the monomer droplets to the micelles, and also MMA molecules slightly dissolved in water would polymerize from the 2-HEI initiating dormant species dissolved in water to generate oligomers,

which would also enter the micelles. 2-HEI and catalysts may also diffuse into the micelles and initiate the polymerization in the micelles. Through these processes, nucleation would occur. Subsequently, MMA molecules would continue to diffuse from the monomer droplets to the particles, and the polymerization would mainly occur in the particles (organic phase).

To probe the roles of NaI and BNI, we studied no use of catalyst and single use of NaI or BNI. In the absence of any catalysts, the M_n value (53,000) largely deviated from the theoretical value (10,000), and the $Đ$ value was as large as 2.39 (Table 4.1 (entry 5), showing no control of the polymerization. In this system, the polymerization was induced by the azo initiator (V50). Because of the use of the alkyl iodide dormant species, degenerative chain transfer could operate. However, the degenerative chain transfer constant in the MMA polymerization is not so large (2.6 at 80 °C and 1.6 at 90 °C)[38] that a small $Đ$ value could not be achieved in this system.

Figure 4.3 and Table 4.1 (entries 3, 6, and 7) compare the results with dual use of NaI and BNI, single use of NaI, and single use of BNI. The single use of NaI afforded polymers with relatively large $Đ$ values (~1.5) throughout the polymerization (Figure 4.3 (triangles) and Table 4.1 (entry 6)), probably because of the lack of a sufficient amount of catalyst in the organic (particle) phase. The single use of BNI led to relatively small $Đ$ values (1.18–1.33) but gave a large deviation of the M_n values from the theoretical values by a factor of 4–10 (Figure 4.3 (squares) and Table 4.1 (entry 7)), suggesting the low initiation efficiency from the alkyl iodide (2-HEI). The low initiation efficiency would be ascribed to the lack of a sufficient amount of catalyst in the water phase to initiate 2-HEI present in water. As already described, the dual use of NaI and BNI resulted in relatively small $Đ$ values (1.18–1.33) and at the same time gave relatively small deviation in the M_n values (Figure 4.3 (circles) and Table 4.1 (entry 3)). The presence of the catalysts in both water (NaI) and organic (BNI) phases is important.

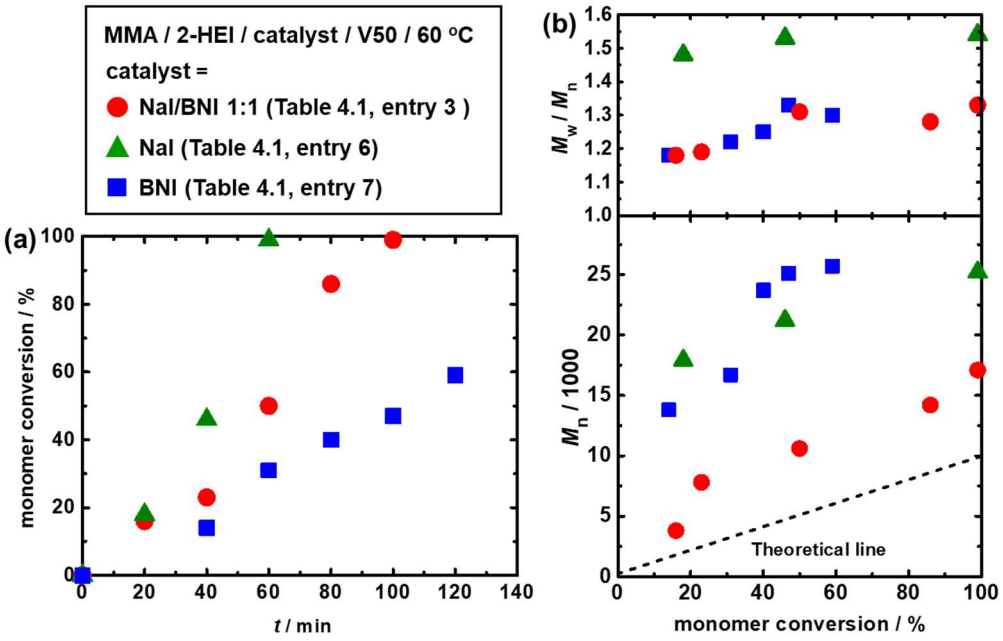

Figure 4.3. Plots of (a) monomer conversion vs t and (b) M_n and M_w/M_n vs conversion for the MMA/2-HEI/Catalyst/V50 systems using a mixture of Tween80 and FES77 emulsifiers (60 °C): $[MMA]_0$ = 8 M; $[2\text{-HEI}]_0$ = 80 mM; $[catalyst]_0$ = 160 mM; $[V50]_0$ = 40 mM (Table 4.1, entries 3, 6, and 7). The symbols are indicated in the figure.

We also studied combinations of other catalysts. We combined BNI with potassium iodide (KI) instead of NaI (Table 4.1 (entry 8) and Figure 4.4 (squares)) and combined NaI with tributylmethylphosphonium iodide (BMPI) instead of BNI (Table 4.1 (entry 9) and Figure 4.4 (triangles)). These systems afforded similar results to that using NaI and BNI (Table 4.1 (entry 3)), generated polymers with $Đ$ = 1.38–1.49. The results suggest a wide catalyst scope in the present system. In what follows, we kept using the combination of NaI and BNI.

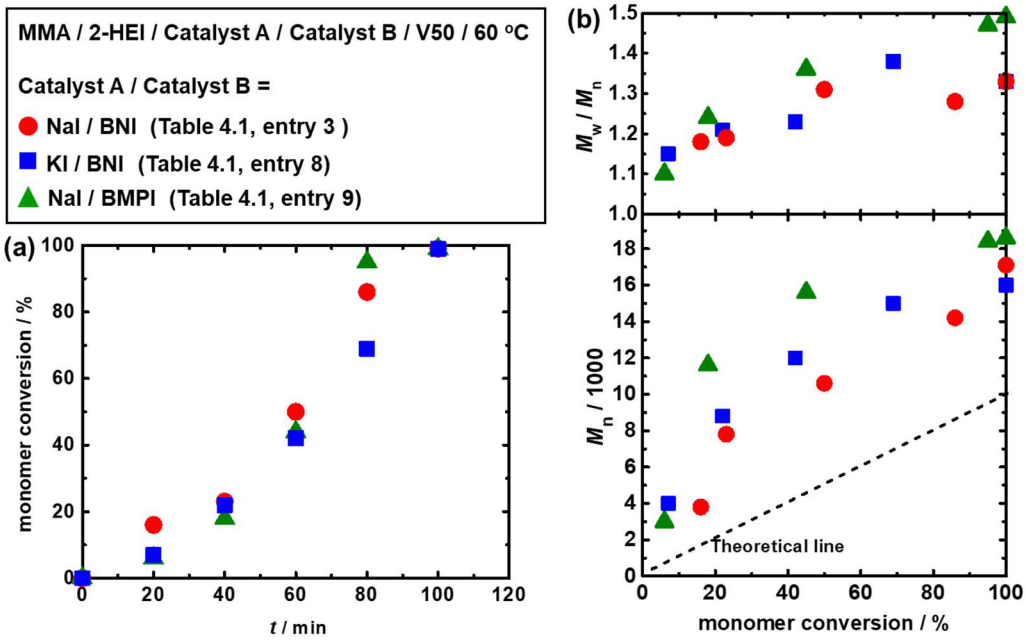

Figure 4.4. Plots of (a) monomer conversion vs *t* and (b) M_n and M_w/M_n vs conversion for the MMA/2-HEI/catalysts/V50 systems (60 °C) (Table 4.1, entries 3, 8, and 9). The symbols are indicated in the figure.

Studies on Alkyl Iodide Dormant Species.

2-HEI (alkyl iodide dormant species) bears a hydroxyl group and has an amphiphilic nature. We also studied more hydrophobic 2-hydroxyethyl 2-iodo-2-phenylacetate (2-HEPhI) bearing an aromatic ring (Figure 4.1) and hydrophilic 2-iodo-2-phenylacetic acid (2-IPhA) bearing a carboxylic acid (Figure 4.1).

We carried out a partitioning test of 2-HEI, 2-HEPhI, and 2-IPhA in organic and aqueous phases. We vigorously stirred a mixture of MMA (6 g, 100 equiv), alkyl iodide (1 equiv), and water (12 g) at 60 °C for 30 min (with no surfactant). After 30 min, the stirring was stopped to separate out the organic (MMA) and aqueous phases at 60 °C for 10 min. Each phase was then 1000 times diluted with methanol, and the UV-Vis absorption was measured. Figure 4.5 shows the absorption spectra of the MMA phase (red lines) and aqueous phase (blue lines) for 2-HEI (Figure 4.5a), 2-HEPhI (Figure 4.5b), and 2-IPhA (Figure 4.5c). Black lines

(Figure 4.5) show the alkyl iodides in pure methanol for reference. The alkyl iodides had an absorption peak at 284 nm (2-HEI) or 243 nm (2-HEPhI and 2-IPhA), and their absorption tailed to approximately 350 nm. From the absorbance in the MMA (red lines) and aqueous phases (blue lines), we calculated the partition of the alkyl iodides in each phase. The partition of 2-HEI was 96% in the MMA phase and 4% in the aqueous phase. While 2-HEI is amphiphilic, the result shows that 2-HEI tends to be soluble in an organic phase more than in an aqueous phase. The partition of 2-HEPhI was virtually 100% in the MMA phase, as expected from the hydrophobic nature of 2-HEPhI. The partition of 2-IPhA was virtually 100% in the aqueous phase, also as expected from the hydrophilic nature of 2-IPhA.

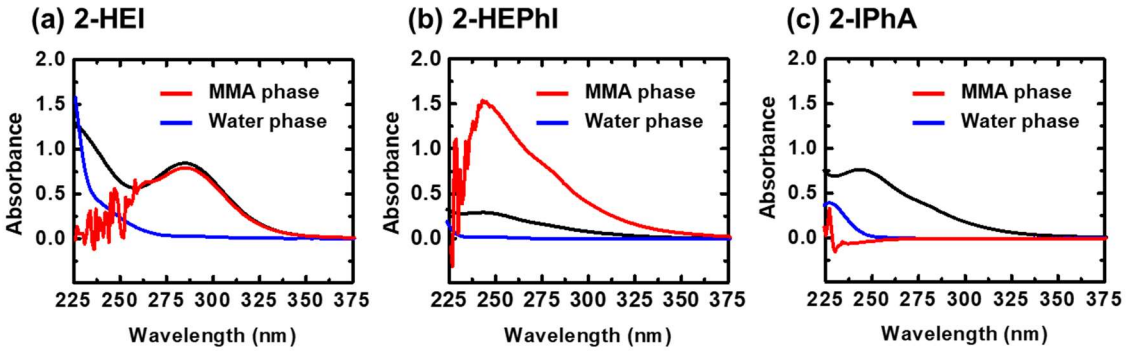

Figure 4.5. UV-Vis spectra for partitioning tests of (a) 2-HEI, (b) 2-HEPhI, and (c) 2-IPhA present in the MMA phase (red line) and the water phase (blue line). Each phase was diluted with methanol (1000 times). The black line represents the alkyl iodide in methanol (0.004 wt% in methanol) for reference.

Table 4.2. Emulsion polymerizations of MMA using Different Alkyl Iodide Initiating Dormant Species (R–I).[a]

Entry	Target DP[b]	R–I	$[MMA]_0/[R–I]_0/[NaI]_0/[BNI]_0/[V50]_0$ (mM)	T (°C)	t (min)	conv (%)	M_n ($M_{n,theo}$)[c]	$Đ$
1[d]	100	2-HEPhI	8000/80/80/80/40	60	120	94	8800 (9400)	1.20
2[d]	100	2-IPhA	8000/80/80/80/40	60	80	94	19000 (9400)	1.41
3[d]	200	2-HEPhI	8000/40/160/160/20	60	240	100	18000 (20000)	1.29
4[d]	400	2-HEPhI	8000/20/160/160/10	60	240	70	25000 (28000)	1.34
5[d]	800	2-HEPhI	8000/10/160/160/10	60	480	82	32000 (65000)	1.27
6[e]	100	2-HEPhI	8000/80/80/80/40	60	120	95	7100 (9500)	1.14
7[f]	100	2-HEPhI	8000/80/80/80/40	60	180	100	11000 (10000)	1.28
C1	100	2-HEPhI	8000/80/80/80/40 (in bulk)	60	150	25	3700 (2500)	1.10

[a]The emulsifier was Tween80/FES77 = (3/1 (w/w)). [b]Target degree of polymerization (DP) at 100% monomer conversion as calculated according to $[MMA]_0/[R–I]_0$. [c]Theoretical M_n value calculated according to $([MMA]_0/[R–I]_0)$ × (monomer conversion) × (molecular weight of MMA). [d]$[MMA]_0/[emulsifier]_0/[water]_0$ = 30.0/3.3/66.7 (w/w/w). [e]$[MMA]_0/[emulsifier]_0/[water]_0$ = 40.0/4.4/55.6 (w/w/w). [f]$[MMA]_0/[emulsifier]_0/[water]_0$ = 50.0/5.6/44.4 (w/w/w).

We compared the polymerizations using 2-HEI (Figure 4.6 (circles) and Table 4.1 (entry 3)), 2-HEPhI (Figure 4.6 (squares) and Table 4.2 (entry 1)), and 2-IPhA (Figure 4.6 (triangles) and Table 4.2 (entry 2)). While the M_n values somewhat deviated from the theoretical values in the 2-HEI system (Figure 4.6 (circles)), the M_n values almost perfectly matched the theoretical values in the 2-HEPhI system (Figure 4.6 (squares)), indicating a high and almost quantitative initiation from 2-HEPhI. 2-HEPhI is hydrophobic but bears a hydroxyl group and may still diffuse through the aqueous phase. A part of 2-HEPhI would initiate in the aqueous phase to generate oligomers to help the nucleation, and the rest of 2-HEPhI would be captured in the micelles and initiate inside the micelles. 2-HEPhI is more hydrophobic than 2-HEI and would efficiently be captured in the micelle. The balance of the initiation in the aqueous phase and the initiation in the micelles seemed just appropriate. The capture of 2-HEPhI in the micelles seemed quantitative, which would result in the nearly quantitative initiation. Another important factor would be the initiation (activation) rate. We previously

experimentally determined the activation rate constant k_a (Scheme 4.1a) of several alkyl iodides (R-I) catalyzed by BMPI at 70 °C. The k_a value for R = phenylacetate (13×10^{-3} M^{-1} s^{-1}) was approximately 6 times larger than that for R = isobutyrate (2.3×10^{-3} M^{-1} s^{-1}).[43] While the absolute k_a values depend on the catalyst (NaI and BNI in the present work) and temperature (60 °C in the present work), the kinetic result suggests that the initiation of 2-HEPhI with R = phenylacetate is faster than that of 2-HEI with R = isobutyrate in the present system. The faster initiation of 2-HEPhI would also contribute to the higher initiation efficiency of 2-HEPhI than that of 2-HEI.

In contrast, the use of the hydrophilic 2-IPhA resulted in a deviation of the M_n values from the theoretical values (Figure 6 (triangles)), although 2-IPhA has a phenylacetate structure as 2-HEPhI does. 2-IPhA tends to be partitioned in the aqueous phase, as mentioned above. Thus, 2-IPhA would not efficiently be captured in the micelle, which would explain the deviation of the M_n value (lower initiation efficiency). In RAFT emulsion polymerization, it was reported that oil-soluble (hydrophobic) macroRAFT agents led to higher initiation efficiency and better control in the polymerization with relatively low $Đ$ value.[44] According to the results from emulsion RCMP, we could also conclude that hydrophobic initiating dormant species have higher initiation efficiency, and can better control the polymerization.

Among all of the studied conditions (described above), the 2-HEPhI system using NaI and BNI as catalysts with Tween80 and FES77 as emulsifiers was the most optimized system (Figure 4.6 (squares) and Table 4.2 (entry 1)). The M_n value well matched the theoretical value, and the $Đ$ value was as low as 1.06−1.20 throughout the polymerization (up to 94% monomer conversion). The polymerization was also fast, as the monomer conversion reached 94% in 120 min.

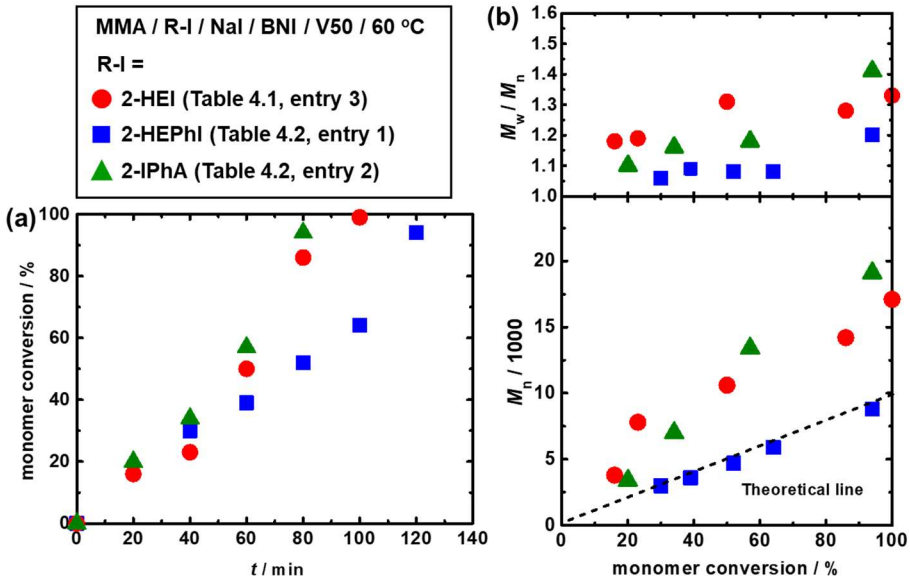

Figure 4.6. Plots of (a) monomer conversion vs t and (b) M_n and M_w/M_n vs conversion for the MMA/R–I/NaI/BNI/V50 systems using a mixture of Tween80 and FES77 emulsifiers (60 °C): $[MMA]_0 = 8$ M; $[R\text{-}I]_0 = 80$ mM; $[NaI]_0 = 80$ mM; $[BNI]_0 = 80$ mM; $[V50]_0 = 40$ mM (Table 4.1, entry 3, and Table 4.2, entries 1 and 2). The symbols are indicated in the figure.

The polymerization rate in the emulsion polymerization (Table 4.2 (entry 1)) was faster than that in the corresponding bulk polymerization (Table 4.2 (entry C1)). The polymerization rate in emulsion LRP is generally characterized by the segregation effect and the confined space effect.[2] The segregation effect increases the polymerization rate. It is a phenomenon that propagating radicals in separated particles ~~(micelles)~~ are segregated and cannot undergo termination (hence promote the polymerization). The observed increased polymerization rate would be explained by the segregation effect. The confined space effect decreases the polymerization rate and can operate when the particle size is small ~~(mini-emulsion)~~.[45] RCMP contains deactivators ($I_2^{\bullet-}$ and I_3^-) (Scheme 4.1), and their concentrations should be higher than that of the propagating radicals because of the so-called persistent radical effect.[46-47] The confined space effect operates when the particle size is so small (<15 nm, for example)[48-49] that even one deactivator molecule in one particle exceeds the corresponding bulk concentration of the deactivator. In such a case, the deactivation rate in the emulsion system is larger than that

in the bulk system, which brings about a decreased polymerization rate. ~~The present system is not a mini-emulsion system.~~ The observed particle sizes in the present work were typically 122–190 nm, as shown below. Therefore, the confined space effect would hardly operate in the present emulsion RCMP.

Study on Nucleation.

A possible mechanism of the nucleation in the present system is as follows when hydrophobic initiating dormant species is used (Figure 4.7a). This is a possible mechanism and other nucleation mechanisms may also operate. As mentioned above, in the beginning of the polymerization, hydrophobic MMA monomer droplets are dispersed in water. Emulsifiers form micelles in water. At an early stage of polymerization, MMA molecules diffuse from the monomer droplets to the micelles, and also MMA molecules slightly dissolved in water would polymerize from hydrophobic alkyl iodide initiating dormant species (2-HEI or 2-HEPhI) dissolved in water to generate oligomers, which would enter the micelles. Alkyl iodide initiating dormant species and catalysts may also diffuse into the micelles and initiate the polymerization in the micelles. Through these processes, nucleation would occur. The nucleation would usually be complete at an early stage of polymerization. Subsequently, MMA molecules continue to diffuse from the monomer droplets to the particles, and the polymerization would mainly occur in the particles, results in small deviation between the molecular weight and the theoretical value. When hydrophilic initiating dormant species (2-IPhA) is applied, the dormant species (initiator and short oligomers) will not be effectively captured by the micelles (discussed above in studies of alkyl iodide dormant species). Hence, polymers grow and terminate both in the partilcles and in the reaction medium, which causes large deviation between the molecular weight and the theoretical value (Figure 4.7b).

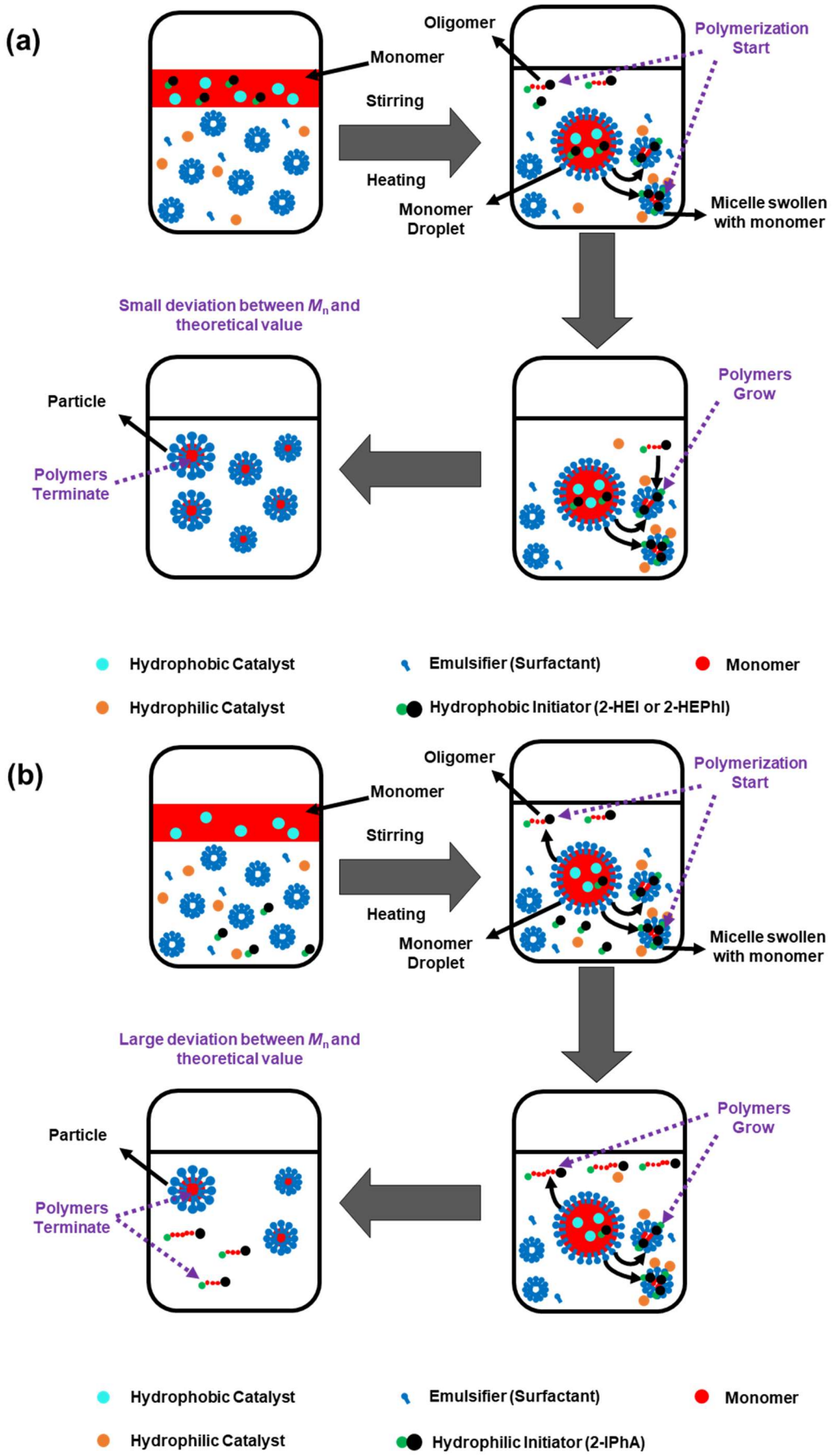

Figure 4.7. Proposed mechanism of emulsion RCMP if (a) using hydrophobic intiatiaor 2-HEI or 2-HEPhI; (b) using hydrophilic initiator 2-IPhA.

If this mechanism operates, the number of the particles would remain constant throughout the polymerization after the nucleation stage. To probe the mechanism, we calculated the number of particles in a representative system shown in Table 4.2 (entry 1), where the M_n values well matched the theoretical values and the $Đ$ values were $\leq$ 1.20 throughout the polymerization (up to 94% monomer conversion). An aliquot of the polymerization mixture was taken out at 40, 60, 80, 100, and 120 min of the polymerization, dried completely, and weighed, from which the solid content (sum of PMMA and emulsifier) was calculated (Table 4.3). Another aliquot was taken out at each time, diluted with water (25 times), and analyzed with dynamic light scattering (DLS). The DLS intensity-distribution curve (Figure 4.8) showed a mono-modal peak for all studied samples, and the peak-top particle size was 122–190 nm (Table 4.3). Assuming that the peak-top particle size is the diameter of the particle and the emulsifier was used up to cover the particle, and using 1.19 g/cm^3 for the density of PMMA[50] and 1.06 g/cm^3 for the average density of Tween80 and FES77,[51,52] we calculated the number of particle in 1 g of the polymerization mixture. The number of the particles (5.3×10^{13}–10.1×10^{13} particles/g) was in nearly the same order of magnitude at all studied polymerization times (above the 30% monomer conversion) (Table 4.3). The result suggests that the nucleation completed at an early stage of polymerization (below the 30% monomer conversion) and the number of the particles was virtually constant thereafter, as expected from the mentioned mechanism. (If we assume no emulsifier attached on the particle, the number of the particle was 4.0×10^{13}–8.7×10^{13} particles/g (Table 4.3)). The order of magnitude is the same and the number of the particles is virtually constant at all polymerization times on this assumption, too. The actual number of particles (the actual amount of emulsifier attached on the particle) would be between those on the two assumptions.)

Table 4.3. Solid Content and Particle Number in Emulsion Polymerization of MMA.[a]

Entry	$[MMA]_0/[2\text{-}HEPhI]_0/[NaI]_0/[BNI]_0/[V50]_0$ (mM)[b]	T (°C)	t (min)	conv (%)	Solid content (PMMA and emulsifier) (%)	Particle diameter (DLS) (nm)	Particle number calculated from solid content (PMMA and emulsifier) (particles/g)	Particle number calculated from PMMA only (particles/g)
1	8000/80/80/80/40	60	40	30	10.7	122	9.8×10^{13}	6.5×10^{13}
			60	39	14.2	164	5.3×10^{13}	4.0×10^{13}
			80	52	18.8	142	10.1×10^{13}	8.7×10^{13}
			100	64	24.0	164	8.9×10^{13}	7.5×10^{13}
			120	94	28.6	190	6.8×10^{13}	5.9×10^{13}

[a]The same system as Table 4.2 (entry 1). [b]$[MMA]_0/[emulsifier]_0/[water]_0$ = 30.0/3.3/66.7 (w/w/w). The emulsifier was a mixture of Tween80 and FES77 (3/1 (w/w)).

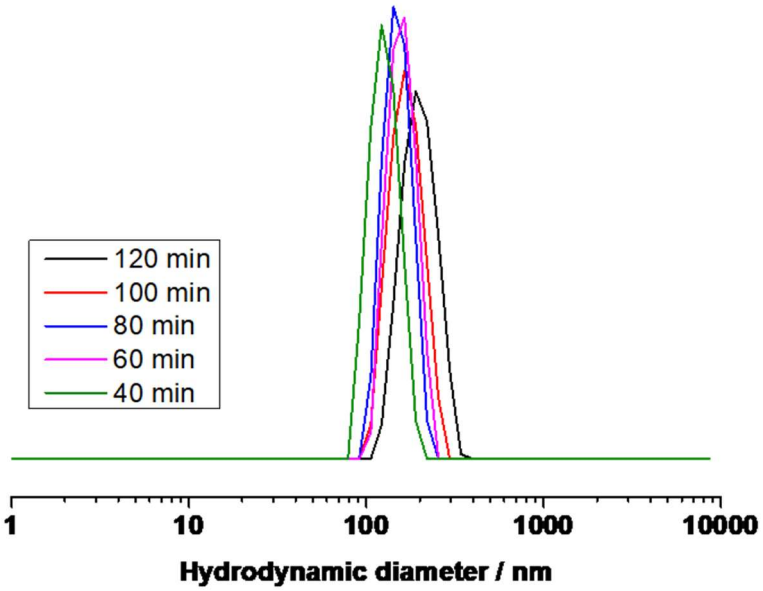

Figure 4.8. DLS intensity-distribution curves for the MMA/2-HEPhI/NaI/BNI/V50 (8000/80/80/80/40 mM) system using a mixture of Tween80 and FES77 emulsifiers (3/1 (w/w)) (Table 4.3 (entry 1)). The polymerization times are indicated in the figure.

Chain-end Fidelity.

We studied the iodide chain-end fidelity (livingness) of a PMMA-iodide (PMMA-I) synthesized in the representative system shown in Table 4.2 (entry 1). The polymer obtained at 60 min was purified by the reprecipitation (in a mixture of methanol and water (2/1 (v/v))) and further purified using preparative gel permeation chromatography (GPC) (M_n = 3900 and

$Đ$ = 1.09 after purification). Figure 4.9 shows ^{1}H NMR spectrum of the purified polymer. The methoxy protons (OCH_3) at the side chain (*a*, *a'*, and *a"*) appeared at 3.53–3.62 ppm. The main peak at 3.53-3.59 ppm is assigned to the repeating monomer units (*a*) in the middle of the chain. The terminal chain end unit (*a'*) adjacent to the iodide chain end appeared at 3.60–3.62 ppm, and the terminal chain end unit (*a"*) adjacent to the initiating 2-HEPh chain end appeared at 3.59–3.60 ppm. According to the ^{1}H NMR peak area and the M_n value (= 3900), the fraction of the iodide chain end was calculated to be nearly 100% (98% as calculated) with an experiment error, suggesting a high iodide chain-end fidelity. A small amount of dead polymers should be generated via radical-radical termination because the polymerization is a radical polymerization. V50 (0.5 equiv to 2-HEPhI) should also generate new chains, although the amount of the new chains would be relatively small because only 20% of V50 (hence 0.1 equiv to 2-HEPhI) decomposed for 60 min at the studied temperature of 60 °C and not all but a part of the generated radicals generate polymers or enter the particles. Nevertheless, the result indicates the dead polymer was relatively little in the present system.

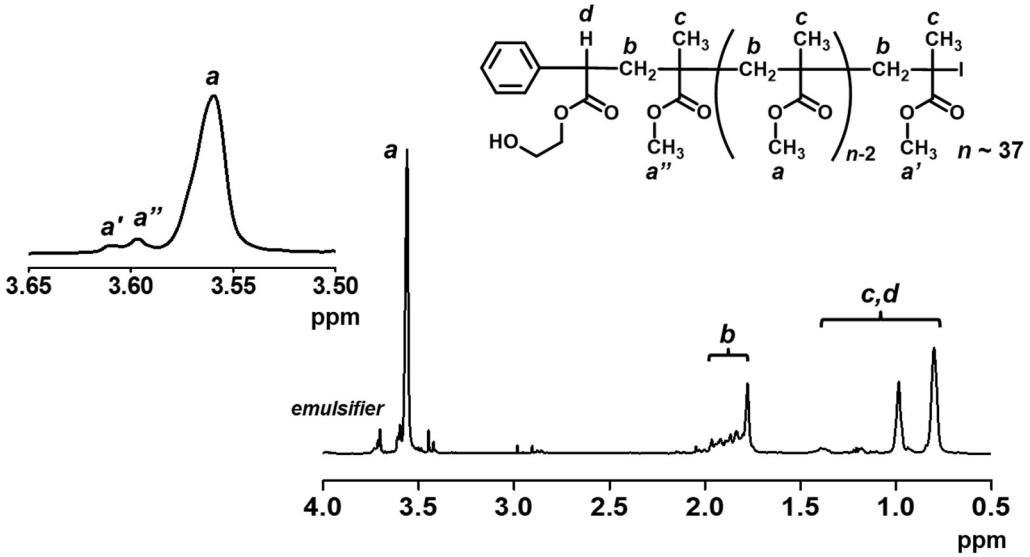

Figure 4.9. ^{1}H NMR spectrum ($CDCl_3$) of PMMA–I obtained in Table 4.2 (entry 1) after 60 min (M_n= 3900 and $Đ$ = 1.09 after purification).

Higher Molecular Weights and Higher Solid Contents.

We targeted higher degrees of polymerization (DPs) in the polymerizations of MMA using 2-HEPhI (alkyl iodide) and BNI and NaI (catalysts). We obtained low-dispersity ($Đ$ =1.27–1.34) polymers at high monomer conversions (70–100%) in relatively short times (240−480 min) up to the M_n values of 18000–32000 (Table 4.2 (entries 3-5)).

We also targeted the higher solid content by increasing the amount of MMA monomer from 30 wt% to 40 and 50 wt% in the polymerization mixture (Table 4.2 (entries 6 and 7)). We obtained stable particles with up to high (95–100%) monomer conversions even in these high solid content systems. The polymerizations were also relatively fast (95–100% monomer conversions for 120–180 min). The result shows the high productivity of the present emulsion RCMP, which would be attractive for industrial applications.

Functional Methacrylates.

Besides MMA, we studied functional methacrylates, i.e., benzyl methacrylate (BzMA) with a benzyl group, glycidyl methacrylate (GMA) with an epoxide, and 2-hydroxyethyl methacrylate (HEMA) with a hydroxyl group, using 2-HEPhI as an initiating dormant species (Table 4.4 (entries 1-3)). The polymerization of BzMA completed in 1 h (monomer conversion = 100%), generating a polymer with M_n = 18000 and $Đ$ = 1.42. BzMA is more hydrophobic than MMA and the generated particles in the BzMA system would be easier to be stabilized. The hydrolysis of the epoxide of GMA is significant at high temperatures such as 80 °C.[53] Tan et al. reported a successful emulsion RAFT polymerization of GMA at 50 °C with a 98% epoxide functionality retention.[54] Hence, we carried out the emulsion polymerization of GMA at 60 °C. The polymerization proceeded to a 64% monomer conversion for 2 h, attaining a relatively low $Đ$ (= 1.43) value. The CH proton in the epoxide group (*c*) and the CH_3 protons

in the polymer backbone (*a*) appeared at 3.24 and 0.84−1.35 ppm, respectively. According to the peak area for proton *c* and protons *a* in the ^{1}H NMR spectrum, the fraction of the retained epoxide functionality in the polymer chain was nearly 100% (98% as calculated). (Figure 4.10). The polymerization of HEMA (Table 4.4 (entry 3)) is an example of dispersion polymerization (not emulsion polymerization). HEMA (monomer) is soluble in water, but PHEMA (polymer) is not soluble in water. Therefore, mechanistically, the polymerization of HEMA started in the water phase, and after reaching a critical chain length, particles were formed and the polymerization proceeded inside the particles. After 3 h, the monomer conversion reached 57%, a polymer with $Đ$ = 1.47 was generated.

Table 4.4. Emulsion Polymerizations of Functional Methacrylates.[a]

Entry	Target DP[b]	Monomer	R–I	[Monomer]$_0$/[2-HEPhI]$_0$/[NaI]$_0$/[BNI]$_0$/[V50]$_0$ (mM)	T (°C)	t (h)	Conv (%)	M_n[c] ($M_{n,theo}$)[d]	$Đ$[c]
1	100	BzMA	2-HEPhI	8000/80/80/80/40	60	1	100	18000 (18000)	1.42
2	100	GMA	2-HEPhI	8000/80/80/80/40	60	2	64	14000 (8900)	1.43
3	100	HEMA	2-HEPhI	8000/80/80/80/40	60	3	57	10000 (7400)	1.47

[a][Monomer]$_0$/[emulsifier]$_0$/[water]$_0$ = 30.0/3.3/66.7 (w/w/w). The emulsifier was a mixture of Tween80 and FES77 (3/1 (w/w)). [b]Target degree of polymerization (DP) at 100% monomer conversion as calculated according to [Monomer]$_0$/[R–I]$_0$. [c]PMMA-calibrated GPC values (DMF eluent). [d]Theoretical M_n value calculated according to ([Monomer]$_0$/[R–I]$_0$) × (monomer conversion) × (molecular weight of monomer).

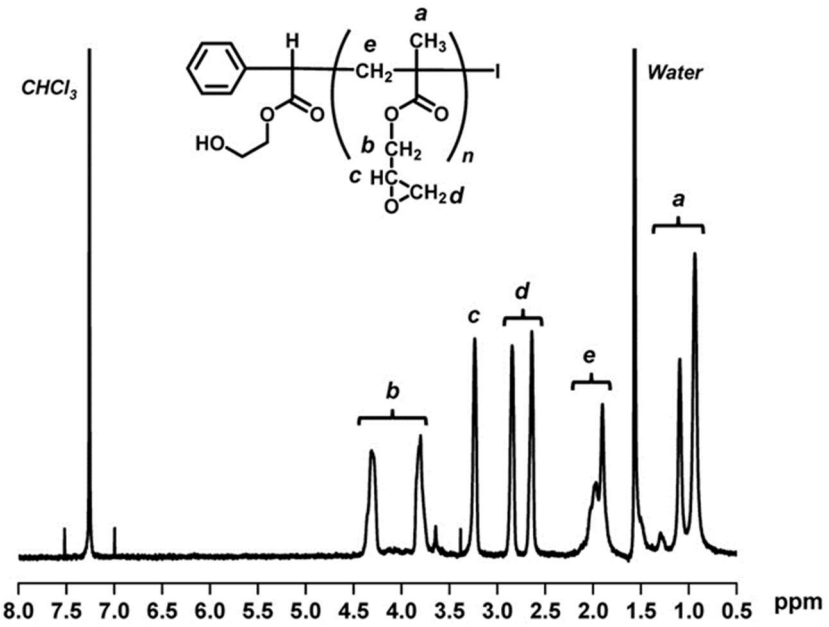

Figure 4.10. ^{1}H NMR ($CDCl_3$) spectrum of PGMA obtained in Table 4.4 (entry 2) (M_n = 16000 and $Đ$ = 1.50 after purification).

Styrene.

We studied another family of monomer, i.e., styrene (St). In contrast to the MMA system, where a combined use of Tween80 and FES77 was required, the styrene system required only the single use of Tween80. The ionic surfactant (FES77) was not required, because of the higher stability of the particles generated from the more hydrophobic St. No precipitation was observed by solely using Tween80.

We used 2-HEI as an alkyl iodide initiating dormant species and co-used NaI and BNI as catalysts. We heated a mixture of St (100 equiv, 30.0 wt%), 2-HEI (1 equiv), NaI (2 equiv), BNI (2 equiv), V50 (1 equiv), Tween80 (5.0 wt%), and water (65.0 wt%) at 60 and 70 ˚C (Table 4.5 (entries 1 and 2)). The monomer conversion reached 82-90% in 4 h, generating a low-dispersity polymer ($Đ$ = 1.24−1.29) in both cases. At the higher temperature of 70 °C, the polymerization was faster, and thus we further studied the amount of surfactant (Tween80) at 70 °C. We increased the amount of Tween80 from 5.0% (Table 4.5 (entry 2)) to 10.0% (Table 4.5 (entry 3) and Figure 4.11). A high monomer conversion (92%) was attained in 3 h with 10% of Tween80, yielding a polystyrene with M_n = 16000 and $Đ$ = 1.25. The relatively faster

polymerization from 2.5 h to 3 h could be attributed to gel effect.[55-56] We further increased the temperature to 80 °C. The polymerization was fast and the monomer conversion reached 99% for 4 h. However, the M_n values nearly twice deviated from the theoretical values even at 80 °C, suggesting an approximately 50% initiation efficiency of 2-HEI. Thus, instead of 2-HEI, 2-HEPhI, which showed higher initiation efficiency in the MMA system, was used in the St system at 70 °C (Table 4.5 (entry 5)). While the low $Đ$ value (= 1.24) was attained, the M_n value still nearly twice deviated from the theoretical value. The reason for the deviation is not clear at this moment. In addition, around 70% of V50 (0.7 equiv to 2-HEPhI) decomposed for 3 h at the studied temperature of 70 °C, hence the obtained polystyrene contained approximately 35% dead chains generated from V50, although the $Đ$ value was small. Without the catalyst (NaI/BNI), the $Đ$ value was large (1.75) (Table 4.5 (entry 6)), which is the iodide transfer (pure degenerative chain transfer) system. The degenerative chain transfer constant in the St system at 70 °C is 3.8,[57-58] which is relatively small and explains the observed large $Đ$ value. The results (Table 4.5 (entries 5 and 6)) clearly show the effectiveness of the catalysts (NaI/BNI) to achieve the low dispersity. Thus, the emulsion RCMP of St generated low-dispersity polymers, although the initiation efficiency was approximately 50% for an unclear reason.

Table 4.5. Emulsion Polymerization of St.

Entry	target DP[a]	R–I	Emulsifier[b]/ water (wt%)	$[St]_0/[R\text{-}I]_0/[NaI]_0/[BNI]_0/[V50]_0$ (mM)	T (°C)	t (h)	conv (%)	M_n ($M_{n,theo}$)[c]	$Đ$
1	100	2-HEI	5.0/65.0	8000/80/160/160/80	60	4	82	18000 (8500)	1.24
2	100	2-HEI	5.0/65.0	8000/80/160/160/80	70	4	90	13000 (9400)	1.29
3	100	2-HEI	10.0/60.0	8000/80/160/160/40	70	3	92	16000 (9600)	1.25
4	100	2-HEI	10.0/60.0	8000/80/160/160/40	80	4	99	20000 (10000)	1.27
5	100	2-HEPhI	10.0/60.0	8000/80/160/160/40	70	4	92	18000 (9600)	1.24
6	100	2-HEPhI	10.0/60.0	8000/80/0/0/40	70	4	70	36000 (7300)	1.75

[a]Target degree of polymerization at 100% monomer conversion (calculated by $[St]_0/[R–I]_0$). [b]The emulsifier was Tween80. [c]Theoretical M_n value calculated according to $([St]_0/[R–I]_0)$ × (monomer conversion) × (molecular weight of St).

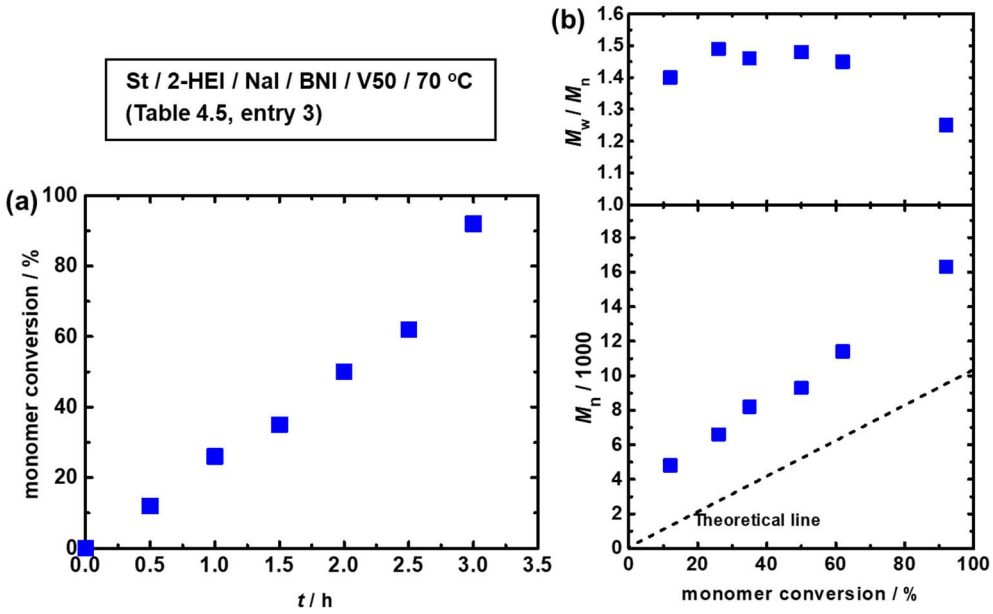

Figure 4.11. Plots of (a) monomer conversion vs t and (b) M_n and M_w/M_n vs conversion for the St/2-HEI/NaI/BNI/V50 system using Tween80 as an emulsifier (70 °C) (Table 4.5, entry 3): $[St]_0 = 8$ M; $[2\text{-HEI}]_0 = 80$ mM; $[NaI]_0 = 160$ mM; [BNI] = 160 mM; $[V50]_0 = 40$ mM.

4.3. Conclusions.

The emulsion RCMPs of MMA successfully generated stable polymer particles using the mixture of (non-ionic) Tween80 and (ionic) FES77 emulsifiers. The co-use of NaI and BNI as catalysts and the use of 2-HEPhI as an alkyl iodide initiator achieved nearly quantitative initiation and generated low-dispersity polymers ($Đ$ = 1.1−1.3) at high (30-50%) contents of MMA monomer. The emulsion RCMPs of functional methacrylates and St also generated stable particles and low-dispersity polymers. The emulsion RCMP combines the advantages of emulsion polymerization such as efficient heat transfer, low viscosity, and high polymerization rate with those of RCMP such as no use of special capping agents or toxic catalysts. The high solid content, high chain-end fidelity, good monomer versatility achievable in the emulsion RCMP would also be attractive for polymer material design and industrial applications.

4.4. Experimental.

Materials.

Methyl methacrylate (MMA) (>99.8%, Tokyo Chemical Industry (TCI), Japan), styrene (>99.0%, TCI), benzyl methacrylate (BzMA) (>98.0%, TCI), glycidyl methacrylate (GMA) (>95.0%, TCI), 2-hydroxyethyl methacrylate (HEMA) (>95.0%, TCI), sodium iodide (NaI) (>99.0%, Sigma-Aldrich, USA), potassium iodide (KI) (>99.5%, TCI), tetrabutylammonium iodide (BNI) (>98.0%, TCI), tributylmethylphosphonium iodide (BMPI) (>98.0%, TCI), Tween-80 (the ester group derived from oleic acid (≥58.0%) and from primarily linoleic, palmitic, and stearic acids (balance), Sigma-Aldrich), FES-77 (33.0% of FES and 67.0% of water, BASF, Shanghai), and 2,2'-azobis(2-methylpropionamide) dihydrochloride (V50) (95%, Wako Pure Chemical, Japan) were used as received. 2-Hydroxyethyl 2-iodoisobutyrate (2-HEI) (>90.0%), 2-hydroxyethyl 2-iodo-2-phenylacetate (2-HEPhI) (>85.0%), and 2-iodophenylacetic acid (2-IPhA) (>94.0%) were provided through the courtesy of Godo Shigen Co., Ltd. (Japan) and used as received.

Measurements.

The GPC analysis was performed using same instruments as mentioned in Chapter 2 (Section 2.4). GPCs were equipped with same columns as Chapter 2 and columns were calibrated with standard poly(methyl methacrylate)s (PMMAs) for THF-GPC, and poly(methyl methacrylate)s (PMMAs) and polystyrenes (PSts) for DMF-GPC. The flow rate was 0.7 mL/min (40 °C) for THF eluent and 0.34 mL/min (40 °C) for DMF eluent.

The ^{1}H NMR spectra were recorded on Bruker (Germany) AV500 spectrometer (500 MHz) or AV300 (300 MHz) at ambient temperature. $CDCl_3$ (for purified polymers), acetone-d_6 (for crude methacrylate polymers), and tetrahydrofuran-d_8 (for crude styrene polymers) (Cambridge Isotope Laboratories, USA) were used as the solvents for the NMR analysis, and

the chemical shift was calibrated using residual undeuterated solvents or tetramethylsilane (TMS) as the internal standard. The monomer conversion was determined with ^{1}H NMR.

The polymer shown in Figure 4.9 was purified with a preparative GPC. The instrument and procedure were the same as mentioned in Chapter 2.

The DLS measurement was carried out on a Malvern Zetasizer Nano ZSP (Worcestershire, UK) at room temperature. The test angle for the DLS analysis was 173° (backscattering detection).

The UV-Vis absorption spectra were recorded on a Shimadzu UV-3600 (Kyoto, Japan) at room temperature with a quartz cell with an optical path length of 1 cm.

General procedure for polymerization.

In a typical run, a mixture of a monomer (25.0 g, 30.0-50.0 wt%), an alkyl iodide initiator, an azo initiator, catalysts, emulsifier (1.7-10.0 wt%), and deionized water (44.4-66.7 wt%) was heated in a reaction vessel at 60−80 °C under argon atmosphere with mechanical stirring (1000 rpm). The vessel was a 100 mL jacketed cylindrical reaction vessel (ChemGlass, USA) connected with an overhead mechanical stirrer (Heidolph, Germany) and immersed in a water bath (Lauda, Germany). After a prescribed time *t*, an aliquot (2 mL) of the solution was taken out by a syringe, cooled to room temperature, and analyzed with GPC (DMF as eluent) and ^{1}H NMR.

Synthesis of PMMA−I for chain-end fidelity analysis (Figure 4.9).

A mixture of MMA (25.0 g, 8 M, 30.0 wt%), 2-HEPhI (0.8 g, 80 mM), V50 (0.3 g, 40 mM), BNI (0.9 g, 80 mM), NaI (0.4 g, 80 mM), emulsifiers (Tween80/FES77 (3:1 (w/w))) (2.8 g, 3.3 wt%), and deionized water (54.9 g, 66.7 wt%) was heated in a reaction vessel at 60 °C for 1 h under argon atmosphere with mechanical stirring. At 1 h (monomer conversion = 43%), an aliquot (10 mL) of the mixture was taken out, cooled to room temperature, reprecipitated in

methanol/water (2/1 (v/v)) (200 mL), and dried. The polymer was diluted with chloroform (10 mL) and subsequently purified with preparative GPC. The purified PMMA−I (M_n = 3900 and $Đ$ = 1.09) was obtained as a yellow solid and subsequently analyzed with GPC (THF as eluent) and ^{1}H NMR.

Partitioning test of initiators using UV-Visible spectroscopy.

A mixture of MMA (6.0 g, 100 equiv), alkyl iodide (1 equiv), and water (12.0 g) was stirred at 60 °C for 30 min under magnetic stirring. After 30 min, stirring was stopped, reaction mixture was settled down at 60 °C for 10 min to separate the organic (MMA) and aqueous phases. An aliquot (0.005 g) of each phase was separately taken out, diluted with 5 g methanol, and the absorption was measured with UV-Vis spectrophotometer (Figure 4.5). The partitions of the initiator in the two phases were calculated from equations 1 and 2:

(Partition of initiator in MMA) = (absorbance of the initiator in organic (MMA) phase) / [(absorbance of initiator in organic phase) + 2 × (absorbance of initiator in aqueous phase)] (equation 1)

(Partition of initiator in water) = 1 – (partition of initiator in MMA) (equation 2)

Solid content test (Table 4.3 (entry 1)).

An empty dry glass petri dish covered with aluminum foil was weighed (G1). An aliquot (1.5 g) of the MMA polymerization mixture (Table 4.3 (entry 1)) was put on the petri dish and weighed (G2). After that, the petri dish was dried in the oven at 90 °C for 1 day, subsequently desiccated for overnight, and reweighed (G3). The solid content is calculated from equation 3:

(Solid content) = (G3 – G1) / (G2 – G1) (equation 3).

Particle size analysis (Table 4.3 (entry 1)).

Particle size was analyzed using DLS for the samples in Table 4.3 (entry 1). An aliquot (0.01 g) of the reaction mixture was diluted with water (25 times) and analyzed using DLS (Figure 4.8).

References.

1. Yamak, H. B. In *Polymer Science*, IntechOpen, **2013**; pp 35-72
2. Zetterlund, P. B.; Kagawa, Y.; Okubo, M. *Chem. Rev.* **2008**, 108, 3747-3794.
3. Zetterlund, P. B.; Thickett, S. C.; Perrier, S.; Bourgeat-Lami, E.; Lansalot, M. *Chem. Rev.* **2015**, 115, 9745-9800.
4. Qiu, J.; Gaynor, S. G. Matyjaszewski, K. *Macromolecules* **1999**, 32, 2872-2875.
5. Peng, H.; Cheng, S.; Fan, Z. *Polymer Engineering & Science* **2005**, 45*,* 297-302.
6. Min, K.; Gao, H.; Yoon, J. A.; Wu, W.; Kowalewski, T. Matyjaszewski, K. *Macromolecules* **2009**, 42, 1597-1603.
7. Cordero, R.; Jawaid, A.; Hsiao, M.-S.; Lequeux, Z.; Vaia, R. A.; Ober, C. K. *ACS Macro Lett* **2018**, 7, 459-463.
8. Banin, G.; Vieira, R. P.; lona, L. M. F. *Chemical Engineering Jornal* **2021**, 407, 126999.
9. Dong, H.; Matyjaszewski, K. *Macromolecules* **2010,** 43, 4623-4628.
10. Wang, Y.; Lorandi, F.; Fantin, M.; Chmielarz, P.; Isse, A. A.; Gennaro, A.; Matyjaszewski, K. *Macromolecules* **2017**, 50, 8417-8425.
11. Kagawa, Y.; Kawasaki, M.; Zetterlund, P. B.; Minami, H.; Okubo, M. *Macromol. Rapid Commun.* **2007**, 28, 2354-2360.
12. Cuneo, T.; Wang, X.; Shi, Y.; Gao, H. *Macromol. Chem. Phys.* **2020**, 221, 2000008.
13. Wang, Y.; Dadashi-Silab, S.; Lorandi, F.; Matyjaszewski, K. *Polymer* **2019**, 165, 163-167.
14. Ciftci, M.; Tasdelen, M. A.; Li, W.; Matyjaszewski, K.; Yagci, Y. *Macromolecules* **2013**, 46, 9537-9543.
15. Fantin, M.; Park, S.; Wang, Y.; Matyjaszewski, K. *Macromolecules* **2016**, 49, 8838-8847.
16. Fantin, M.; Chmielarz, P.; Wang, Y.; Lorandi, F.; Isse, A. A.; Gennaro, A.; Matyjaszewski, K. *Macromolecules* **2017**, 50, 3726-3732.
17. Ferguson, C. J.; Hughes, R. J.; Pham, B. T. T.; Hawkett, B. S.; Gilbert, R. G.; Serelis, A. K.; Such, C. H. *Macromolecules* **2002**, 35, 9243-9245.
18. Zhou, J.; Yao, H.; Ma, J. *Polym. Chem.* **2018**, 9, 2532-2561.
19. Karagoz, B.; Esser, L.; Duong, H. T.; Basuki, J. S.; Boyer, C.; Davis, T. P. *Polym. Chem.* **2014**, 5, 350-355.
20. Liu, C.; Hong, C.-Y.; Pan, C.-Y. *Polym. Chem.* **2020**, 11, 3673-3689.
21. Poon, C. K.; Tang, O.; Chen, X.-M.; Pham, B. T. T.; Gody, G.; Pollock, C. A.; Hawkett, B. S.; Perrier, S. *Biomacromolecules* **2016**, 17, 965-973.
22. Poon, C. K.; Tang, O.; Chen, X.-M.; Kim, B.; Hartlieb, M.; Pollock, C. A.; Hawkett, B. S.; Perrier, S. *Macromol. Biosci* **2017**, 17, 1600366.
23. Engström, J.; Hatton, F. L.; Wågberg, L.; D'Agosto, F.; Lansalot, M.; Malmströma, E.; Carlmark, A. *Polym. Chem.* **2017**, 8, 1061-1073.
24. Gurnani, P.; Perrier, S. *Prog. Polym. Sci.* **2020**, 102, 101209.
25. Marestin, C.; Noël, C.; Guyot, A.; Claverie, J. *Macromolecules* **1998**, 31, 4041-4044.
26. Nicolas, J.; Charleux, B.; Guerret, O.; Magnet, S. *Angew. Chem. Int. Ed.* **2004**, 43, 6186-6189.
27. Nicolas, J.; Ruzette, A.-V.; Farcet, C.; Ge´rard, P.; Magnet, S.; Charleux, B. *Polymer* **2007**, 48, 7029-7040.
28. Tajbakhsh, S.; Hajiali, F.; Marić, M. *Ind. Eng. Chem. Res* **2020**, 59, 8921-8936.
29. Okubo, M.; Sugihara, Y.; Kitayama, Y.; Kagawa, Y.; Minami, H. *Macromolecules* **2009**, 42, 1979-1984.
30. Su, X.; Jiang, Y.; Jessop, P. G.; Cunningham, M. F.; Feng, Y. *Macromolecules* **2020**, 53, 6018-6023.
31. Tonnar, J.; Lacroix-Desmazes, P. *Polymer* **2016**, 106, 267-274.

32. Sue-eng, S.; Boonchuwong, T.; Chaiyasat, P.; Okubo, M.; Chaiyasat, A. *Polymer* **2017**, 110, 124-130.
33. Tonnar, J.; Lacroix-Desmazes, P.; Boutevin, B. *Macromolecules* **2007**, 40, 186-190
34. Tonnar, J.; Lacroix-Desmazes, P.; Boutevin, B. *Macromolecules* **2007**, 40, 6076-6081
35. Goto, A.; Suzuki, T.; Ohfuji, H.; Tanishima, M.; Fukuda, T.; Tsujii, Y.; Kaji, H. *Macromolecules* **2011**, 44, 8709-8715.
36. Goto, A.; Ohtsuki, A.; Ohfuji, H.; Tanishima, M.; Kaji, H. *J. Am. Chem. Soc*. **2013**, 135, 11131-11139.
37. Wang, C.-G.; Chong, A. L. C.; Pan, H. M.; Sarkar, J.; Tay, X. T.; Goto, A. *Polym. Chem.* **2020**, 11, 5559-5571.
38. Sarkar, J.; Xiao, L.; Goto, A. *Macromolecules* **2016**, 49, 5033-5042.
39. Wang, C.-G.; Hanindita, F.; Goto, A. *ACS Macro Lett.* **2018**, 7, 263-268.
40. Mao, W.; Wang, C.-G.; Goto, A. *Polym. Chem.* **2020**, 11, 53-60.
41. Sarkar, J.; Xiao, L.; Jackson, A. W.; van Herk, A. M.; Goto, A. *Polym. Chem.* **2018**, 9, 4900-4907.
42. Sarkar, J.; Chan, K. B. J.; Goto, A. *Polym. Chem.* **2021**, 12, 1060-1067.
43. Lei, L.; Tanishima, M.; Goto, A.; Kaji, H.; Yamaguchi, Y.; Komatsu, H.; Jitsukawa, T.; Miyamoto, M.. *Macromolecules* **2014**, 47, 6610-6618.
44. Luo, Y.; Wang, X.; Li, B.-G.; Zhu, S. *Macromolecules* **2011**, 44, 221-229.
45. Simms, R. W.; Cunningham, F. *Macromolecules* **2008**, 41, 5148-5155.
46. Fischer, H. *J. Polym. Sci., Part A: Polym. Chem.* **1999**, 37, 1885-1901.
47. Fischer, H. *Chem. Rev.* **2001**, 101, 3581-3610.
48. Tomoeda, S.; Kitayama, Y.; Wakamatsu, J.; Minami, H.; Zetterlund, P. B.; Okubo, M. *Macromolecules* **2011**, 44, 5599-5604
49. Zetterlund, P. B. *Polym. Chem.* **2011**, 2, 534-549.
50. Van der Lee, A.; Hamon, L.; Holl, Y.; Grohens, Y. *Langmuir* **2001**, 17, 7664-7669.
51. The density of Tween80 is 1.06 g/cm^3, https://www.sigmaaldrich.com/SG/en/product/sial/p1754, (accessed 9 June 2021).
52. The density of FES77 is 1.05 g/cm^3, https://chemical.carytrad.com.tw/uploads/1/2/3/8/123848866/tds_disponil_bes_fes_types_en.pdf, (accessed 9 June 2021).
53. Weaver, J. V. M.; Bannister, I.; Robinson, K. L.; Bories-Azeau, X.; Armes, S. P. *Macromolecules* **2004**, 37, 2395-2403.
54. Zhang, Y.; He, J.; Dai, X.; Yu, L.; Tan, J.; Zhang, L. *Polym. Chem.* **2019**, 10, 3902-3911.
55. Yang, L.; Luo, Y.; Liu, X.; Li, B. *Polymers* **2009**, 50, 4334-4342.
56. Xu, S.; Huang, J.; Xu, S.; Luo, Y. *Polymers* **2013**, 54, 1779-1785.
57. Goto, A.; Ohno, K.; Fukuda, T. *Macromolecules* **1998**, 31, 2809-2814.
58. Lansalot, M.; Farcet, C.; Charleux, B.; Vairon, J.-P. *Macromolecules* **1999**, 32, 7354-7360.

Chapter 5. Systematic Studies of Copolymer Synthesis in Aqueous Media via RCMP

Abstract.

Copolymerizations via reversible complexation mediated polymerization (RCMP) were systematically studied in aqueous media. Based on the success in developing emulsion RCMP in Chapter 4, we carried out block copolymerizations using poly(methyl methacrylate)–I (PMMA–I) polymers as macroinitiators in emulsion RCMP. Well-defined hydrophobic-hydrophobic block copolymers ($Đ$ = 1.36–1.47) were successfully synthesized through one-pot reactions with high monomer conversions in relatively short reaction times, where $Đ$ is the dispersity. Random copolymerizations of methyl methacrylate (MMA) and butyl acrylate (BA), MMA and styrene (St), and MMA and benzyl methacrylate (BzMA) via emulsion RCMP yielded random and gradient copolymers with high monomer conversions, and the gradient sequence was tuned by the reaction temperature. Monomers with anti-fouling properties were utilized to synthesize various hydrophilic-amphiphilic block copolymers via solution RCMP in water, ethanol, or a mixture of water and ethanol. The polymers were used for surface modification of membranes, and anti-fouling tests were carried out. The accessibility to a range of copolymers via the RCMP in aqueous media was demonstrated.

5.1 Introduction.

Water is widely used as a reaction solvent due to several reasons: (i) water is abundant, inexpensive, non-flammable, and non-toxic, (ii) water has the highest value of specific heat capacity among liquids, and (iii) water can provide regulatable reaction environments such as biphasic systems and control in pH and ionic strength.[1-2] As mentioned in the previous chapters, water is also used as a solvent in living radical polymerization (LRP) for, e.g., solution polymerization, dispersion polymerization, and emulsion polymerization.

Aqueous emulsion LRP is used to synthesize not only homopolymers but also random and block copolymers. For block copolymerizations, polymerization-induced self-assembly (PISA) has been studied in recent years. In PISA, a hydrophilic homopolymer (A) is chain-extended by a second monomer (B). The generated block copolymer gradually becomes insoluble in the solvent, which drives the self-assembly of the copolymer. By varying the degrees of polymerization (DPs) of the two blocks, spheres, worms, vesicles and other nano-structures are formed.[4-5] The combination of emulsion LRP with PISA provides such nano-structures with high colloidal stabilities and high solid contents.[5] PISA was introduced in emulsion reversible addition-fragmentation chain transfer (RAFT) polymerization in 2002 for the synthesis of poly(acrylic acid)-*block*-poly(butyl acrylate) copolymer.[6] For emulsion LRP-PISA, emulsion RAFT-PISA is used in many cases due to the amenability of the RAFT polymerization to various monomers and solvents.[7-9] Emulsion RAFT copolymerization is also used for synthesizing multiblock copolymers. The obtained multiblock copolymers have been used for, e.g., thermoplastic elastomers, polymeric phase separation, and drug delivery.[10-13]

In emulsion LRP copolymerizations, the copolymers are generally prepared in two-step synthesis, requiring a purification step between the two steps. For example, in emulsion RAFT copolymerizations, macroRAFT agents are synthesized and purified first, and subsequently react with the second monomer.[14-15] Similarly, emulsion nitroxide-mediated polymerization

(NMP) uses purified macroinitiators with alkoxyamine chain end for block copolymerization.[16-17] The two-step synthesis and purification require time and cost in operation.

In Chapter 4, we demonstrated emulsion polymerizations of methacrylates and styrene via RCMP to yield low-dispersity homopolymers with high solid contents. In Chapter 4, we obtained a poly(methyl methacrylate)–I (PMMA–I) with high iodide chain-end fidelity, which may further be used as a macroinitiator for synthesizing copolymers via emulsion RCMP. Emulsion RCMP may also be used for random copolymerizations. Temperature-dependent one-pot synthesis of random, gradient, and block-like copolymers may be attained by exploiting different monomer reactivity ratios, different solubilities in water, and different terminal carbon-iodine bond energies of the dormant species for studied monomers. Gradient copolymers are copolymers that have a gradual change in monomer composition along the chain are gradient copolymers (Scheme 5.1c). Unlike random (Scheme 5.1a) and block copolymers (Scheme 5.1b), gradient copolymers can have unique properties such as broad glass transition temperature (T_g) and relaxation time distribution.[18] Gradient copolymers can also serve as alternatives of block copolymers in applications for, e.g., dispersants and compatibilizers.[19-22]

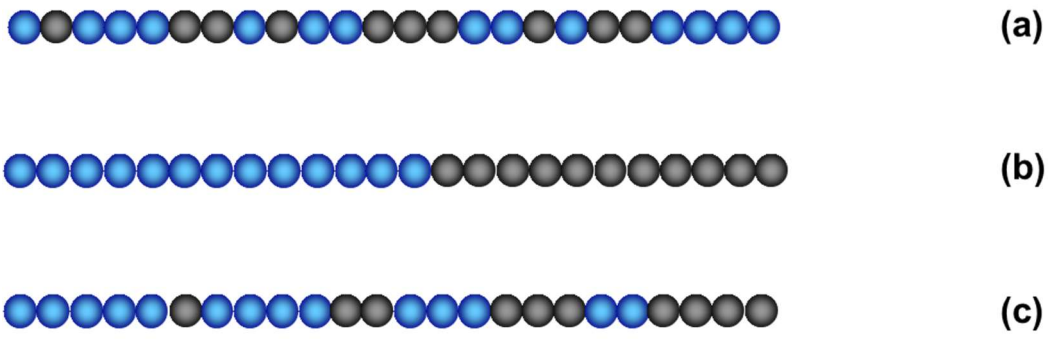

Scheme 5.1. Example of a (a) random copolymer, (b) block copolymer, and (c) gradient copolymer.

As another research topic, we are interested in polymers that can contribute to water purification. In 2018, UN World Water Development Report updated the water risk situation; namely, 47% of the global population faces a shortage of freshwater.[23] To deal with the demand for freshwater, desalination is extensively utilized to convert saline water to freshwater.[24] Membrane technologies are involved in desalination, and reverse osmosis (RO) is utilized for energy-saving and simple operations.[25] However, a common challenge that limits membrane performance is membrane fouling, which is caused by microbial growth, undesirable chemisorption, and pore-clogging. The fouling reduces the water flux, increases the energy consumption and operation cost, and shortens the membrane lifespan.[25-26] Therefore, the development of membranes with anti-fouling properties has been an important research topic in recent years.

In general, with an increase in the hydrophilicity of the membrane surface, a denser hydration layer is generated on the surface, thereby effectively blocking foulants such as proteins, polysaccharides, and enzymes which are hydrophobic in nature.[27] Thus, modification of membrane surfaces with hydrophilic molecules is an effective approach for anti-fouling. A particularly useful approach is to graft polymers on membrane surfaces. Representative polymers are poly(ethylene glycol) (PEG), poly(2-hydroxyethyl methacrylate) (PHEMA), poly(2-methacryloyloxyethyl phosphorylcholine) (PMPC), and poly(sulfobetaine methacrylate) (PSBMA).[28-30] Random copolymers are also used to provide multiple functionalities. An example is a random copolymer that contains 3-(trimethoxysilyl) propyl methacrylate for surface anchoring, poly(ethylene glycol) methacrylate for anti-fouling, and *N*-acryloylsuccinimide for immobilization of biomolecules.[31] For the synthesis of such random copolymers, free radical polymerization is often used. However, conventional free radical polymerization is not able to finely control the polymer structures. Because RCMP is a useful

method to synthesize various copolymers in a controlled manner, RCMP may be used to synthesize efficient copolymers for anti-fouling of membrane surfaces.

The present chapter describes two studies. One is the synthesis of block and gradient copolymers in emulsion RCMP using water as a solvent. We studied block copolymerizations using purified PMMA–I polymers as macroinitiators. We also studied random copolymerizations of several monomers to yield gradient copolymers by exploiting different monomer reactivities and solubilities of the studied monomers. The other is the synthesis of hydrophilic-amphiphilic block copolymers via solution (not emulsion) RCMP for anti-fouling of membrane surfaces. The polymerization solvents are water, ethanol, and a mixture of water and ethanol. The obtained hydrophilic-amphiphilic block copolymers were tested for membrane anti-fouling.

5.2 Results and Discussion.

Synthesis of Block Copolymers via Emulsion RCMP.

In Chapter 4, we studied the iodide chain-end fidelity of PMMA–I (M_n = 3900 and $Đ$ = 1.09) synthesized via emulsion RCMP (Table 4.2 (entry 1) for 1 h), showing a nearly 100% iodide chain-end fidelity. Taking advantage of the high chain-end fidelity, we studied the synthesis of block copolymers. We carried out the first polymerization (the synthesis of the first block segment) under the same reaction condition described in Chapter 4 (Table 4.2 (entry 1)). Namely, we heated a mixture of MMA (100 equiv, 30.0 wt%), 2-hydroxyethyl 2-iodo-2-phenylacetate (2-HEPhI (Figure 4.1 in Chapter 4)) (1 equiv) as an alkyl iodide initiating dormant species, NaI (1 equiv) as a water-soluble catalyst, tetrabutylammonium iodide (BNI) (1 equiv) as an organic-soluble catalyst, 2,2'-azobis(2-methylpropionamidine) dihydrochloride (V50) (0.5 equiv) as a conventional radical initiator, a mixture of Tween80 and FES77 (3/1 (w/w), 3.3 wt%) as emulsifiers, and deionized (DI) water (66.7 wt%) as reaction medium for 2 h, yielding PMMA–I polymers with M_n = 10000–13000 and $Đ$ (= M_w/M_n) = 1.18–1.28 at a 100 % monomer (MMA) conversion (Table 5.1 (entries 1-1 and 2-1)), where M_n and M_w are number-average molecular weight and weight-average molecular weight, and $Đ$ is dispersity. Without purification, we used the PMMA–I polymers as macroinitiators in the second polymerizations (in the synthesis of block copolymers). Namely, to the reaction mixture of the first polymerization, we directly added the second monomer, i.e., butyl acrylate (BA) or benzyl methacrylate (BzMA). The target degree of polymerization (DP) at a full (100%) monomer conversion in the second polymerization was set to 100. We carried out the second polymerization at 60–70 °C for 0.75–3 h (Table 5.1 (entries 1-2 and 2-2) and Figure 5.1), yielding block copolymers with M_n = 27000–34000 and $Đ$ = 1.36–1.47 (after purification via reprecipitation in methanol). Figure 5.1 shows the gel permeation chromatography (GPC) charts. In both cases, large fractions of the macroinitiators successfully extended to block

copolymers, demonstrating high block efficiency. Compared with PMMA-*b*-PBzMA (methacrylate-methacrylate block copolymer), PMMA-*b*-PBA (methacrylate-acrylate block copolymer) had a larger *Đ* value (1.36 vs 1.47), where PBzMA is poly(benzyl methacrylate) and PBA is poly(butyl acrylate). The reason would be a slow activation of the acrylate (secondary alkyl) terminal unit capped with iodide at the studied mild temperature (70 °C). Thus, the emulsion RCMP started from PMMA–I successfully yielded block copolymers with relatively small *Đ* values of 1.36–1.47 at high conversion (100% (first block) and 82–96% (second block)) in relatively short reaction times (2 h (first block) + 0.75-3 h (second block)). The low-dispersity block copolymers were obtained without purifying the macroinitiators, which would be attractive for practical use. Emulsion NMP, ATRP, and RAFT copolymerization can produce block copolymer particles with various morphologies, such as core-shell, vesicle, and onion-like structures.[13,16-17] It is also attractive to study the morphogy of the obtained particles in emulsion RCMP in the future, which could be helpful to explore the applications for the block copolymers.

Table 5.1. Block Copolymerizations use PMMA–I as Macroinitiator via Emulsion RCMP.

Entry	$[MMA]_0/[2\text{-}HEPhI]_0/[BNI]_0/[NaI]_0/[V50]_0$ (mM)[a]	Second Block Monomer	Second Block DP[b]	T (°C)	t (h)	Conv (MMA/M) (%)	M_n ($M_{n,theo}$[c])	$Đ$
1-1	8000/80/80/80/40	-	-	60	2	100/0	13000 (10000)	1.28
1-2	-	+BA[d]	100	70	0.75	100/96	34000 (22000)	1.47
2-1	8000/80/80/80/40	-	-	60	2	100/0	10000 (10000)	1.18
2-2	-	+BzMA[d]	100	60	3	100/82	27000 (24000)	1.36

[a]$[MMA]_0/[emulsifier]_0/[water]_0$ = 30/3.3/66.7 (w/w/w). The emulsifier was a mixture of Tween80 and FES77 (3/1 (w/w)). [b]Target degree of polymerization (DP) at 100% monomer conversion as calculated according to $[Monomer]_0/[PMMA{-}I]_0$. [c]Theoretical M_n calculated with $[Monomer]_0$, $[R{-}I]_0$, and monomer conversion. [d]$[Monomer]_0/[water]_0$ = 30/70 (w/w).

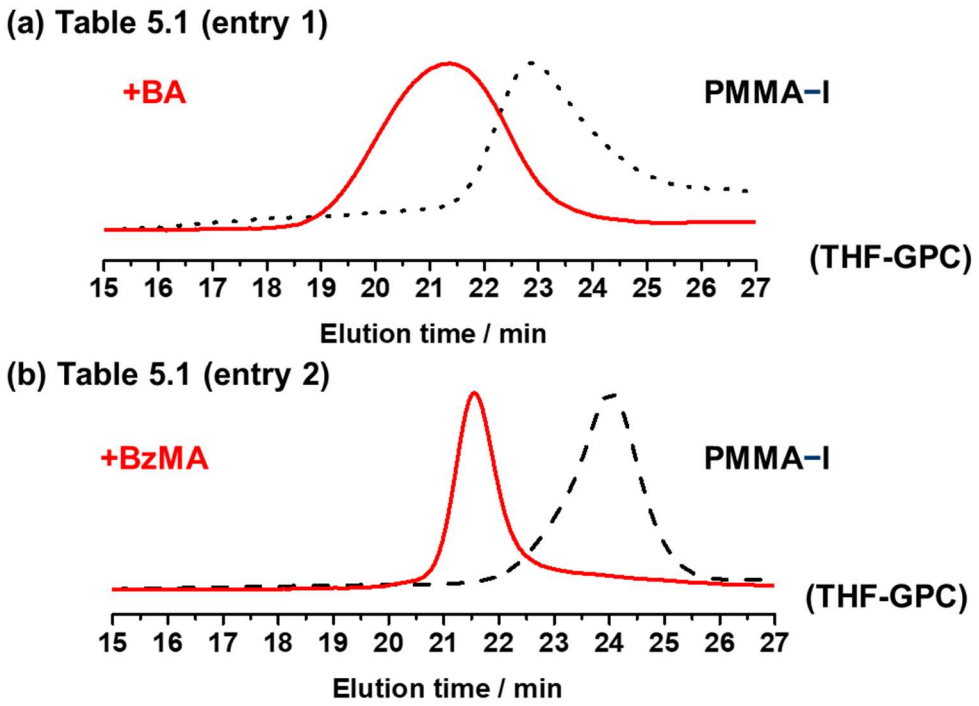

Figure 5.1. GPC chromatograms before (dashed lines) and after (solid lines) the block polymerizations in Table 5.1.

Synthesis of Gradient Copolymers via Emulsion RCMP.

We synthesized gradient copolymers via random copolymerizations of two monomers with different reactivities. We studied random copolymerizations of MMA (monomer 1) and BA (monomer 2) via emulsion RCMP. The monomer reactivity ratios (r_1 and r_2) are 2.64 and 0.32, respectively, at 70 °C.[32] MMA is more reactive than BA. Hence, MMA is consumed faster than BA, and polymer chains contain more MMA units at an early stage of polymerization and more BA units at a later stage of polymerization and become gradient copolymers. We heated a solution of mixed monomers of MMA and BA (50/50 equiv, 30.0 wt%), 2-hydroxyethyl 2-iodoisobutyrate (2-HEI (Figure 4.1 in Chapter 4)) (1 equiv) as an alkyl iodide initiating dormant species, BNI (4 equiv) as an organic-soluble catalyst, NaI (4 equiv) as a water-soluble catalyst, V50 (0.34 equiv) as a conventional radical initiator, a mixture of Tween80 and FES77 (3/1 (w/w), 3.3 wt%) as emulsifiers, and DI water (66.7 wt%) as reaction medium at 70 °C (Table 5.2 (entry 1) and Figure 5.2a). As expected, MMA was consumed faster than BA (Figure 5.2a).

In the first 20 min, virtually only MMA was consumed (38% MMA conversion and 0% BA conversion). At 40 min, MMA was further consumed (72% MMA conversion), and BA started to be consumed (16% BA conversion). At 80 min, MMA was fully consumed (100% MMA conversion), while BA continued to be consumed (84% BA conversion). After 80 min, the remaining BA was consumed, reaching a 92% BA conversion in 2 h. Thus, we obtained a gradient copolymer with pure MMA units in the beginning, MMA-rich to BA-rich gradient in the middle, and pure BA units in the last. However, the *Đ* value (= 1.50–1.77) was relatively large (Table 5.2 (entry 1)). Thus, we reduced the amount of V50 from 27 mM (Table 5.2 (entry 1) and Figure 5.2a) to 10 mM (Table 5.2 (entry 2) and Figure 5.2b) for reducing the generation of additional chains. However, the *Đ* value (= 1.50–1.90) was still relatively large.

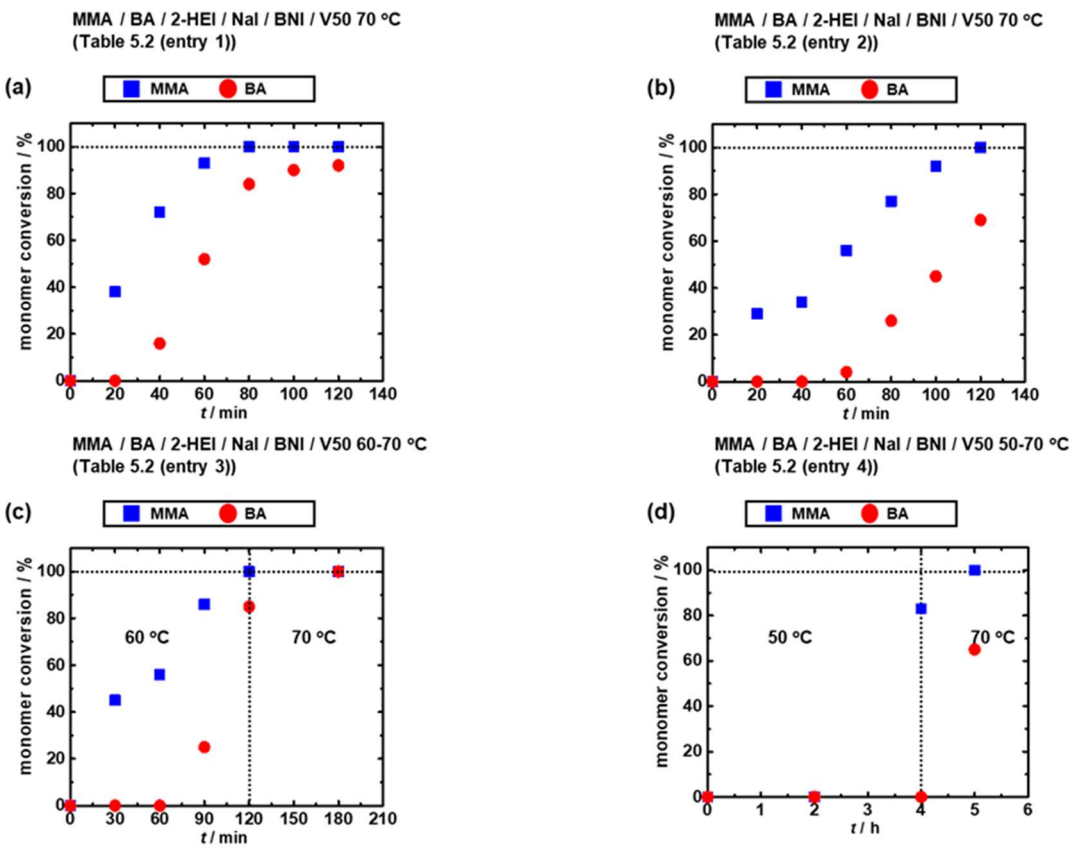

Figure 5.2. Plots of monomer conversion vs *t* for the MMA/BA/2-HEI/NaI/BNI/V50 systems at different temperatures: $[MMA]_0$ = 8 M; $[BA]_0$ = 8 M; $[2\text{-HEI}]_0$ = 80 mM; $[BNI]_0$ = 320 mM; $[NaI]_0$ = 320 mM; $[V50]_0$ = 27 or 10 mM (Table 5.2 (entries 1-4)). The symbols are indicated in the figure.

In order to reduce possible side reactions such as elimination of HI from polymer chain-end, we decreased the reaction temperature from 70 °C (Table 5.2 (entry 2) and Figure 5.2b) to 60 °C (Table 5.2 (entry 3) and Figure 5.2c). The $Đ$ value became low at an early stage of polymerization ($Đ$ = 1.15–1.41) but increased to 1.78–1.91 at a later stage of polymerization (Table 5.2 (entry 3)). Notably, because of the lower temperature, the difference in the reactivities of MMA and BA increased. As a result, the sole consumption of MMA was prolonged to a 56% conversion. We further decreased the polymerization temperature to 50 °C (Table 5.2 (entry 4) and Figure 5.2d). The sole consumption of MMA was even more prolonged to an 83% MMA conversion (for 4 h). Subsequently (after 4h), the temperature was elevated from 50 °C to 70 °C for the remaining BA to polymerize, successfully yielding gradient copolymer with low polydispersity (M_n = 13000 and $Đ$ = 1.31). Thus, we obtained gradient copolymers of MMA and BA with different sequences (pure MMA units, gradient, and pure BA units) by changing temperature.

Table 5.2. Synthesis of Gradient Copolymers via Emulsion RCMP.

Entry	Target DP[a]	Monomer (A/B)[c]	R–I	$[A]_0/[B]_0/[R–I]_0/[BNI]_0/[NaI]_0/[V50]_0$ (mM)[d]	T (°C)	t (h)	conv (%) (A/B)	M_n ($M_{n,theo}$[b])	$Đ$
1	200	MMA/BA	2-HEI	8000/8000/80/320/320/27	70	0.33	38/0	8000 (3800)	1.50
						2	100/92	22000 (22000)	1.77
2	200	MMA/BA	2-HEI	8000/8000/80/320/320/10	70	0.66	34/0	13000 (3400)	1.50
						1	56/4	25000 (6100)	1.73
						2	100/69	23000 (19000)	1.90
3	200	MMA/BA	2-HEI	8000/8000/80/320/320/10	60	0.5	45/0	3500 (4500)	1.15
						1	56/0	14000 (5600)	1.41
						1.5	86/25	29000 (12000)	1.91
						2	100/85	27000 (21000)	1.78
					70	3	100/100	24000 (23000)	1.91
4	200	MMA/BA	2-HEI	8000/8000/80/320/320/10	50	4	83/0	7000 (8300)	1.30
					70	5	100/65	13000 (18000)	1.31
5	100	MMA/St	2-HEI	4000/4000/80/160/160/40	70	1	56/0	5000 (2800)	1.34
						2	90/38	8800 (6500)	1.32
						3	100/74	9600 (8800)	1.34
						4	100/97	9900 (10000)	1.35
6	100	MMA/BzMA	2-HEPhI	4000/4000/80/160/160/40	60	2	39/20	8000 (3700)	1.10

[a]Target degree of polymerization at 100% monomer conversion (calculated by $([A]_0+[B]_0)/[R–I]_0$). [b]Theoretical M_n calculated with $[A]_0$, $[B]_0$, $[R–I]_0$, and monomer conversion. [c]$[Monomer]_0/[emulsifier]_0/[water]_0$ = 30/3.3/66.7 (w/w/w). The emulsifier was a mixture of Tween80 and FES77 (3/1 (w/w)).

We further studied a random copolymerization of MMA (monomer 1) and styrene (St) (monomer 2) via emulsion RCMP. The monomer reactivity ratios (r_1 and r_2) are 0.46 and 0.44, respectively, at 44 °C.[33] MMA is slightly more reactive than St. Table 5.2 (entry 5) and Figure 5.3 show the polymerization result at 70 °C. MMA was polymerized first and reached 56% monomer conversion at 1 h, and subsequently St was gradually consumed until 4 h. The conversion of MMA and St reached 100% and 97% at 4 h, yielded a low-dispersity gradient copolymer with M_n = 9900 and $Đ$ = 1.35. The r_1 and r_2 values are smaller than 1 and suggest

an alternative tendency in the MMA/St random copolymerizaiton. The generation of the gradient copolymer would be because of different solubilites of the two monomers in water; namely, MMA (15.9 g/L at 25 °C) is more soluble in water than St (0.24 g/L at 25 °C), and the transportation from the monomer droplet to the polymerization loci (particle) would be more effective for MMA than St. [34-35]

We also studied a copolymerization of two methacrylates, i.e., MMA (monomer 1) and BzMA (monomer 2). Because the two monomers are the same monomer family (methacrylate), r_1 and r_2 tend to be close to 1 (random tendency). At an early stage of polymerization (30 min), only MMA was consumed, and subsequently MMA and BzMA were consumed (Table 5.2 (entry 6) and Figure 5.4). This result would also be ascribed to the different solubilities of MMA and BzMA in water; namely, MMA is less hydrophobic (is more transported through water) than BzMA (1.04 g/L at 25 °C).[34,36]

These results demonstrate that emulsion RCMP is effective in synthesizing gradient copolymers with different monomer combinations and different monomers sequences.

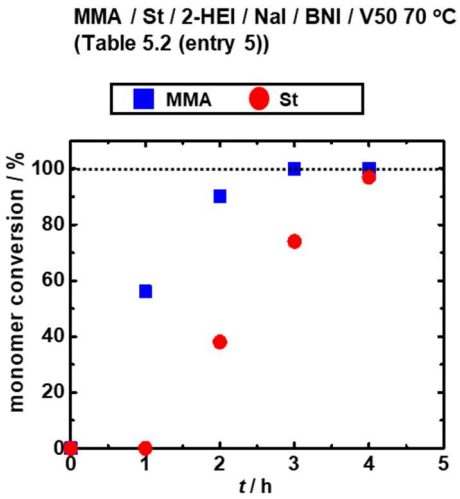

Figure 5.3. Plots of monomer conversion vs *t* for the MMA/St/2-HEI/NaI/BNI/V50 systems at 70 °C: $[MMA]_0 = 4$ M; $[St]_0 = 4$ M; $[2\text{-HEI}]_0 = 80$ mM; $[BNI]_0 = 160$ mM; $[NaI]_0 = 160$ mM; $[V50]_0 = 40$ mM (Table 5.2 (entry 5)). The symbols are indicated in the figure.

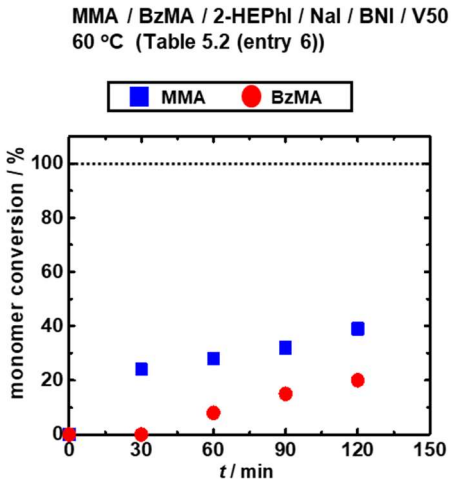

Figure 5.4. Plots of monomer conversion vs *t* for the MMA/BzMA/2-HEI/NaI/BNI/V50 systems at 60 °C: $[MMA]_0 = 4$ M; $[BzMA]_0 = 4$ M; $[2\text{-HEPhI}]_0 = 80$ mM; $[BNI]_0 = 160$ mM; $[NaI]_0 = 160$ mM; $[V50]_0 = 40$ mM (Table 5.2 (entry 6)). The symbols are indicated in the figure.

Preparation of Macroinitiators via Solution RCMP for the Synthesis of Anti-fouling Block Copolymers.

We studied the synthesis of hydrophilic-amphiphilic block copolymers for membrane anti-fouling. The hydrophilic segment is expected to provide anti-fouling properties, and the amphiphilic segment is expected to anchor membrane surfaces. We used glyceryl monomethacrylate (GLMMA) and glycerol monoacrylate (GLMA) with two hydroxyl functional groups and SBMA and MPC with zwitterionic functional groups (Figure 5.5) as hydrophilic monomers, which can form hydration layers and provide anti-fouling properties. We used poly(ethylene glycol) methyl ether acrylate (PEGA) (average M_n = 480 g/mol) and poly(ethylene glycol) methyl ether methacrylate (PEMGA) (average M_n = 300 g/mol) (Figure 5.5) as amphiphilic monomers, which are biocompatible and also can anchor membrane surfaces.[37-40] We synthesized those block copolymers via solution RCMP.

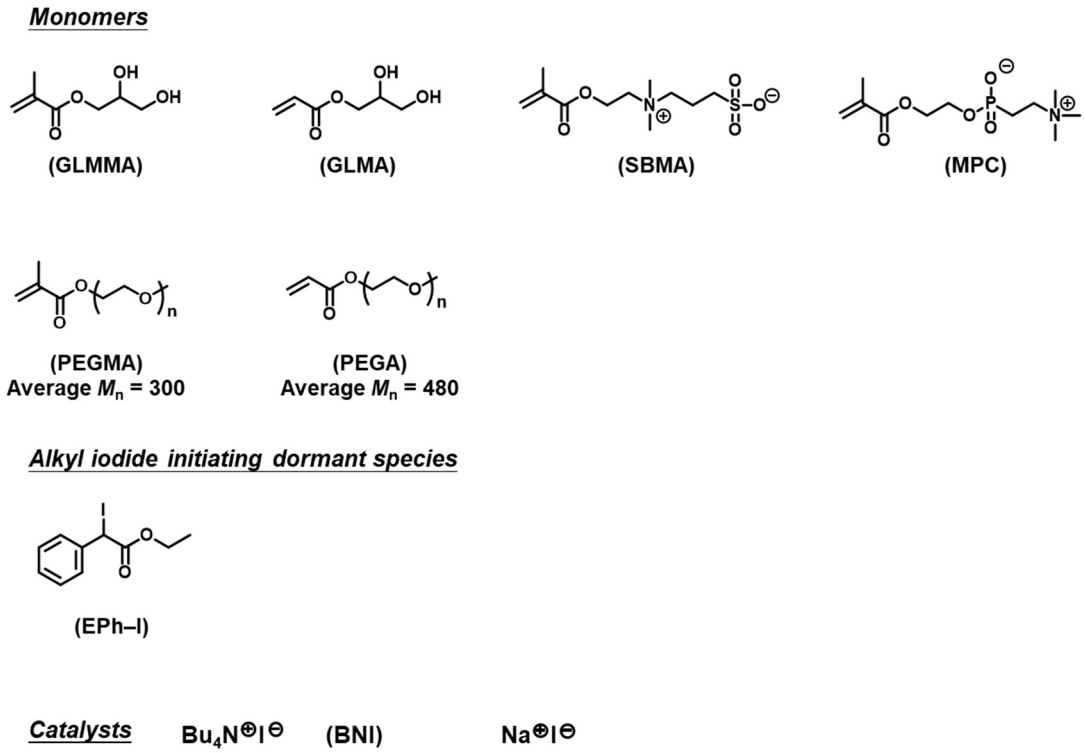

Figure 5.5. Structures of monomers, alkyl iodides, and catalysts used in solution RCMP.

We synthesized PGLMMA–I macroinitiators, where PGLMMA is poly(glyceryl monomethacrylate). We heated a mixture of GLMMA (8M, 100 equiv), ethyl α-iodophenylacetate (EPh−I) (40 mM, 0.5 equiv) as an alkyl iodide initiating dormant species, BNI (100 mM, 1.25 equiv) as a catalyst, 2,2′-azobis (2,4-dimethylvaleronitrile) (V65) (10 mM, 0.125 equiv) as a conventional radical initiator, and ethanol (60% wt of the total mixture) as a solvent at 60 ˚C for 15, 25, and 40 min, yielding PGLMMA–I macroinitiators with different M_n values (= 5900–15000) and low polydispersity ($Đ$ = 1.36–1.48) (Table 5.3 (entry 1)). We also synthesized PGLMA–I macroinitiators, where PGLMA is poly(glycerol monoacrylate). The temperature was increased to 70 ˚C because GLMA is an acrylate monomer and RCMP of acrylates requires a higher temperature than that of methacrylates. We used NaI (400 mM, 5 equiv) as a catalyst instead of BNI, because NaI has better solubility in the mixture of GLMA and ethanol, which is a more hydrophilic environment than the mixture of GLMMA and ethanol. 4,4'-Azobis(4-cyanovaleric acid) (V501) (20 mM, 0.25 equiv) with higher water-

solubility was also used instead of V65 for the GLMA polymerization. By varying the molar ratio of GLMA (monomer) to EPh–I (initiating dormant species), we also successfully synthesized PGLMA–I with different M_n values (= 9000–17000) in a controlled manner ($Đ$ = 1.34–1.41) (Table 5.3 (entries 2 and 3)). We also carried out the polymerizations of PEGMA in bulk and in solution (25% wt ethanol) and obtained two PPEGMA–I macroinitiators (M_n = 22000, $Đ$ = 1.10 and M_n = 8000, $Đ$ = 1.48, respectively) (Table 5.3 (entries 4 and 5)), where PPEGMA is poly(poly(ethylene glycol) methyl ether methacrylate).

Table 5.3. Synthesis of Macroinitiators for Solution Block Copolymerization.

Entry	Monomer	Target DP[a]	$[M]_0/[EPh–I]_0/[BNI]_0/[NaI]_0/[V65]_0$ (mM)[b]	T (°C)	t (min)	conv (%)	M_n[c] ($M_{n,theo}$[d])	$Đ$[c]
1	GLMMA	200	8000/40/100/0/10	60	15	8	5900 (2600)	1.48
					25	16	7500 (5100)	1.36
					40	40	15000 (13000)	1.41
2	GLMA	40	8000/200/0/400/0[e]	70	30	32	17000 (2000)	1.41
3	GLMA	20	8000/400/0/400/0[e]	70	30	90	9000 (2600)	1.34
4	PEGMA	100	8000/80/80/0/120 (bulk)	50	60	35	22000 (10000)	1.10
5	PEGMA	100	8000/80/80/0/80	60	240	30	8000 (9000)	1.48

[a]Target degree of polymerization at 100% monomer conversion (calculated by $[M]_0/[EPh–I]_0$). [b]Diluted with 60% wt ethanol (entries 1-3) and 25% wt ethanol (entry 5). [c]PMMA-calibrated DMF-GPC values for entry 1. PEG-calibrated water-GPC values for entries 2-5. [d]Theoretical M_n calculated with $[M]_0$, $[EPh–I]_0$, and monomer conversion. [e]Additional $[V501]_0$ = 20 mM.

Synthesis of Block Copolymers via Solution RCMP.

We purified the macroinitiators via reprecipitation in diethyl ether (for PGLMMA–I and PGLMA–I) or a mixture of diethyl ether and hexane mixture (1/1 (v/v)) (for PPEGMA–I) and used them in the subsequent (second block) polymerizations. We used water, a mixture of water and ethanol, or ethanol as the polymerization solvent and NaI as the catalyst, because NaI is soluble in water and ethanol. PGLMMA–I and PGLMA–I reacted with PEGA, yielding PGLMMA-*b*-PPEGA and PGLMA-*b*-PPEGA block copolymers with M_n = 14000, $Đ$ = 1.58 and M_n = 29000, $Đ$ = 1.45, respectively, where PPGEA is poly(poly(ethylene glycol) methyl ether acrylate). PPEGMA–I macroinitiators were also used as to synthesize a PPEGMA-*b*-PSBMA block copolymer with M_n = 48000, $Đ$ = 1.58 and a PPEGMA-b-PMPC copolymer

with M_n = 29000, $Đ$ = 1.56. The $Đ$ values of the obtained hydrophilic-amphiphilic block copolymers were relatively large ($Đ$ = 1.45–1.58). Nevertheless, in the studied four systems, large fractions of the macroinitiators successfully extended to block copolymers (Figure 5.6). Thus, hydrophilic-amphiphilic block copolymers were successfully obtained via solution RCMP.

Table 5.4. Block Copolymerization via Solution RCMP.

Entry	Reaction Conditions (mM)	Solvent (wt%)	T (°C)	t (h)	macroinitiator M_n	M_n[a] (units)	$Đ$[a]
1	PGLMMA–I/PEGA/NaI/V501 = 40/8000/320/120	H_2O (95)	90	3	5900	14000 (17)	1.58
2	PGLMA–I/PEGA/NaI/V501 = 8000/200/300/200	H_2O (66.7)	90	5	17000	29000 (25)	1.45
3	PPEGMA–I/SBMA/NaI/V65 = 40/8000/20/150	H_2O/EtOH (80)[b]	60	3	8000	48000 (143)	1.56
4	PPEGMA–I/MPC/NaI/V65 =80/8000/160/80	EtOH (75)	55	2	22000	29000 (24)	1.56

[a]PMMA-calibrated DMF-GPC values for entry 1. PEG-calibrated water-GPC values for entries 2-4. [b]Solvent is a mixture of H_2O/EtOH (4/1 (v/v)).

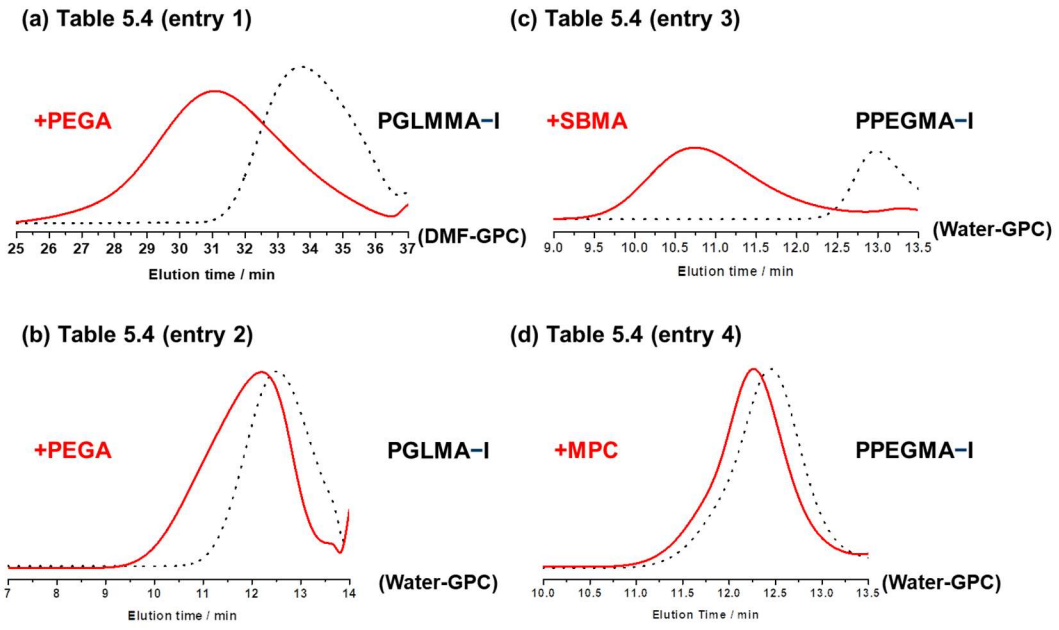

Figure 5.6. GPC chromatograms before (dashed lines) and after (solid lines) the block polymerizations in Table 5.4.

Anti-fouling Test.

We tested the anti-fouling properties of the obtained block copolymers on a polyethersulfone (PES) ultrafiltration (UF) membrane, which is frequently used in RO systems.[41-42] We used bovine serum albumin (BSA) as a foulant, which is a common foulant used in this test.[43-44] The block copolymers obtained above were tested together with the relevant two other PGLMMA-*b*-PPEGA block copolymers synthesized by E. Seah in our research group, and random copolymers and homopolymers synthesized by Nippon Shoukubai Co. Ltd. In an anti-fouling test, an aqueous solution of a polymer (2 g/L) was prepared, and a PES UF membrane was subsequently dipped in the solution for 24 h. The polymer was anchored on the membrane via physical adsorption. The obtained membrane was mounted in a circulated testing loop. In one test cycle, DI water was pumped to permeate through the membrane. Subsequently, the DI water was replaced by an aqueous BSA solution (0.2% wt of BSA) for fouling. After the fouling, the membrane was rinsed with DI water and subsequently an aqueous NaOH solution (0.2% wt of NaOH). Three continuous cycles were conducted for each sample. After the three cycles, the final water flux (LMH/bar) in DI water was recorded as F_1. Similarly, the same procedures were performed on a membrane without modification (without polymer coating). The final water flux in DI water was recorded as F_0. The relative permeability was defined as:

$$\text{Relative permeability (\%)} = F_1 / F_0 \times 100.$$

If a polymer exhibits anti-fouling property, the relative permeability will be greater than 100% because of the less deposition of BSA and higher water flux. Table 5.5 shows the results. Except the PGLMA-*b*-PPEGA block copolymer (entry 2-1) (relative permeability 85%), all the other studied membranes modified with polymers (PGLMMA homopolymer (entry 1-1),

PGLMMA-*r*-PPEGA random copolymer (entry 1-2), PGLMMA-*b*-PPEGA block copolymers (entries 1-3, 1-4, and 1-5), PSBMA-*r*-PPEGA random copolymer (entry 3-1), and PSBMA homopolymer (entry 3-2)) exhibited relative permeability values greater than 100%, exhibiting anti-fouling properties. Comparing the GLMMA/PEGA random (entry 1-2) and block copolymers (entries 1-3, 1-4, and 1-5), the block copolymers (relative permeability = 102–124%) did not afford a better anti-fouling property than the random copolymer (relative permeability = 124%) in contrast to our expectation. The reason is unclear at the moment. Nevertheless, block copolymers were successfully synthesized and tested for BSA-fouling in the present work (Chapter 5), which enabled a more comprehensive and detailed study on the surface modification of membranes and their anti-fouling properties carried out by our collaborators.[45]

Table 5.5. Anti-fouling test results.

Entry	Composition (unit ratio)	M_w	Copolymer type	Relative permeability compared with control during BSA test (%)
1-1[a]	GLMMA=100	47000	-	115
1-2[a]	GLMMA/PEGA=80/20	60000	random	124
1-3[b]	GLMMA/PEGA=78/22	23000	block	102
1-4	GLMMA/PEGA=67/33 (Same polymer in Table 5.4 (entry 1))	22000	block	124
1-5[b]	GLMMA/PEGA=71/29	24000	block	108
2-1	GLMA/PEGA=85/15 (Same polymer in Table 5.4 (entry 2))	53000	block	85
3-1[a]	SBMA/PEGA=20/80	51000	random	142
3-2[a]	SBMA=100	30000	-	141

[a]Polymer provided by Nippon Shoukubai Co. Ltd. [b]These two block copolymers were synthesized by E. Seah in her FYP project in our research group.

5.3 Conclusion.

We successfully used emulsion RCMP for the synthesis of copolymers. Block copolymers with narrow molecular weight distributions were synthesized using PMMA–I macroinitiators. Various gradient copolymers were obtained via emulsion RCMP random copolymerizations, and the monomer sequence was tuned by the reaction temperature. For membrane anti-fouling applications, solution RCMP was successfully used to synthesize hydrophilic-amphiphilic block copolymers with different molecular weights and different monomer compositions. Thus, RCMP in aqueous media can serve as a useful synthetic system for a range of copolymers.

5.4 Experimental.

Materials.

Glyceryl monomethacrylate (GLMMA) (NOF Corporation, Japan), glycerol monoacrylate (GLMA) (NOF), poly(ethylene glycol) methyl ether methacrylate (PEGMA) (average M_n = 300 g/mol) (Sigma-Aldrich, USA), poly(ethylene glycol) methyl ether acrylate (PEGA) (average M_n = 480 g/mol) (Sigma-Aldrich), sulfobetaine methacrylate (SBMA) (95%, Sigma-Aldrich), 2-methacryloyloxyethyl phosphorylcholine (MPC) (97%, Sigma-Aldrich), ethyl α-iodophenylacetate (EPh−I) (>98%, Tokyo Chemical Industry (TCI), Japan), 2,2′-azobis (2,4-dimethylvaleronitrile) (V65) (95%, Wako Pure Chemical, Japan), 4,4'-Azobis(4-cyanovaleric acid) (V501) (98%, Sigma-Aldrich), ethanol (≥99.5%, absolute, Fisher Scientific), diethyl ether (ACS reagent grade, VWR International), and hexane (>99%, International Scientific, Singapore) were used as received. The details of other used materials in this work were mentioned in Chapter 4 (Section 4.4).

Measurements.

The GPC analysis using THF or DMF as the eluent was performed using the same instruments and procedures mentioned in Chapter 4 (Section 4.4).

The GPC analysis using water as the eluent was performed on a Shimazu (Kyoto, Japan) GPC-101 liquid chromatograph equipped with two Shodex SB-804 HQ columns (300 × 8.0 mm; bead size = 10 μm; pore size = 200 Å). The eluent (water) contained NaH_2PO_4 (44 mM) and Na_2HPO_4 (26mM). The flow rate was 1.50 mL/min (40 °C). The sample detection and quantification were conducted using a Shimadzu differential refractometer RI-101. The column system was calibrated with standard poly(ethylene glycol)s (PEGs).

The ^{1}H NMR spectra were recorded on Bruker (Germany) AV500 spectrometer (500 MHz) or AV300 (300 MHz) at ambient temperature. Acetone-d_6 (for copolymers synthesized via emulsion RCMP without styrene), tetrahydrofuran-d_8 (for copolymers synthesized via

emulsion RCMP containing styrene), and methanol-d_4 (for polymers synthesized via solution RCMP) (Cambridge Isotope Laboratories, USA) were used as the solvents for the NMR analysis, and the chemical shift was calibrated using residual undeuterated solvents or tetramethylsilane (TMS) as the internal standard. The monomer conversion was determined with ^{1}H NMR.

Block copolymerization via emulsion RCMP.

The synthesis of macroinitiators was the same as "General procedure for polymerization" in Chapter 4 (section 4.4). In a typical run, after the macroinitiator was synthesized, a mixture of the second monomer (30.0 wt%) and DI water (70.0 wt%) was heated in a reaction vessel at 60-70 °C under argon atmosphere with mechanical stirring (1000 rpm). The vessel was a 250 mL jacketed cylindrical reaction vessel (ChemGlass, USA) connected with an overhead mechanical stirrer (Heidolph, Germany) and immersed in a water bath (Lauda, Germany). After a prescribed time *t*, an aliquot (1 mL) of the solution was taken out by a syringe, cooled to room temperature, and analyzed with ^{1}H NMR. Another aliquot (10 mL) of the mixture was taken out, cooled to room temperature, reprecipitated in methanol (200 mL), and dried. The purified copolymer was analyzed with GPC (THF as eluent).

Gradient copolymerization via emulsion RCMP.

In a typical run, a mixture of comonomers (30.0 wt%), an alkyl iodide initiator, a conventional radical initiator, catalysts, emulsifier (3.3 wt%), and DI water (66.7 wt%) was heated in a reaction vessel at 50–70 °C under argon atmosphere with mechanical stirring (1000 rpm). The vessel was a 250 mL jacketed cylindrical reaction vessel (ChemGlass, USA) connected with an overhead mechanical stirrer (Heidolph, Germany) and immersed in a water bath (Lauda, Germany). After a prescribed time *t*, an aliquot (2 mL) of the solution was taken out by a syringe, cooled to room temperature, and analyzed with GPC (DMF as eluent) and ^{1}H NMR.

Synthesis of macroinitiators via solution RCMP.

In a typical run, a mixture of monomer (8 M), EPh–I (40–400 mM), catalyst (80–400 mM), a conventional radical initiator (10–120 mM), and ethanol (0-60 wt% of the total mixture) was heated in a Schlenk flask at 50–70 °C under argon atmosphere with magnetic stirring. After polymerization, an aliquot (1 mL) of the solution was taken out, cooled to room temperature, and analyzed with GPC (DMF or water as eluent) and ^{1}H NMR. The reaction mixture was diluted with ethanol (5 mL) and reprecipitated in diethyl ether (for PGLMMA–I and PGLMA–I) or a mixture of diethyl ether and hexane (1/1 (v/v)) (for PPEGMA–I) (100 mL). The obtained polymer was dried in vacuo and used as macroinitiators for block copolymerizations.

Block copolymerization via solution RCMP.

In a typical run, a mixture of monomer, macroinitiator, a catalyst, a conventional radical initiator, and solvent (water, ethanol, and a mixture of water and ethanol (4/1 (v/v)) was heated in a Schlenk flask at 55–90 °C under argon atmosphere with magnetic stirring. After cooling to room temperature, the solution was reprecipitated in diethyl ether and dried under vacuum. The obtained copolymers were analyzed by GPC (DMF or water as eluent) and ^{1}H NMR.

Anti-fouling test.

Purified copolymers were sent to our collaborator (Prof R. Wang) in Nanyang Environment & Water Research Institute (NEWRI) in NTU for the anti-fouling performance test on a Singapore Membrane Technology Centre (SMTC) PES UF membrane for anti-fouling test. In a typical run, a polymer solution (2 g/L) was prepared, UF membrane was dipped in the solution for 24 h. The polymer was anchored on the membrane via physical adsorption. After modification, the water permeability of the membrane was first measured with pure water (flow velocity 0.8 m/s) at 1 bar. Then the feed water was replaced by 0.5 wt% BSA aqueous solution for the fouling test at 1 bar for 2 h. After the fouling test, the membrane was cleaned by first

DI water then NaOH aqueous solution (0.2 wt%), and tested again for another cycle. Three continuous cycles were conducted in total. After three cycles, the final water flux (LMH/bar) in DI water was recorded as F_1. Similarly, the same procedures were performed on a membrane without modification and the final water flux in DI water was recorded as F_0. The relative permeability was defined as:

$$\text{Relative permeability (\%)} = F_1 / F_0 \times 100.$$

References.

1. Hailes, H. C. *Organic Process Research & Development* **2007**, 11, 114-120.
2. Lubineau, A.; Augé, J., Chapter 1 - Water as Solvent in Organic Synthesis. In *Modern Solvents in Organic Synthesis*, Knochel, P., Eds. Springer: **1999**; pp 1-39.
3. Asua, J. M. *Prog. Polym. Sci.* **2002***,* 27, 1283-1346.
4. Liu, C.; Hong, C.-Y.; Pan, C.-Y. *Polym. Chem.* **2020**, 11, 3673-3689.
5. Canning, S. L.; Smith, G. N.; Armes, S. P.; *Macromolecules* **2016**, 49, 1985-2001.
6. Ferguson, C. J.; Hughes, R. J.; Pham, B. T. T.; Hawkett, B. S.; Gilbert, R. G.; Serelis, A. K.; Such, C. H. *Macromolecules* **2002**, 35, 9243-9245.
7. György, C.; Lovett, J. R.; Penfold, N. J. W.; Armes, S. P. *Macromol. Rapid Commun.* **2019**, 40, 1800289.
8. Galanopoulo, P.; Dugas, P.-Y.; Lansalot, M.; D'Agosto, F. *Polym. Chem.* **2020**, 11, 3922-3930.
9. Boussiron, C.; Bechec, M. L.; Sabalot, J.; Lacombe, S.; Save, M. *Polym. Chem.* **2021**, 12, 134-147.
10. Engelis, N. G.; Anastasaki, A.; Nurumbetov, G.; Truong, N. P.; Nikolaou, V.; Shegiwal, A.; Whittaker, M. R.; Davis, T. P.; Haddleton, D. M. *Nature chemistry* **2017**, 9, 171-178.
11. Clothier, G. K. K.; Guimarães, T. R.; Khan, M.; Moad, G.; Perrier, S.; Zetterlund, P. B. *ACS Macro Lett.* **2019**, 8, 989-995.
12. Fang, J.; Gao, X.; Luo, Y. *Polymer* **2020**, 201, 122602.
13. Khan, M.; Guimarães, T. R.; Choong, K.; Moad, G.; Perrier, S.; Zetterlund. P. B. *Macromolecules* **2021**, 54, 736-746.
14. Manguian, M.; Save, M.; Charleux, B. *Macromol. Rapid Commun.* **2006**, 27, 399-404.
15. Lee, C.; Hwang, A.; Jose, L.; Park, J. H.; Jang, S.; Song, J. K.;Kim, Y.; Cho, Y.; Jeon, H. B.; Jin, J.-O.; Paik, H. J. *Journal of Industrial and Engineering Chemistry* **2020**, 86, 35-38.
16. Delaittre, G.; Nicolas, J.; Lefay, C.; Save, M.; Charleux, B. *Chem. Commun.* **2005**, 614-616.
17. Groison, E.; Brusseau, S.; D'Agosto, F.; Magnet, S.; Inoubli, R.; Couvreur, L.; Charleux, B. *ACS Macro Lett.* **2012**, 1, 47-51.
18. Beginn, U. *Colloid Polym Sci* **2008,** 286, 1465-1474.
19. Kim, J.; Gray, M. K.; Zhou, H.; Nguyen, S. T.; Torkelson, J. M. *Macromolecules* **2005**, 38, 1037-1040.
20. Tao, Y.; Kim, J.; Torkelson, J. M. *Polymer* **2006**, 47, 6773-6781.
21. Penfold, H. V.; Holder, S. J.; McKenzie, B. E. *Polymer* **2010**, 51, 1904-1913.
22. Sun, D.; Cho, J. *Polymer* **2015**, 66, 192-200.
23. Boretti, A.; Rosa, L. *NPJ Clean Water* **2019**, 2, 1-6.
24. Kavitha, J.; Rajalakshmi, M.; Phani, A. R.; Padaki, M. *Journal of Water Process Engineering* 2019, 32, 100926.
25. Jiang, S.; Li, Y.; Ladewig, B. P. *Science of the Total Environment* **2017**, 595, 567-583.
26. Guo, W.; Ngo, H.-H.; Li, J. *Bioresource Technology* **2012**, 122, 27-34.
27. Beier, S. P.; Enevoldsen, A. D.; Kontogeorgis, G. M.; Hansen, E. B.; Jonsson, G. *Langmuir* **2007**, 23, 9341-9351.
28. Yu, Q.; Zhang, Y.; Wang, H.; Brash, J.; Chen, C. *Acta Biomaterialia* **2011**, 7, 1550-1557.
29. He, M.; Gao, K.; Zhou, L.; Jiao, Z.; Wu, M.; Cao, J.; You, X.; Cai, Z.; Su, Y.; Jiang, Z. *Acta Biomaterialia* **2016**, 40, 142-152.
30. Liu, C.; Lee, J.; Ma, J.; Elimelech, M. *Environ. Sci. Technol.* **2017**, 51, 2161-2169.
31. Park, S.; Lee, K.-B.; Choi, I. S.; Langer, R.; Jon, S. *Langmuir* **2007**, 23, 10902-10905.
32. Jiang, S.; Sudol, E. D.; Dimonie, V.; El-aasser, M. S. *J. Polym. Sci. Part A: Polym. Chem.* **2007**, 45, 2105-2112.

33. Goldwasser, J. M.; Rudin, A. *Journal of Polymer Science: Polymer Chemistry Edition* **1982**, 20, 1993-2006.
34. Solubility of MMA in water is 15.9 g/L at 25 ℃, https://www.chemicalbook.com/ChemicalProductProperty_EN_CB8854425.htm, (accessed 25 Jul 2021).
35. Solubility of St in water is 0.24 g/L at 25 ℃, https://www.chemicalbook.com/ChemicalProductProperty_EN_CB3415111.htm, (accessed 25 Jul 2021).
36. Solubility of BzMA in water is 1.04 g/mL at 25 ℃, https://www.chemicalbook.com/ChemicalProductProperty_EN_CB7306028.htm, (accessed 25 Jul 2021).
37. Dalsin, J. L.; Hu, B.-H.; Lee, B. P.; Messersmith, P. B. *J. Am. Chem. Soc.* **2003**, 125, 4253-4258.
38. Hamming, L. M.; Messersmith, P. B. *Material Matters* **2008**, 3.3, 52.
39. Hu, J.; Chen, Y.; Lu, J.; Fan, X.; Li, J.; Li, Z.; Zeng, G.; Liu, W. *Polymer* **2020**, 201, 122531.
40. Mohamed, H; Hudziak, S.; Arumuganathan, V.; Meng, Z.; Coppens, M.-O. *Mol. Syst. Des. Eng.* **2020**, 5, 1219-1229.
41. Bezuidenhout, D.; Hurndall, M. J. Sanderson, R. D.; van Reenen, A. J. *Desalination* **1998**, 116, 35-43.
42. Vatsha, B.; Ngila, J. C.; Moutloali, R. M. *Physics and Chemistry of the Earth* **2014**, 67-69, 125-131.
43. Ang, W. S.; Elimelech, M. *Journal of Membrane Science* **2007**, 296, 83-92.
44. Yin, Z.; Wen, T.; Li, Y; Li, A.; Long, C. *Journal of Membrane Science* **2020**, 595, 117546.
45. Tian, M.; Wang, R.; Goto, A.; Mao, W.; Miyoshi, Y.; Mizoguchi, H. *Journal of Water Process Engineering* **2020**, 33, 101034.

Chapter 6. Conclusions.

In Chapter 2, we successfully utilized oxyanions (carboxylate, nitrate, sulfonate, and phosphate) as catalysts in RCMP. Among the studied catalysts, carboxylate and nitrate anions exhibited higher reactivities. Naturally existing non-toxic carboxylate compounds were also employed as RCMP catalysts. These catalysts were amenable to methacrylates, styrene, and acrylonitrile. Block copolymers were also successfully synthesized exploiting the high iodide chain-end livingness. Oxyanions are low-toxic and inexpensive. The development of carboxylate anion as RCMP catalyst also contributed to the exploration of air-tolerant RCMP in Chapter 3.

In Chapter 3, we successfully developed air-tolerant RCMP using cyclohexanecarboxaldehyde (CHCA), *N*-hydroxyphthalimide (NHPI), and 2,4,6-trimethylpyridine (TMP). Oxygen was consumed via NHPI-catalyzed oxidation of CHCA (aldehyde) to the carboxylic acid. The carboxylic acid was further converted to the carboxylate anion in the presence of TMP (base), and the carboxylate anion worked as an efficient catalyst of RCMP. The air-tolerant RCMP system afforded polymers with low dispersity and relatively high monomer conversions. The development of air-tolerant RCMP enhanced the usefulness of RCMP.

In Chapter 4, we successfully employed RCMP in emulsion system for homopolymerization. We systematically studied the effects of different emulsifiers, catalysts, and alkyl iodide dormant species. The co-use of Tween80 and FES77 mixed emulsifiers, NaI and BNI as catalysts, and the use of 2-HEPhI as an alkyl iodide initiator achieved nearly quantitative initiation and generated low-dispersity polymers ($Đ$ = 1.1−1.3) at high (30−50%) contents of methyl methacrylate (MMA) monomer. Emulsion RCMP is also amenable to functional methacrylates and styrene. The advantages of both emulsion polymerization and

RCMP were successfully combined in emulsion RCMP, which are attractive for polymer material design and industrial applications.

In Chapter 5, we further explored RCMP in aqueous media for copolymer synthesis. As one part of the work, we carried out block copolymerizations using poly(methacrylate)−I (PMMA−I) synthesized in Chapter 4 as the macroinitiator, yielding well-defined hydrophobic-hydrophobic block copolymers with methacrylate and acrylate monomers. Random copolymerizations via emulsion RCMP also yielded various hydrophobic-hydrophobic gradient copolymers utilizing the different monomer reactivity ratios and different solubilites in water, and the monomer sequence was tuned by the reaction temperature. Solution RCMP in water, ethanol, and a mixture of water and ethanol produced various hydrophilic-amphiphilic block copolymers containing anti-fouling segment and anchoring segment. The anti-fouling test of membranes modified with these copolymers was performed. RCMP was proved to be an effective method for copolymer synthesis in the aqueous media.

In total, polymerizations were successfully carried out in emulsion, solution, and bulk systems via iodide- and oxyanion-catalyzed RCMP, yielding well-defined polymers. The applications of oxyanion catalysts in air-tolerant RCMP and block copolymers synthesized via solution RCMP for anti-fouling membrane coating were demonstrated. The use of little toxic or naturally existing oxyanion compounds as RCMP catalysts greatly expanded the catalyst scope in RCMP and also contributed towards green chemistry. In the future, vinyl monomers containing oxyanion functional groups may be used as a monomer and a catalyst simultaneously. The use of such catalytic monomers may also enable self-catalyzed RCMP in which the polymerization is catalyzed by the catalytic monomers and does not require an extra catalyst. Based on the development of oxyanion catalysts, the first air-tolerant RCMP method was developed. This development gave an impact not only in polymer chemistry but also in synthetic chemistry, as it expands applications of the reported NHPI-catalyzed oxidation of

aldehydes developed for small molecule to the synthesis of polymers under air. The air -tolerant RCMP also facilitates the use of RCMP for large-scale synthesis and low-volume reactions and increases the accessibility of RCMP for non-experts and new learners. The development of emulsion RCMP opens another new avenue for large-scale polymer synthesis that may be useful in industries and has led to research collaboration with a chemical company on this topic. Last but not least, the application of RCMP in aqueous solution for anti-fouling membrane coating, as well as other works in thesis, proves that RCMP is a versatile LRP method, which is tolerant to different reaction media (in bulk, solution, and emulsion) and has large potential in industrial applications.

Currently, there is still much to explore for RCMP. For example, the polymerizations of acrylamides and non-conjugated monomers (such as vinyl acetate and *N*-vinylpyrrolidone) are still challenging. The further design of new RCMP catalysts for monomer scope expansion and the further development of RCMP in aqueous media may widen the applications of RCMP in the future.